Kinetic Factors In Miniemulsion Polymerization.

Order Number 9130012

Kinetic factors in miniemulsion polymerization

Tang, Phan Linh, Ph.D.

Lehigh University, 1991

U·M·I
300 N. Zeeb Rd.
Ann Arbor, MI 48106

KINETIC FACTORS
IN
MINIEMULSION POLYMERIZATION

by

Phan L. Tang

A Dissertation

Presented to the Graduate Committee

of Lehigh University

in Candidacy for the Degree of

Doctor of Philosophy

in

Chemical Engineering

Lehigh University

1991

Certificate of Approval

This dissertation is accepted in partial fulfillment of the requirements for the degree of Doctor of Philosophy.

APRIL 2, 1991
(date)

M.S. El-Aasser
Professor in Charge

MAY 13, 1991
(date accepted)

Special committee directing
the doctoral work of
Phan L. Tang

M.S. El-Aasser, Chairman & Advisor

M.E. Adams

A. Klein

C. Silebi, Co-Advisor

E.D. Sudol, Co-Advisor

Acknowledgements

I would like to express my appreciation to:

Dr. M. S. El-Aasser for his advice, guidance, support and encouragement throughout this project, and especially for his idea of monthly miniemulsion meeting.

Dr. E. D. Sudol for his advice, discussion of the results and editing this dissertation.

Dr. M. E. Adams for her advice during this work and help in parameter estimation.

Dr. C. Silebi for his advice during this work, time in miniemulsion meetings and help in the calculation of the ionic strength.

Dr. A. Klein for his advice and introduction to the polymer chain distribution in the swollen polymer particles.

The staff and colleagues of the Emulsion Polymers Institute for their help and friendship.

The Emulsion Polymers Institute, the Graduate School of Lehigh University, the National Science Foundation Grant No. CTS-8907600 and the United States Department of Education Graduate Fellow Program in Chemical Engineering.

My wife for her love and support.

Dedication

To my parents
and my wife

Table of Contents

List of Figures

List of Tables

Abstract

The kinetics of miniemulsion polymerization were examined by three separate investigations: 1) the effect of preparative variables on miniemulsion polymerization kinetics and resulting particle sizes; 2) the effect of cetyl alcohol on the entry and exit of radicals in seeded polymerizations; and 3) applying a mathematical model incorporating various possible mechanisms for predicting miniemulsion polymerization kinetics.

Variations in the conditions used to prepare miniemulsions of monomers in water have resulted in substantial differences in polymerization kinetics and final particle sizes and distributions. These variations have included: 1) surfactant amount and type; 2) co-surfactant amount and type; 3) monomer(s) type; 4) temperature of preparation and polymerization; 5) means and conditions of homogenization; and 6) degree of aging of the emulsion. In an effort to unify some of the disparate information of previous work, a systematic study of some of the above variables was undertaken using styrene as the oil phase, sodium lauryl sulfate as surfactant, and hexadecane or cetyl alcohol as co-surfactant. Based on the polymerization kinetics and particle sizes obtained for styrene miniemulsions, the following conclusions are drawn. The finest droplet size miniemulsions are obtained by: 1) using a co-surfactant; 2) homogenizing at elevated temperature (when cetyl alcohol is used as co-surfactant); 3) homogenizing using a uniform high shear device (Microfluidizer); and 4) limiting the aging time prior to polymerization (when a co-surfactant is not used).

Seeded emulsion polymerizations of styrene in polystyrene were carried out to study the effect of cetyl alcohol on the entry and exit of radicals in miniemulsion polymerization. A monodisperse seed was used to maintain a

constant particle concentration throughout the reactions, a requirement for determining the entry and exit rate coefficients. Cetyl alcohol was added to the system to mimic the oil/water interphase in miniemulsions. Comparisons were made between experiments including cetyl alcohol and those without. A different seed size was also employed to separate the effects of entry and exit. The chain transfer constant for cetyl alcohol was experimentally obtained to determine its effect on exit in emulsion polymerization and was found to be more than an order of magnitude greater than that of styrene. The results show that cetyl alcohol does not measurably affect entry but does decrease the exit of radicals from the polymer particles, thus resulting in a faster reaction. These results suggest that when a water insoluble compound (such as cetyl alcohol) is present in the monomer swollen particles and it has a higher chain transfer constant than that of the monomer and when $\bar{n} < 0.5$, it would increase the polymerization rate by decreasing the exit rate of radicals from the polymer particles. The results also suggests that the difference in the entry rate coefficients for droplets and particles is likely due to the difference in their physico-chemical nature.

A mathematical model which takes into account the nucleation of monomer droplets, the equilibrium swelling thermodynamics, the desorption of radicals from the polymer particles and the coagulation of droplets and particles based on the DLVO theory and the Muller Equation, was applied to predict the experimental data. The modeling results suggest that the co-surfactant is very important in the nucleation of particles in miniemulsion polymerization. It was found that the entry rate coefficient for radicals into the monomer droplets, prepared with cetyl alcohol as cosurfactant, was about an order of magnitude smaller than that of the polymer particle; but the entry rate coefficient for radicals into the monomer droplets, prepared with hexadecane as cosurfactant,

was similar to that of the polymer particles. The co-surfactant was also found to be important in miniemulsion polymerization kinetics by decreasing the concentration of monomer in the particles while the monomer droplets exist, which in turn decreases the rate of polymerization. The stability of the monomer droplets was found to be a function of the size, number and surface charge density of the droplets and particles.

Chapter 1
General Introduction

The purpose of this research is to investigate the kinetic factors that affect miniemulsion polymerization. This chapter provides some background on the types of emulsions, the polymerization of emulsions, and particle nucleation in emulsion polymerization.

1.1 Macro, Mini and Microemulsions

Emulsions are dispersions of small droplets of one liquid in a second liquid which is immiscible in the first, such as dispersions of oil in water. Emulsions often are classified into one of three types according to their physical properties: macroemulsions, miniemulsions and microemulsions. Macroemulsions, often referred to as conventional emulsions, are opaque and milky, and tend to separate upon standing[1]; their average droplet diameter is larger than 1000 nm. Miniemulsions are also opaque and milky, but are relatively stable emulsions with average droplet diameters[2] ranging from 50 nm to 400 nm. Microemulsions, on the other hand, are clear or translucent and somewhat viscous, and thermodynamically stable; their average droplet diameter ranges from 10 nm to 100 nm[1, 3].

Macroemulsions are usually prepared by mixing two immiscible liquids with surfactant, ionic or nonionic, or a mixture of both, where the concentration of surfactant is about 1 to 3%. Microemulsions are usually prepared by using a mixture of ionic surfactant and a co-surfactant such as a short chain alcohol (usually 1-pentanol or 1-hexanol), where the concentration of the total surfactant and co-surfactant is about 15 to 30%. Miniemulsions, on the other hand, require a co-surfactant consisting of a long chain alcohol or alkane of at

least 12 carbon atoms in length, where the total concentration of surfactant plus co-surfactant is about 1 to 3%.

The preparation of stable miniemulsions involves some special techniques. In the case of a long chain alcohol co-surfactant, such as hexadecanol, the usual procedure to prepare stable miniemulsions requires a pre-emulsifying step, in which the surfactant and long-chain alcohol are mixed in the aqueous phase at a temperature above the melting point of the alcohol for a period of at least 30 minutes. The oil phase is then added to the aqueous phase, and mild agitation such as a magnetic stirrer is usually sufficient to prepare stable miniemulsions[4]. When using a long-chain alkane such as hexadecane as co-surfactant, stable miniemulsions are prepared by adding hexadecane to an oil phase while dissolving the surfactant in the aqueous phase. The two phases are then mixed in a high-shear device such as a sonifier[2, 5, 6, 7].

The chain-length of the co-surfactant and the co-surfactant/surfactant molar ratio are important factors in determining the stability of a miniemulsion. Ugelstad et al.[8] studied a series of n-alkanes with chain-lengths of 10 to 16 carbon atoms and demonstrated that the longer the chain-length of the co-surfactant, the more stable the miniemulsion. If a long-chain alcohol was used as a cosurfactant, the most stable miniemulsion was formed when the long-chain alcohol/emulsifier molar ratio was between 2:1 and 3:1[4, 9, 10, 11, 12].

When an alkane such as hexadecane was used, no optimum molar ratio of alkane/emulsifier was found to provide maximum stability. Delgado[13] studied the miniemulsion copolymerization of vinyl acetate and n-butyl acrylate and found that a plateau in emulsifier adsorption or stability existed for hexadecane/sodium hexadecyl sulfate molar ratios greater than three. This result was also observed for the system of styrene and methyl methacrylate with hexadecane and sodium lauryl sulfate[14], and also for the system of vinyl acetate

and methyl acrylate where hexadecane and Aerosol MA 80 were used[15].

1.2 Emulsion Polymerization

Emulsion polymerization is a widely used process for producing a large number of industrial polymers. It is a unique process which produces polymers with both high molecular weight and fast reaction rate. The physical state of the emulsion system makes it easy to control the process; thermal and viscosity problems are much less significant than in bulk polymerization. The products of emulsion polymerizations in some instances can be used directly without further separation, as long as appropriate blending is done. Such applications include coatings, finishes, floor polishes, and paints[16].

Emulsion polymerization can be divided into three stages: particle nucleation, particle growth and monomer droplet disappearance. The particle nucleation stage is considered to be the most important one because it determines the number of particles present in the system and thus the polymerization rate. Therefore, only particle nucleation is discussed here.

In addition to being important, particle nucleation is also more controversial because it is experimentally difficult to assess. The initial particles are too small (with radius < 5 nm) to be resolved by transmission electron microscopy and the time dependence of the number of particles during the nucleation period is extremely difficult to obtain due to the short duration of this period[17].

There are three types of oil-in-water emulsion polymerizations: macroemulsion polymerization, miniemulsion polymerization and microemulsion polymerization.

1.2.1 Macroemulsion Polymerization

The most widely used process is the macroemulsion or conventional emulsion polymerization. In macroemulsion polymerization, the monomer is emulsified in an aqueous phase using an oil-in-water emulsifier to produce an emulsion with droplets ranging from 1000 to 10,000 nm in diameter. The polymerization is accomplished by introducing a water-soluble or oil-soluble initiator into the emulsion to produce a colloidal dispersion of polymer particles in water. The polymer particles typically range from 100 to 300 nm in diameter[18].

Harkins[19] proposed that monomer-swollen micelles were the main locus of particle nucleation. The monomer droplets act as reservoirs which only supply monomer to the monomer-swollen micelles and the formed polymer particles.

Another major nucleation mechanism was proposed by Priest[20]. Here the aqueous phase was the main locus of particle nucleation. Radicals generated in an aqueous phase grow to a critical length becoming insoluble in the aqueous phase and precipitate to form particles.

1.2.2 Miniemulsion Polymerization

In macroemulsion polymerization, monomer droplets are not considered a significant locus for particle nucleation. The reason for this behavior is that monomer droplets have a relatively small total surface area, which makes them unable to compete with nucleation in micelles and in the aqueous phase. Ugelstad, El-Aasser and Vanderhoff[21] have shown that when very small monomer droplets are used, they may become the main locus for particle nucleation and polymerization. This polymerization of these smaller droplets has come to be known as miniemulsion polymerization.

Recently, many studies have been carried out for monomers such as

styrene[22, 23, 24, 25] and vinyl chloride[26, 27]; and for comonomers such as vinyl acetate-butyl acrylate[13], vinyl acetate-methyl acrylate[15], and styrene-methyl methacrylate[14].

1.2.3 Microemulsion Polymerization

Microemulsion polymerization was developed around 1980 and is a relatively new area compared to macroemulsion and miniemulsion polymerizations. Atik and Thomas[28] polymerized microemulsions containing styrene, using azo-bis-isobutyronitrile and a γ-ray source to obtain particles 20 to 35 nm in diameter. Leong and Candau[29] published results on inverse microemulsion polymerizations of an aqueous solution of acrylamide in toluene. Small particles and high molecular weights were found.

Guo et al.[30, 31] studied the microemulsion polymerization of styrene and proposed that the monomer-droplets capture radicals from the aqueous phase for both water-soluble and oil-soluble initiators to form polymer particles. The microemulsion droplets, which did not capture radicals, served as reservoirs to supply monomer to the polymer particles. However, the possibility of homogeneous nucleation could not be ruled out.

1.3 Mechanisms of Particle Nucleation in Emulsion Polymerization

Four mechanisms of particle nucleation have been proposed: nucleation in monomer-swollen micelles[19], nucleation in the aqueous phase[20, 32, 33, 34, 35], nucleation in emulsifier layers[36, 37], and nucleation in monomer droplets[21].

1.3.1 Nucleation in Monomer-Swollen Micelles

In studying the polymerization of styrene and isoprene in the presence and absence of monomer-swollen micelles, Harkins[19] observed that the rates of polymerization were much greater when micelles were present. As a result, he proposed that monomer-swollen micelles were the principal locus of particle nucleation, and that monomer droplets acted only as a reservoir to supply monomer to the monomer-swollen micelles and the formed particles. Particle nucleation stops when all micelles have either captured a radical or disbanded.

Smith and Ewart[38] derived an equation for the number of particles with i radicals in terms of the rate of radical entry into the particles, rate of radical transfer out of the particles, and rate of termination within the particles. Smith and Ewart did not obtain a general solution to this equation, instead, solved it for three limiting cases: case 1, $\bar{n} \ll 0.5$; case 2, $\bar{n} \approx 0.5$; and case 3, $\bar{n} \gg 0.5$ (where $\bar{n}$ is the average number of radicals per particle).

By the assumption of case 2 conditions, Smith and Ewart obtained a satisfactory model for the emulsion polymerization of styrene:

$$R_p = k_p C_m^p N_p / 2 \tag{1.1}$$

where R_p is the rate of polymerization, k_p is the rate constant for propagation, C_m^p is the monomer concentration in the particles, and N_p is the number of particles. Smith and Ewart also developed an expression for the number of particles initiated:

$$N_p = k_N (R_i/\mu)^{0.4} (a_s S)^{0.6} \tag{1.2}$$

where k_N is a constant, R_i is the rate of radical entry into the particles, μ is the rate of volume increase of the particles, a_s is the area occupied by the emulsifier, and S is the amount of emulsifier present. The equation was verified experimentally by Smith[39, 40].

Smith-Ewart case 2 is a rational explanation which fitted the styrene

system reasonably well. Its most important advantage is that it is amenable to experimental verification. Therefore, it stimulated much experimental work, not only with styrene, but with other monomers as well. Many investigators carried out extensions or modifications of the Smith-Ewart theory. Stockmayer[41] developed a general solution for the Smith-Ewart steady-state equation. Van der Hoff[42] and O'Toole[43] further extended the work of Stockmayer. Ugelstad et al.[44] considered the desorption and readsorption of radicals from the aqueous phase. Gardon[45] carried out a detailed and extensive reconsideration of the Smith-Ewart case 2 and the deviations from it arising from decreased rates of termination within the particles. He treated all parameters including latex particle size and molecular weight distributions and correlated the experimental values with the theoretically calculated values. Gilbert and Napper[46] developed a time dependent solution for the Smith-Ewart equation and applied these analytical solutions to explain the seeded polymerization of vinyl acetate.

According to Hansen and Ugelstad[47], many investigators have argued against the Smith-Ewart theory on the grounds that: (1) particles are formed even if no micelles are present; (2) the equation for the particle number gives an estimate that is a factor of 2 higher than that found experimentally; (3) more water-soluble monomers do not fit the theory; and (4) a maximum polymerization rate is predicted for the end of the nucleation but rarely has been observed. Because of these arguments, other theories of particle nucleation have been put forward, based on the idea of self-nucleation of oligomeric radicals produced in the aqueous phase.

1.3.2 Nucleation in the Aqueous Phase

From the studies of particle size distribution in vinyl acetate polymerizations initiated by potassium persulfate in the presence of varying amounts of different stabilizers and inhibitors at several temperatures, Priest[20] has laid out all the basic qualitative features of the theory of homogeneous nucleation in emulsion polymerization. Priest proposed that initiation in solution is the initial process which is then followed by the growth of a given polymer chain until the polymer is no longer soluble, and collapses to become a primary particle. The number of particles may be reduced by coagulation depending upon the quantity and efficiency of the surfactant; and micelles, when present, act as reservoirs of surfactant which maintain the concentration of surfactant in the aqueous phase at a constant level equal to the critical micelle concentration.

These proposals led to a quantitative treatment by Fitch et al.[33], which is based on the belief that there are three processes involved in homogeneous nucleation whose rates are R_i (radical generation), R_c (radical capture by existing particles), and R_f (particle flocculation). The rate of particle formation was expressed as:

$$\frac{dN_p}{dt} = R_i - R_c - R_f \tag{1.3}$$

This equation says that the number of particles increases at a rate equal to the rate of free radical generation, reduced at a rate equal to the rate of radicals captured by particles, and further reduced at a rate equal to the rate of flocculation.

Flocculation of primary particles must be limited because it increases the surface electrical potential, and consequently increases stabilization[33]. Flocculation will occur until a critical surface potential developes to prevent

further flocculation[48]. When the primary particles are stable, particle flocculation is negligible.

Coagulative nucleation, an extension of homogeneous nucleation, has been proposed by Napper, Gilbert et al.[17, 49]. They did extensive work on the time evolution of the particle size distribution of the latex some time after the end of nucleation. They also applied the DLVO[50] theory and Muller Equation[51] to explain the coagulation mechanism of precursor particles. Based on theoretical and experimental results, they proposed that: (1) the polymerization reaction starts with the formation of colloidally unstable precursor particles, which form by the homogeneous nucleation mechanism discussed above; (2) this is followed by their coagulation to form colloidally stable particles; and (3) the precursor particles are presumed to grow mainly by coagulation, although some growth must occur by polymerization.

In the coagulative nucleation theory, the initiation takes place in the aqueous phase followed by growth of a given polymer chain until the polymer is no longer soluble and nucleates to become a precursor particle. These precursor particles grow mostly by coagulation with each other. As time proceeds, the rate at which flocs coagulate with other flocs of comparable size becomes progressively smaller, whereas the rate of coagulation increases between the large particles (stable particles formed from coagulation of numerous precursor particles) and the precursor particles. The nucleation stage ends when the rate of coagulation between particles and precursor particles is so large that the probability of coagulation between precursor particles themselves to form stable particles is negligible.

1.3.3 Particle Initiation in Emulsifier Layer

Medvedev[36, 37] proposed that the adsorbed emulsifier layer, whether it is in micelles, monomer-swollen polymer particles, or emulsion droplets, is the principal locus for particle formation. Thus the most important parameter of Medvedev's theory is the total surface area stabilized by adsorbed emulsifier.

Medvedev showed theoretically that the polymerization rate should vary as the 1.0 power of the emulsifier concentration and the 0.5 power of the initiator concentration. This result was compared with experimental results from polymerizations of isoprene in aqueous emulsifier solutions. The agreement between theoretical and experimental results was good for the variation in the emulsifier concentration, but poor for the variation with initiator concentration.

1.3.4 Particle Initiation in Monomer Droplets

Monomer droplets are usually not considered a significant locus for initiation of polymerization because they are relatively large and few and have a relatively small total surface area, which makes them unable to compete with initiation in micelles or in the aqueous phase. However, if the droplet size is small enough, the droplets should be able to compete with initiation in micelles or in the aqueous phase.

In some systems such as miniemulsion polymerization, monomer droplets are the principal locus of particle nucleation. This behavior was first demonstrated by Ugelstad, El-Aasser and Vanderhoff[21] in using styrene with a mixed emulsifier system of ionic surfactant and fatty alcohol. They showed that by dispersing the monomer into smaller stable droplets, the area available for radical capture increases dramatically, and monomer droplets become the main locus for particle formation and polymerization.

Ugelstad et al.[8] gave further evidence of monomer-droplet nucleation in studying the miniemulsion copolymerization of styrene, n-butyl acrylate and methacrylic acid. They showed that the final latex particle size decreased with decreasing initial monomer-droplet size. Rodriguez[14] showed similar results for the miniemulsion copolymerization of styrene and methyl methacrylate. Tang et al.[52] using semicontinuous feed of the miniemulsions to demonstrate that monomer-droplet nucleation takes place whenever miniemulsion droplets exist in the reactor.

Not all monomer droplets end up as particles, only a fraction of droplets become particles and this fraction was found to increase with increasing initiator concentration[9]. Therefore, monomer droplets that are not initiated have to disappear by diffusion of monomer to the polymer particles and/or collision with the polymer particles. Delgado[13] used equilbrium swelling thermodynamics to show that the presence of a low molecular weight and low water-solubility compound in the monomer droplets prevents them from dissappearance by molecular diffusion during the polymerization. The collision mechanism was found to be necessary to explain some experimental data[14]. It is likely that the monomer in the uninitiated monomer droplets diffuses to the polymer particles until the droplets are small enough to coagulate with the polymer particles, because the importance of coagulation increases with increasing the size difference between large and small particles[51].

1.3.5 Importance of Particle Nucleation Mechanisms

The relative importance of a specific particle nucleation mechanism depends on the individual polymerization system. Particle nucleation in micelles and in the aqueous phase are very important in the polymerization of macroemulsions. Whereas, particle nucleation in monomer-droplets is dominant

in the polymerization of miniemulsions and microemulsions. Particle nucleation in adsorbed emulsifier layers has not been widely investigated probably because of its poor prediction of experimental results.

Vanderhoff[18] has stated that in macroemulsion polymerization, the initiation-in-micelles mechanism is generally applied to monomers which are only sparingly soluble in water and the initiation-in-the-aqueous-phase mechanism to monomers with significantly higher solubilities in water. Dunn[53] demonstrated the importance of micelles by carrying out the polymerization of *p*-tert-butyl styrene which has only one-tenth of the solubility in water of styrene. No latex was produced when emulsifier-free emulsion polymerization was attempted, however a latex was formed instantly when emulsifier was introduced.

Nevertheless, Hansen and Ugelstad[54] had pointed out that particle nucleation models should include all three nucleation mechanisms--micellar, homogeneous, and droplet--since all three mechanisms may compete and coexist in the same polymerization system, even if one of them usually dominates.

In some instances, it is difficult to distinguish between different nucleation mechanisms. For example, Smith and Ewart[38] showed that the micellar entry mechanism can lead to a particle number density and thus the polymerization rate being proportional to $[I]^{0.4}[S]^{0.6}$ (where [I] is the initiator concentration and [S] the surfactant concentration). It was later shown by Roe[32] that this behavior is also consistent with homogeneous nucleation. Snuparek[55] showed that the polymerization rate of acrylic monomers in the water phase in the absence of emulsifier is enhanced by an increase of monomer polarity; and in the presence of emulsifier, the initial polymerization rate increases rapidly with increasing emulsifier concentration. This indicates the possibility of a competitive action of homogeneous and micellar nucleations.

1.4 Project Objectives and Overview

The objectives of this research are:

1. To investigate the polymerization kinetics and resulting particle size distributions as a function of the various methods of preparing miniemulsions.

2. To study the effect of cetyl alcohol on the entry and exit of radicals in miniemulsion polymerization.

3. To refine and expand a mathematical model for the kinetics of styrene miniemulsion polymerization.

Subsequent chapters elaborate on the experimental techniques and the discussion of the results. Chapter 2 examines the kinetics and the resulting particle size distributions of the polymerization of miniemulsions which were prepared by different methods. The important variables are the levels of surfactant and co-surfactant, the type of co-surfactant, the age of the emulsions and the devices used for shearing the emulsion. In an attempt to gain further understanding of the particle nucleation mechanism in miniemulsion, chapter 3 examines the effect of cetyl alcohol (co-surfactant) on the entry and exit rate coefficients in miniemulsion polymerization. Comparison between experiments with cetyl alcohol and those without cetyl alcohol will be made. Different seed sizes will be employed to isolate the effect of cetyl alcohol on the entry and exit rate coefficients. Chapter 4 describes the mathematical modeling of the kinetics of miniemulsion polymerization of styrene. The Smith-Ewart[38] Equation will be used for the population balance of the particles. The thermodynamic equilibrium model[13] will be used to calculated the monomer concentrations in various phases and also to predict the average radius of monomer droplets and polymer particles. The desorption model of Asua et al.[56] will be applied. The DLVO[50] theory and the Muller Equation[51] will be used to calculate the coagulation coefficient between droplets and particles. Lastly, chapter 5 offers

some conclusions and recommendations based on the findings of this research project.

1.5 References

1. L. M. Prince, in *"Microemulsions: Theory and Practice"*, L. M. Prince, Ed., Academic Press, New York, 1977, p. 45.

2. M. S. El-Aasser, S. C. Misra, J. W. Vanderhoff and J. A. Manson, *J. Coatings Tech.*, **49**, 71 (1977).

3. D. O. Shah, V. K. Bansal, K. Chan and W. C. Hsieh, in *"Improved Oil Recovery by Surfactant Flooding"*, D. O. Shah and R. S. Schechter, Ed., Academic Press, New York, 1977, p.293.

4. W. L. Grimm, T. I. Min, M. S. El-Aasser and J. W. Vanderhoff, *J. Colloid Interface Sci.*, **94**, 531 (1983).

5. J. W. Vanderhoff, M. S. El-Aasser and J. Ugelstad , U. S. Patent 4,177,177, December, 1977.

6. J. W. Vanderhoff, M. S. El-Aasser and J. D. Hoffman, U. S. Patent 4,070,323, December, 1979.

7. M. S. El-Aasser, G. W. Poehlein and J. W. Vanderhoff, *Coatings and Plastics Preprints*, **37**, 92 (1977).

8. J. Ugelstad, P. C. Mork, K. Herder Kaggerud, T. Ellingsen and A. Berge, *Adv. Colloids Interface Sci.*, **13**, 101 (1980).

9. Y. T. Choi, *Formation and Stabilization of Miniemulsions and Latexes*, Ph. D. Dissertation, Lehigh University, 1986.

10. W. L. Grimm, *The Use of Mixed-Emulsifier Systems in the Preparation and Stabilization of Emulsions and Latexes*, M. S. Thesis, Lehigh University, 1982.

11. M. S. El-Aasser, C. D. Lack, Y. T. Choi, T. I. Min, J. W. Vanderhoff and F. M. Fowkes, *Colloids Surfaces*, **12**, 79 (1984).

12. C. D. Lack, *Emulsion Formation and Stabilization with Mixed Emulsifier Liquid Crystals*, Ph. D. Dissertation, Lehigh University, 1985.

13. J. Delgado, *Miniemulsion Copolymerization of Vinyl Acetate and n-Butyl Acrylate*, Ph. D. Dissertation, Lehigh University, 1986.

14. V. S. Rodriguez, *Interparticle Monomer Transport in Miniemulsion Copolymerization*, Ph. D. Dissertation, Lehigh University, 1988.

15. H. A. Pelsynski, *Batch and Semicontinuous Copolymerization of Vinyl Acetate and Methyl Acrylate*, M. S. Research Report, Lehigh University, 1987.

16. G. Odian, *"Principles of Polymerization"*, 2nd Ed., Wiley-Interscience, New York, 1981, p. 319.

17. G. Lichti, R. G. Gilbert and D. H. Napper, *J. Polym. Sci. Polym. Chem.*

Ed., **21**, 269 (1983).

18. J. W. Vanderhoff, *J. Polym. Sci., Polym. Symp.*, **72**, 161 (1985).

19. W. D. Harkins, *J. Am. Chem. Soc.*, **69**, 1428 (1947).

20. W. J. Priest, *J. Phys. Chem.*, **56**, 1977 (1952).

21. J. Ugelstad, M. S. El-Aasser and J. W. Vanderhoff, *Polym. Lett.*, **11**, 503 (1973).

22. B. J. Chamberlain, D. H. Napper and R. G. Gilbert, *J. Chem. Soc., Faraday Trans. I*, **78**, 591 (1982).

23. Y. T. Choi, M. S. El-Aasser, E. D. Sudol and J. W. Vanderhoff, *J . Polym. Sci., Polym. Chem. Ed.*, **23**, 2973 (1985).

24. J. Ugelstad, F. K. Hansen and S. Lange, *Die Makromol. Chem.*, **175**, 507 (1974).

25. F. K. Hansen, E. Baumann Ofstad and J. Ugelstad, in *"Theory and Practice of Emulsion Polymerization"*, A. L. Smith, Ed., Academic Press, London, 1976, p. 13.

26. R. C. Dewald, L. H. Hart and W. F. Carroll, Jr., *J. Polym. Sci. Polym. Chem. Ed.*, **22**, 2923 (1984).

27. R. C. Dewald, L. H. Hart and W. F. Carroll, Jr., *J. Polym. Sci. Polym. Chem. Ed.*, **22**, 2931 (1984).

28. S. S. Atik and J. K. Thomas, *J. Am. Chem. Soc.*, **103**, 4279 (1981).

29. Y. S. Leong and F. Candau, *J. Phys. Chem.*, **86**, 2269 (1982).

30. J. S. Guo, M. S. El-Aasser and J. W. Vanderhoff, *J. Polym. Sci. Polym. Chem. Ed.*, **27**, 691 (1989).

31. J. S. Guo, *Polymerization of Styrene Oil-in-Water Microemulsions*, Ph.D. Dissertation, Lehigh University, 1990.

32. C. P. Roe, *Ind. Eng. Chem.*, **60**, 20 (1968).

33. R. M. Fitch and C. H. Tsai, in *"Polymer Colloids"*, R. M. Fitch, Ed., Plenum, New York, 1971, p.73.

34. B. Jacobi, *Angew. Chem.*, **64**, 539 (1952).

35. R. Patsiga, M. Litt and V. Stannett, *J. Phys. Chem.*, **64**, 801 (1960).

36. Medvedev, *Ric. Sci., Suppl.*, **25**, 897 (1955).

37. Medvedev, *"International Symposium on Macromolecular Chemistry"*, Pergamon Press, New York, 1959, p.174.

38. W. V. Smith and R. W. Ewart, *J. Chem. Phys.*, **16**, 592 (1948).

39. W. V. Smith, *J. Am. Chem. Soc.*, **70**, 3695 (1948).

40. W. V. Smith, *J. Am. Chem. Soc.*, **71**, 4077 (1949).

41. W. H. Stockmayer, *J. Polym. Sci.*, **24**, 314 (1957).

42. B.M.E. van der Hoff, *J. Polym. Sci.*, **33**, 487 (1958).

43. J. T. O'Toole, *J. Appl. Polym. Sci.*, **9**, 1291 (1965).

44. J. Ugelstad, P. C. Mork and J. O. Aasen, *J. Polym. Sci., Part A-1*, **5**, 2281 (1967).

45. J. C. Gardon, *J. Polym. Sci., Part A-1*, **6**, 623 (1968); ibid. 643 (1968); ibid. 665 (1968); ibid. 687 (1968).

46. R. G. Gilbert and D. H. Napper, *J. C. S. Faraday I*, **70**, 391 (1976).

47. F. K. Hansen and J. Ugelstad, in *"Emulsion Polymerization"*, Irja Piirma, Ed., Acadamic Press, New York, 1982, p.51.

48. A. S. Dunn and L. C. H. Chong, *Br. Polym. J.*, **2**, 49 (1970).

49. P. J. Feeney, D. H. Napper and R. G. Gilbert, *Macromolecules*, **17**, 2520 (1984).

50. J. Th. G. Overbeek, in *Colloid Science*, H. R. Kruyt, Ed., Elsevier, Amsterdam, 1952.

51. H. Muller, *Kolloid.-Beih.*, **26**, 257 (1928).

52. P. L. Tang, E. D. Sudol, M. E. Adams, J. M. Asua and M. S. El-Aasser, *J. Appl. Polym. Sci.*, **42**, 2019 (1991).

53. A. S. Dunn, *Eur. Polym. J.*, Vol. 25, No. 7/8, 691 (1989).

54. F. K. Hansen and J. Ugelstad, *J. Polym. Sci. Polym. Chem. Ed.*, **17**, 3069 (1979).

55. J. Snuparek, Jr., *Angew. Makromol. Chem.*, **88**, 61, 69 (1980).

56. J. M. Asua, E. D. Sudol and M. S. El-Aasser, *J. Polym. Sci., Polym. Chem. Ed.*, **27**, 3903 (1989).

Chapter 2
Miniemulsion Polymerization -- A Comparative Study of Preparative Variables

2.1 Introduction

Miniemulsions are relatively stable submicron (50 to 500 nm) dispersions of oil (such as monomer) in water prepared by shearing a system containing oil, water, surfactant, and additionally, a "co-surfactant". The principle behind the making of stable miniemulsions is the introduction of a low molecular weight and relatively water-insoluble compound (the "co-surfactant") inside the monomer droplets to retard substantially the diffusion of monomer out of the monomer droplets.

It is well known that the chemical potential of a phase is a function of the molal surface area of that phase[1], so a small crystal dissolves much faster than a larger one and small droplets would have a higher vapor pressure than the larger ones. In conventional emulsions the smaller monomer droplets which have a higher chemical potential dissolve while the larger droplets grow at their expense, thus conventional emulsions are not stable and usually phase separate upon standing for a short time. However, in miniemulsions, the presence of a low molecular weight and relatively water insoluble compound such as hexadecane or cetyl alcohol in the monomer droplets retards the diffusion of monomer out of the droplets.

Higuchi and Misra[2] used diffusion theory to show that the diffusion of the more water-soluble compound in the droplets is governed by the diffusion of the water-insoluble one. Initially, when the monomer is broken up into droplets, some monomer would diffuse out of the smaller droplets, thus the concentration

of the water-insoluble compound would be increased in the smaller droplets, until the concentration of the water-insoluble compound is high enough to offset the chemical potential of the smaller droplets and significantly retard the diffusion process. Some miniemulsions can be prepared that are stable upon standing for months.

For the cetyl alcohol system, the enhanced stability is also attributed to the formation of "intermolecular complexes" at the oil/water interface. These complexes would be liquid condensed and electrically charged creating a low interfacial tension and high resistance to droplet coalescence[3,4,5,6]. However, in a similar system the existence of the interfacial complex has been ruled out by Fowkes[7]. He applied the film balance techniques and used mixed monolayers of cetyl alcohol and sodium cetyl sulfate in n-hexane spread on an aqueous substrate containing 5% of sodium chloride (which keeps the sodium cetyl sulfate from dissolving into the substrate) and obtained pressure-area isotherms for a wide range of stoichiometric ratios. Fowkes concluded that the complex formation for the system of cetyl alcohol and cetyl sulfate could not explain the experimental results and as the concentration of cetyl alcohol increases it removes cetyl sulfate from solution in aqueous surface layer. However, it has been suggested that the alcohol prevents the surfactant from desorbing and covers areas of oil/water interphase not occupied by the surfactant[8, 9], and this forms an interfacial film that resists rupture upon collision.

In conventional emulsion polymerization, the principal locus of particle nucleation is the aqueous phase or the monomer swollen micelles depending on the degree of water solubility of the monomers and the amount of surfactant used; lower water solubility monomer and higher amounts of surfactant would favor particle nucleation in monomer swollen micelles[10]. Monomer droplets are only considered to act as monomer reservoirs supplying monomer to the growing

polymer particles. However, in miniemulsion polymerization, the small size of the monomer droplets enables them to become the principal locus of particle nucleation. Thus, different conditions used in their preparation produce miniemulsions with different average droplet sizes and size distributions which in turn exhibit different polymerization kinetics and final particle size distributions.

Since the introduction of miniemulsion polymerization in the early 1970s[11], many investigators have studied the subject and have used many different methods to prepare miniemulsions[12,13,14,15,16,17,18,19,20]. Two important parameters in preparing miniemulsions are the type and amount of co-surfactant (usually hexadecane or cetyl alcohol) and the means of carrying out the homogenization. Hansen and Ugelstad[14] used styrene as monomer, hexadecane as co-surfactant and a two-stage homogenizer (Manton Gaulin S. A.) as the means of homogenization. Chamberlain et al.[17] used styrene, 1-dodecanol and a sonifier. Choi[18] used styrene, cetyl alcohol and the Microfluidizer (Microfluidics Corp.). Delgado[19] used vinyl acetate and butyl acrylate as monomers, hexadecane as co-surfactant and both the Omni mixer (Ivan Sorvall, Inc.) and a sonifier (Branson Sonic Power Co.), and Rodriguez[20] used styrene and methyl methacrylate as monomers, both cetyl alcohol and hexadecane as co-surfactants and a sonifier. This lack of consistency in the preparation of miniemulsions necessitates the evaluation of the effect of the different methods of preparing miniemulsions, particularly the effect on the polymerization kinetics and the final particle size distribution.

2.2 Experimental

2.2.1 Materials

Styrene (Polysciences) was distilled under reduced pressure (20 mm Hg) of nitrogen. The purified monomer was stored at –2°C for no more than four weeks before use. Potassium persulfate (FMC) was recrystallized from distilled deionized water and then dried at room temperature under vacuum. Sodium lauryl sulfate, SLS, (BDH Chemicals), hexadecane (HD), 98% (Aldrich), cetyl alcohol (CA), 98% (Aldrich) and sodium bicarbonate, certified A.C.S. grade (Fisher) were used as received. The water was distilled and deionized (DDI).

2.2.2 Preparation of Miniemulsions

There are some differences in the procedures for preparing styrene miniemulsions with hexadecane versus cetyl alcohol. In the preparation of miniemulsions with hexadecane (Figure 2-1), sodium lauryl sulfate is first dissolved in the water and hexadecane in the styrene monomer. The two solutions are mixed with a magnetic stirrer for 10 minutes to form a uniform emulsion followed by homogenization to break the monomer into the small droplets forming a miniemulsion. A few extra steps are involved in the preparation of miniemulsions with cetyl alcohol[20] (Figure 2-2). Sodium lauryl sulfate, cetyl alcohol, and water are mixed at 65°C for two hours, cooled to room temperature to form the gel phase[21], and sonified to break up the gel phase. Styrene is then mixed with the gel phase for 10 minutes followed by homogenization.

The Microfluidizer-110 (Microfluidics Corp.), Sonifier Disruptor W-350 (Branson Sonic Power Co.) and the Omni mixer (Ivan Sorvall, Inc.) were used to provide the high shear required to produce submicron monomer droplets. In the the Microfluidizer, the inlet stream is pressurized and forced into an interaction

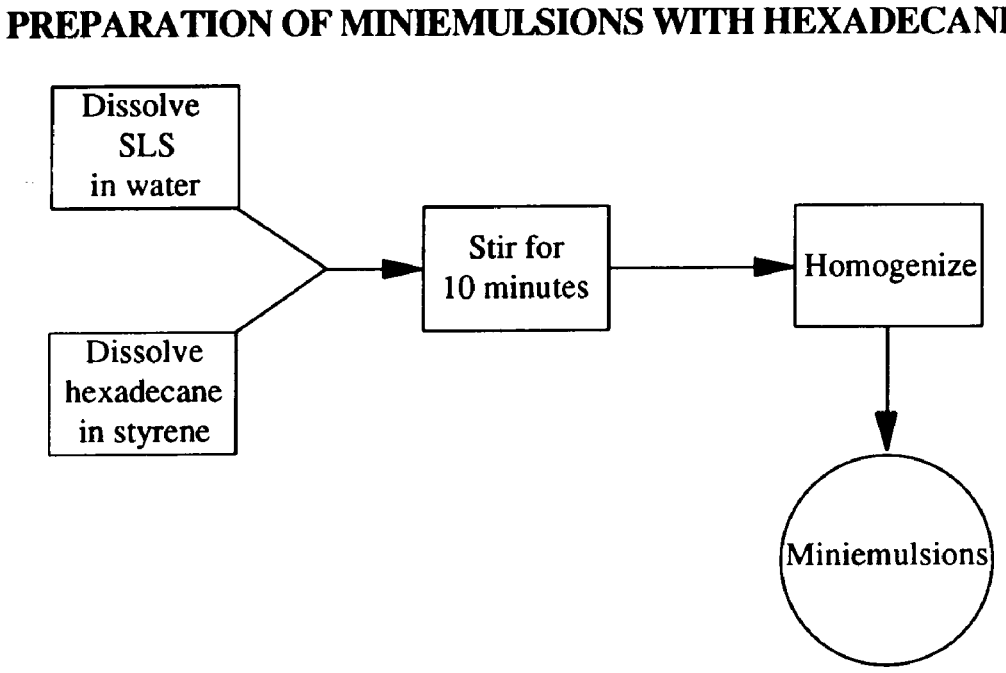

Figure 2-1: Preparation of stable miniemulsions with hexadecane.

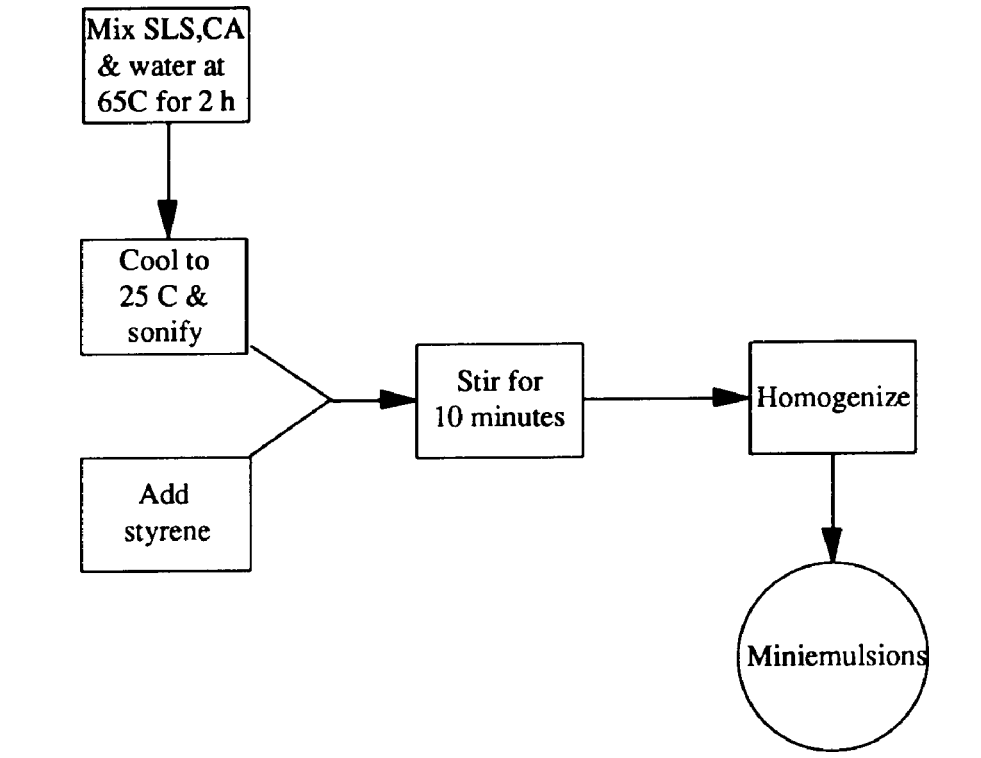

Figure 2-2: Preparation of stable miniemulsions with cetyl alcohol.

chamber. There it is directed into precisely defined microchannels causing the streams to instantly accelerate to high velocities and when recombined in the interaction region, produce an emulsion with fine droplets and a narrow size distribution as a result of shear, turbulence, and cavitation forces[22]. The sonifier produces rapid local pressure variations below the probe tip bringing about cavitation and shear. The Omni mixer produces high speed mixing to shear the liquid around the impeller. Therefore, the Microfluidizer is expected to produce more uniform monomer droplets than the sonifier and the Omni mixer, because of its more uniform exposure of the entire fluid to the shear forces breaking up the oil droplets. In this work, the Microfluidizer was operated at 80 psi inlet pressure and about 7000 psi outlet pressure with the smallest orifice size available (A10), and 10 passes of the emulsion. The sonifier was operated at 50% duty cycle and power 7 for 60 seconds of sonification time. The Omni mixer was operated at about 16,000 rpm (maximum speed of the device) for 20 minutes.

2.2.3 Polymerization Process

The recipe used in this study is shown on Table 2-1 which consists of 80 wt.% DDI water, 20 wt.% styrene, 2.66 mM sodium bicarbonate, 2.66 mM potassium persulfate, 5 or 10 mM sodium lauryl sulfate, and 15--40 mM (all based on water) co-surfactant (cetyl alcohol or hexadecane). When hexadecane was used, the molar ratio of hexadecane to sodium lauryl sulfate was 4 to 1; and when cetyl alcohol was used, the molar ratio of cetyl alcohol to sodium lauryl sulfate was 3 to 1. These co-surfactant to surfactant molar ratios were found to be the optimum ratios to produce stable miniemulsions with minimum amount of surfactant and cosurfactant[3, 20, 23, 24, 25, 26, 27]. The reaction temperature was 70°C.

Table 2-1: Recipe for the of Polymerization of Emulsions Prepared by Different Methods.

Ingredient	Amount
DDI Water	40 g
Styrene	10 g
Potassium Persulfate	2.66 mM *
Sodium Bicarbonate	2.66 mM *
Sodium Lauryl Sulfate, SLS	5 or 10 mM *
Cetyl Alcohol, CA	0 -- 30 mM *
Hexadecane, HD	0 -- 40 mM *

* based on aqueous phase

Dilatometry was applied to monitor the conversion-time behavior of the polymerizations. Its principle is based on the difference in density between monomer and polymer. Polystyrene has a density of 1.037 g/cc at 70°C which is higher than the 0.860 g/cc of styrene at the same temperature[28]. As the polymerization proceeds, styrene is converted to polystyrene and this in turn causes the contraction of the volume of the mixture inside the dilatometer. Therefore the conversion at time t can be calculated from the initial amount of monomer and the volume contraction at time t. The dilatometric method has the advantage over the gravimetric method in that it provides a large number of data which is useful in observing the kinetic transitions.

The apparatus used in this study is shown on Figure 2-3. The dilatometer is immersed in a constant temperature water bath which is controlled by a

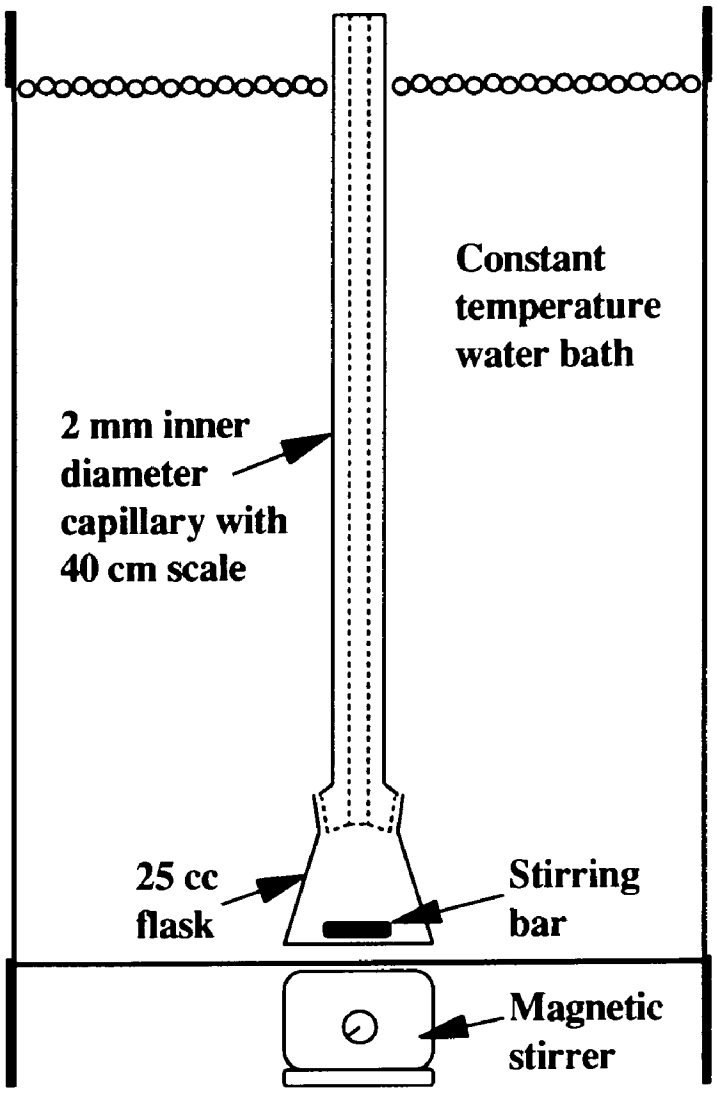

Figure 2-3: Schematic representation of the dilatometer used for monitoring polymerization kinetics.

heating and circulating device. The mixture inside the dilatometer is kept uniform by a stirring bar and a magnetic stirrer. Because the conversion depends on the volume change of the reaction mixture, the emulsion is degassed to avoid any gas bubbles from forming inside the dilatometer during the polymerization. After the emulsion is degassed at a pressure of about 20 mm Hg for 20 minutes using an aspirator, it is loaded into the 25 cc flask and the capillary is quickly inserted to avoid entrapment of air between the flask and the capillary. The dilatometer is placed in the bath which is controlled at a temperature of 70 ± 0.02°C. ; it takes about five minutes for the mixture to be heated from about 25°C to 70°C. To start the polymerization an initiator solution, also at 70°C, is injected into the dilatometer with a micro-syringe connected to a small polyethylene tube. A large number of data can be obtained with frequent readings.

The fractional conversion, x_t, was calculated as:

$$x_t = \frac{G_s - G_{s,t}}{G_s} \tag{2.1}$$

where G_s is the initial grams of styrene in the dilatometer and $G_{s,t}$ the amount at time t, which was calculated from:

$$G_{s,t} = [(1/G_s\rho_s - \Delta V/G_s^2)^{-1} - G_s\rho_{ps}]/(\rho_s - \rho_{ps}) \tag{2.2}$$

where ΔV is volume contraction, ρ_s and ρ_{ps} are the densities of styrene and polystyrene, respectively. This formula was derived by Sudol[28] assuming additive densities of styrene and polystyrene. Typical conversion-time behavior is shown in Figure 2-4 which contains about 100 data points.

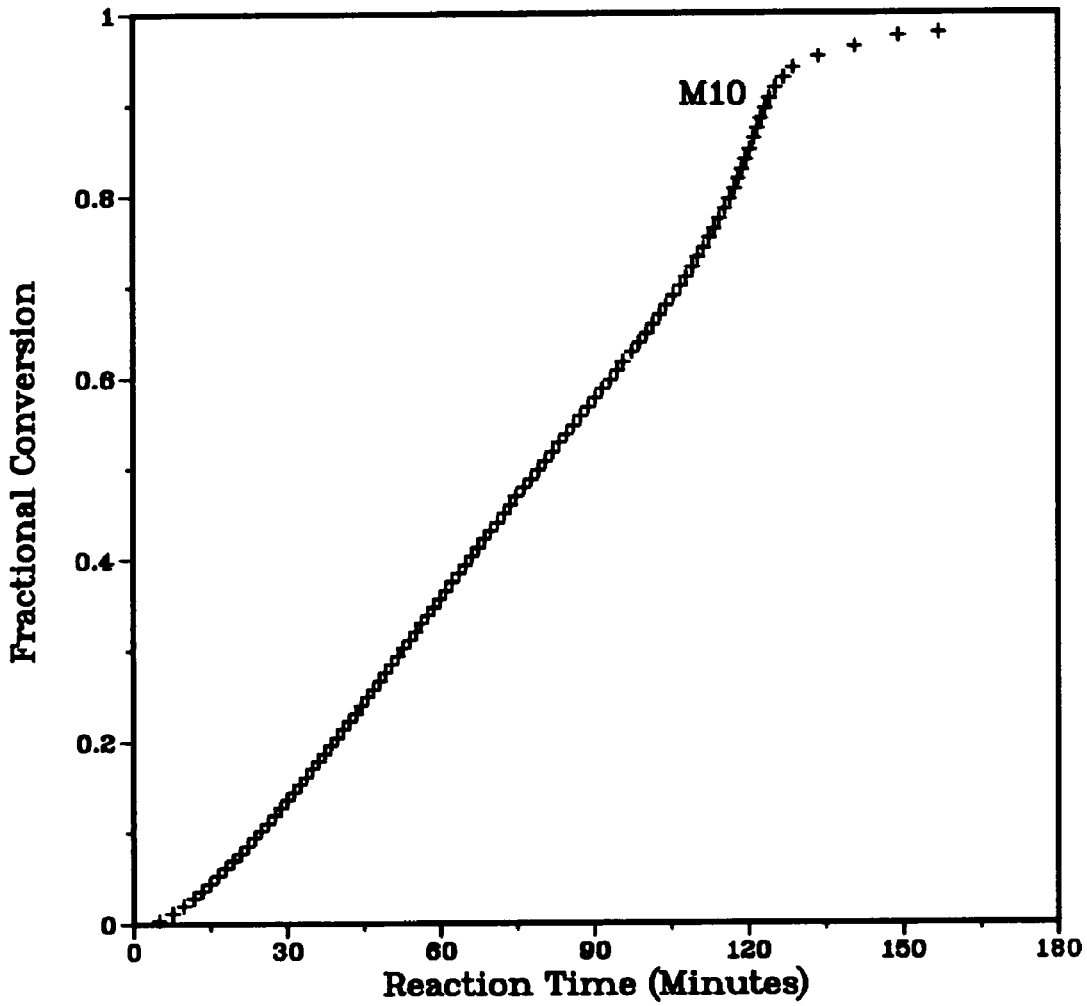

Figure 2-4: Conversion versus time curve of styrene miniemulsion polymerization, run M10, obtained by dilatometry.

2.2.4 Determination of Particle Size Distribution

Calibrated transmission electron microscopy (TEM) was used to determine the final latex particle size distribution. A monodisperse polystyrene standard with diameter of 824 nm was added to a latex sample before the sample was placed on a TEM grid. Micrographs were taken using the Phillips 300 Transmission Electron Microscope. For samples with a wide particle size distribution, at least a thousand particles were counted (using the Zeiss MOP-3 Analyzer) and for narrow particle size distributions, at least five hundred particles were counted. The mean volume diameter was calculated as:

$$D_v = \left[\frac{\sum_j N_j D_j^3}{\sum_j N_j}\right]^{1/3} \tag{2.3}$$

the mean number diameter was calculated as:

$$D_n = \frac{\sum_j N_j D_j}{\sum_j N_j} \tag{2.4}$$

and the standard deviation was calculated as:

$$S_n = \left[\left(\frac{\sum_j N_j D_j^2}{\sum_j N_j} - D_n^2\right)\left(\frac{\sum_j N_j}{\sum_j (N_j - 1)}\right)\right]^{1/2} \tag{2.5}$$

The mean volume diameter, D_v, was used to calculate the number concentration of particles, N_p.

2.2.5 Calculation of the Rate of Polymerization

The rate of polymerization can be calculated from the slope of a conversion-time curve. A typical formula used to compute the slope from two points is given by:

$$y_n' = \frac{y_{n+1} - y_n}{x_{n+1} - x_n} \tag{2.6}$$

This formula can be obtained from a Taylor's expansion of y_{n+1} from y_n:

$$y_{n+1} = y_n + y_n'(\Delta x) + \frac{1}{2!}y_n''(\Delta x)^2 + \frac{1}{3!}y_n'''(\Delta x)^3 + \ldots \quad (2.7)$$

by neglecting all the terms with the order higher than first order. An equally simple but more accurate formula is to compute the slope from three points. A Taylor expansion of the point with the coordinate of (y_{n-1}, x_{n-1}) from (y_n, x_n) can be expressed as:

$$y_{n-1} = y_n + y_n'(-\Delta x) + \frac{1}{2!}y_n''(-\Delta x)^2 + \frac{1}{3!}y_n'''(-\Delta x)^3 + \ldots \quad (2.8)$$

Subtracting Equation (2.8) from Equation (2.7) to obtain:

$$y_{n+1} - y_{n-1} = 2y_n'(\Delta x) + 0y_n''(\Delta x)^2 + \frac{2}{3!}y_n'''(\Delta x)^3 + \ldots \quad (2.9)$$

A three-point formula is obtained by neglecting all the terms with order higher than second order:

$$y_n' = \frac{y_{n+1} - y_{n-1}}{2(\Delta x)} \quad (2.10)$$

Equation (2.10) is more accurate than Equation (2.6) because it neglects the error terms higher than the second degree which is much smaller than the error terms of higher than first degree. This can be seen from Figures 2-5 and 2-6. The calculated data are more scattered using the two-point formula.

2.3 Results and Discussion

The conditions for all experiments are described in Table 2-2. The variables in these experiments are the concentration of sodium lauryl sulfate, the type and amount of co-surfactant, the aging time of the emulsion and the device used for homogenization.

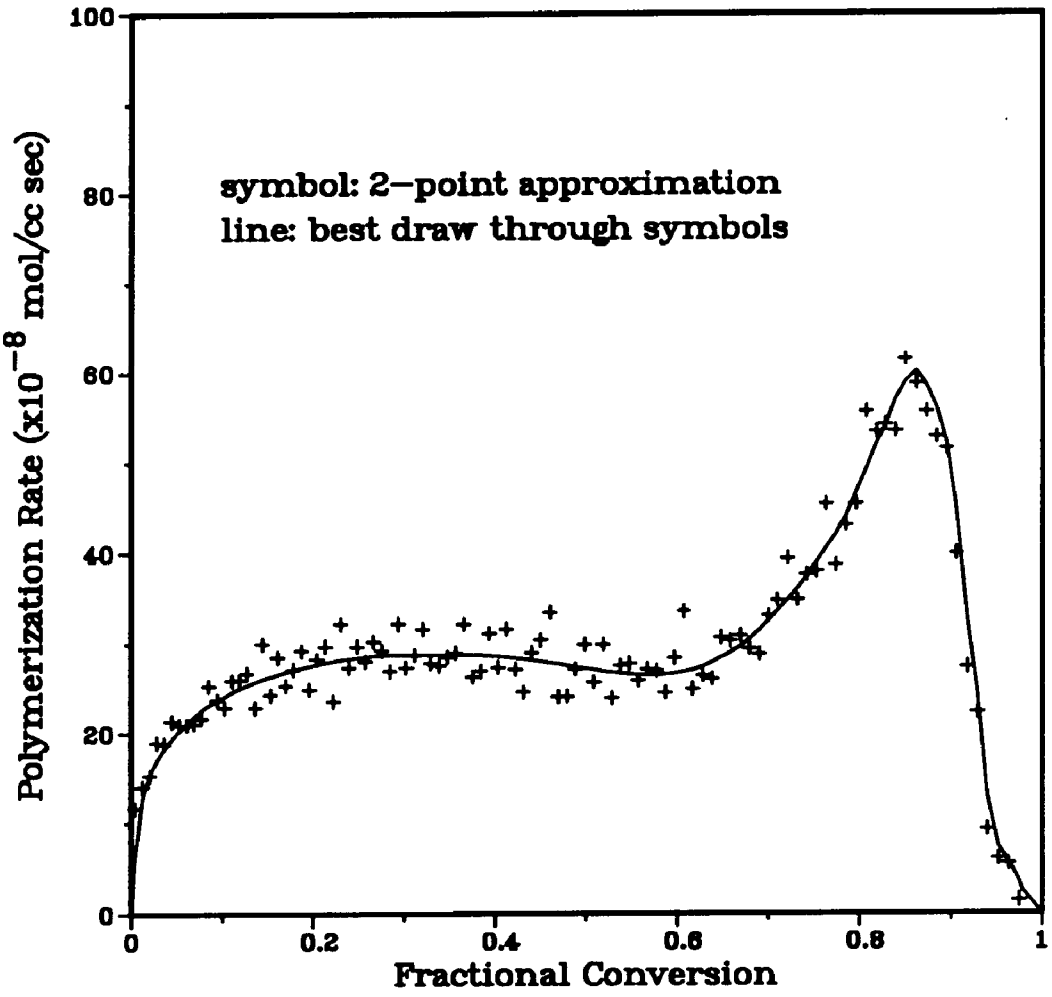

Figure 2-5: Polymerization rate versus conversion curve for miniemulsion polymerization of styrene, run M10, computed using the two-point formula of Equation (2.6).

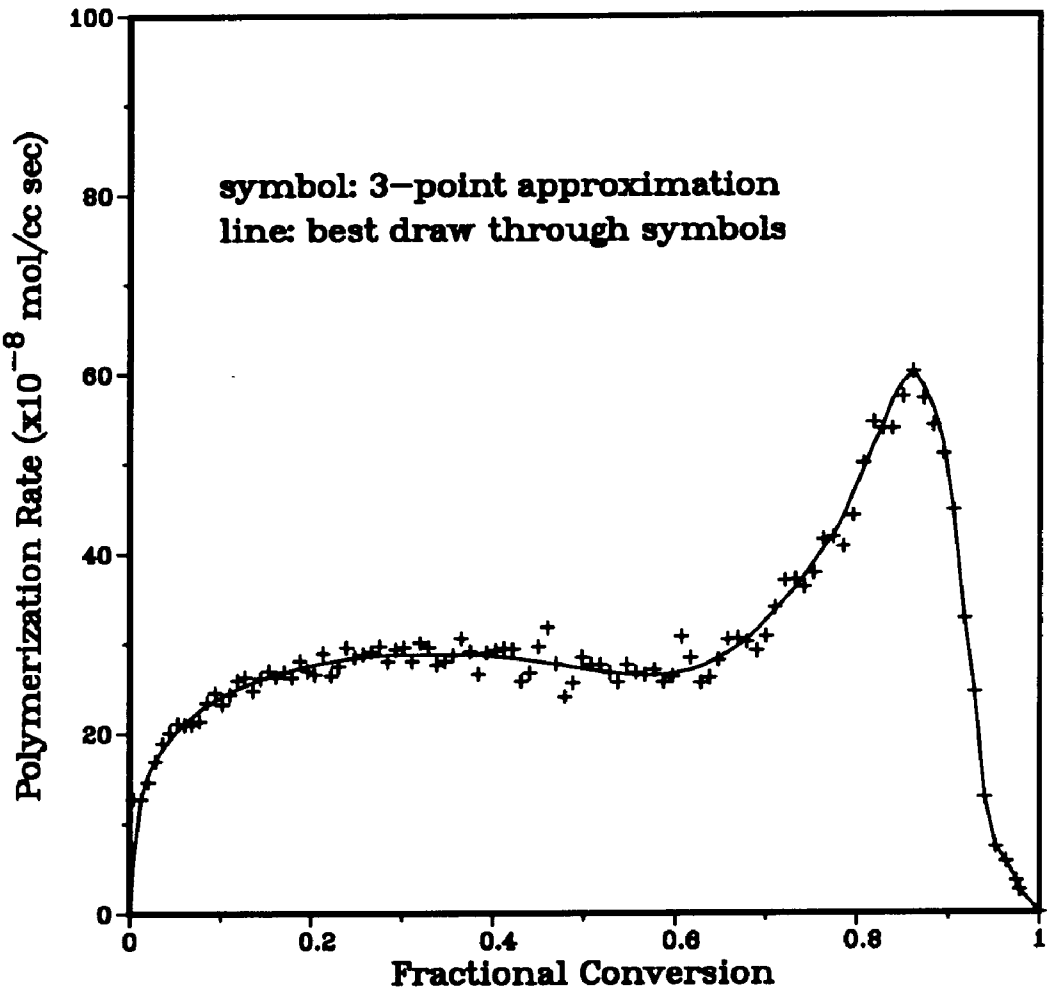

Figure 2-6: Polymerization rate versus conversion curve for miniemulsion polymerization of styrene, run M10, computed using the three-point formula of Equation (2.10).

Table 2-2: Conditions of Polymerization of Emulsions Prepared by Different Methods.

Run	Description
C2	"Conventional", Microfluidizer, 10 mM SLS
C6	"Conventional", Microfluidizer, 5 mM SLS, two hours unstirred at 25°C before initiation
C7	"Conventional", Microfluidizer, 5 mM SLS, one hour with stirring at 70°C before initiation
C8	"Conventional", Microfluidizer, 5 mM SLS
M6	Microfluidizer, 10 mM SLS, 30 mM CA, monomer added to SLS-CA solution at 65°C
M10	Microfluidizer, 5 mM SLS, 15 mM CA, monomer added to SLS-CA solution at 65°C
M11	Microfluidizer, 5 mM SLS, 15 mM CA, monomer added to SLS-CA solution at 25°C
M12	Microfluidizer, 5 mM SLS, 20 mM HD
M13	Sonifier, 5 mM SLS, 20 mM HD
M14	Microfluidizer, 5 mM SLS, 20 mM HD, one hour unstirred at 25°C before initiation
M15	Microfluidizer, 5 mM SLS, 20 mM HD, four hours unstirred at 25°C before initiation
M16	Microfluidizer, 5 mM SLS, 15 mM CA, one hour unstirred at 25°C before initiation
M17	Microfluidizer, 5 mM SLS, 15 mM CA, four hours unstirred at 25°C before initiation
M19	Microfluidizer, 5 mM SLS, 15 mM CA, 20 mM HD
M21	Omni Mixer, 5 mM SLS, 20 mM HD

2.3.1 Effect of Cetyl Alcohol and Sodium Lauryl Sulfate

In order to carry out a "conventional" emulsion polymerization in a dilatometer, the emulsion was first homogenized with the Microfluidizer to avoid monomer separation in the capillary during the polymerization. However, true conventional emulsion polymerization (i.e., without homogenization) were carried out in a reaction calorimeter (RC1, Mettler Instrument Corp.) for comparison and the results are shown on Figure 2-7. The dotted curves are the results obtained without homogenization (i.e., in calorimeter) whereas the solid curves are those from homogenization of the emulsion. The only other variable is the concentration of sodium lauryl sulfate. The results show that above the CMC (7.4 mM, as determined by measuring the conductivity of SLS solutions at different concentrations as shown in Figure 2-8), the run with no homogenization reacted slightly faster than the one with homogenization; but below the CMC, the run with no homogenization reacted slower. This is because above the CMC, the run with no homogenization had more nucleation sites (presumably micelles) as compared to the one with homogenization. Based on the final particle size distribution of the latter (Figure 2-10), it seems plausible that two mechanisms of nucleations were in competition in this system, namely, micellar and droplet. However, below the CMC nucleation is slow in the non-homogenized run (homogeneous nucleation) while it is considerably faster when fine droplets are present as produced by the Microfluidizer.

Delgado[19] found that for the same surfactant concentration, the overall rate of polymerization of a conventional emulsion system is usually faster than that of a miniemulsion system. Most of these comparisons were carried out with a total concentration of surfactant above its critical micelle concentration (cmc). The monomer swollen micelles are an order of magnitude smaller than the miniemulsion droplets which means that the number of monomer swollen

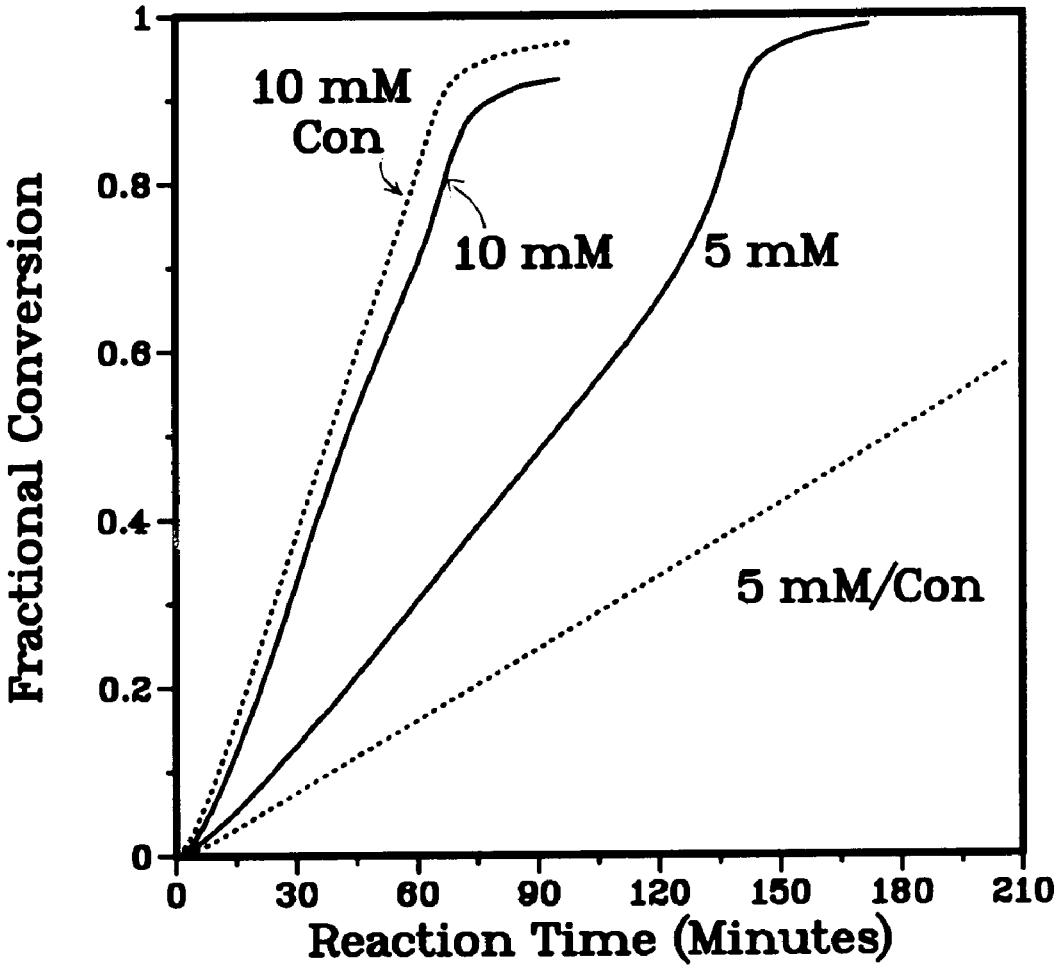

Figure 2-7: Conversion versus time curves for conventional polymerizations of styrene at 5 mM and 10 mM SLS; dotted lines: no homogenization of the emulsion before polymerization in the RC1 reactor, and solid lines: homogenization of the emulsion with the Microfluidizer before polymerization in a dilatometer.

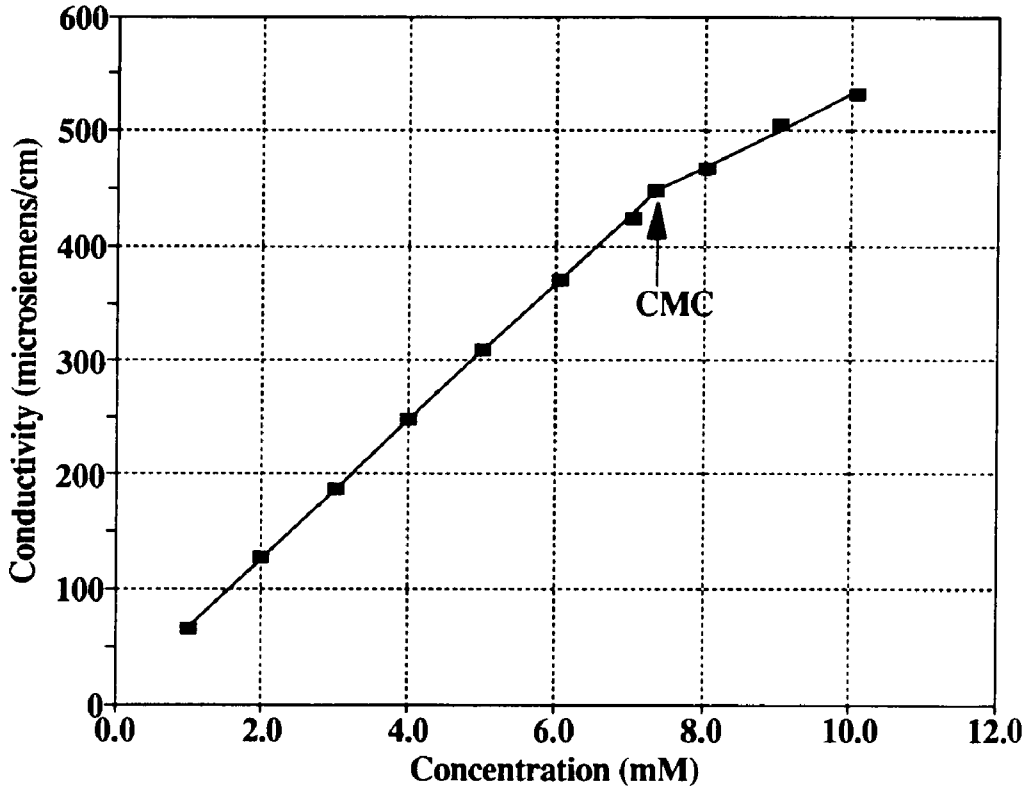

Figure 2-8: Conductivity of aqueous solution of sodium lauryl sulfate as a function of concentration (room temperature).

micelles are much larger than the number of monomer droplets. Thus more particles are nucleated in the conventional system than in the miniemulsion system (if micelles and droplets have similar radical capture efficiency). However, when the concentration of surfactant is below the cmc, the rate of polymerization is greater for the miniemulsion system because there are no monomer swollen micelles present in the conventional emulsion system. This phenomenon can be seen from the results given in Figure 2-9 in which the variables studied were the concentrations of sodium lauryl sulfate and cetyl alcohol. Curves C2 and M6 were obtained using recipes containing 10 mM sodium lauryl sulfate while curves C8 and M10 contained 5 mM. The recipe used to obtain the solid curves (C2 and C8) did not contain any co-surfactant whereas those represented by the dashed curves contained cetyl alcohol. All these emulsions were subjected to high shear with the Microfluidizer prior to polymerization.

The results in Figure 2-9 show that for emulsions prepared with 10 mM sodium lauryl sulfate, the polymerization kinetics of the "conventional" case (C2) are faster than those of the miniemulsion case (M6). However, for those prepared with 5 mM sodium lauryl sulfate, the polymerization kinetics of the "conventional" case (C8) are slower than that of the miniemulsion case (M10). This is likely because above the CMC, the conventional case may have two competing nucleation mechanisms, namely micellar and droplet, thus results in more nucleation sites than the miniemulsion case in which droplet nucleation is the only important mechanism. Figure 2-10 show the corresponding particle size distributions which also suggests the competing nucleation mechanisms existing in run C2 (run C2 has a significant population of large particles beside the main population of about 100 nm in diameter). However, monomer droplet nucleation is predominant below the CMC and the miniemulsion case has faster

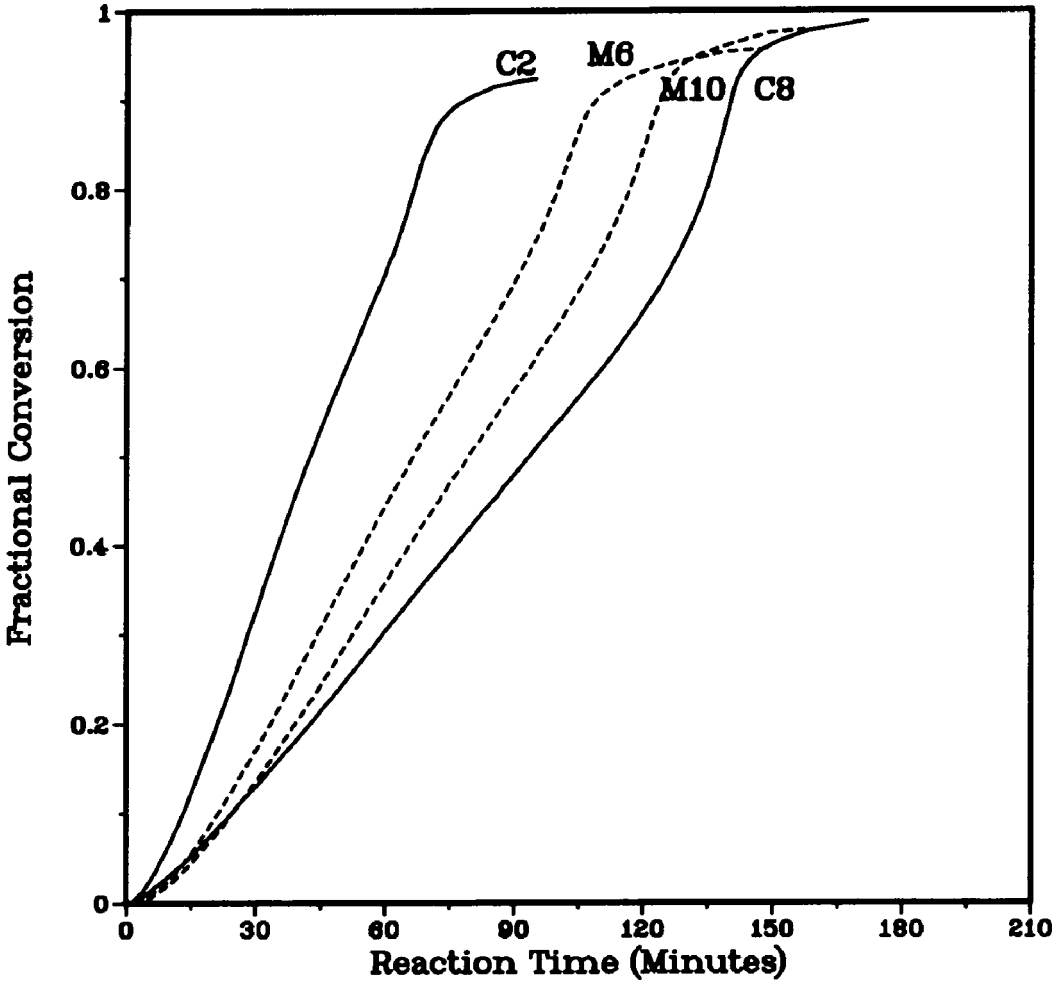

Figure 2-9: Conversion versus time curves for conventional polymerization of styrene: runs C2 (Microfluidizer, 10 mM SLS), C8 (Microfluidizer, 5 mM SLS); and miniemulsion polymerization of styrene: M6 (Microfluidizer, 10 mM SLS/30 mM CA), and M10 (Microfluidizer, 5 mM SLS/15 mM CA).

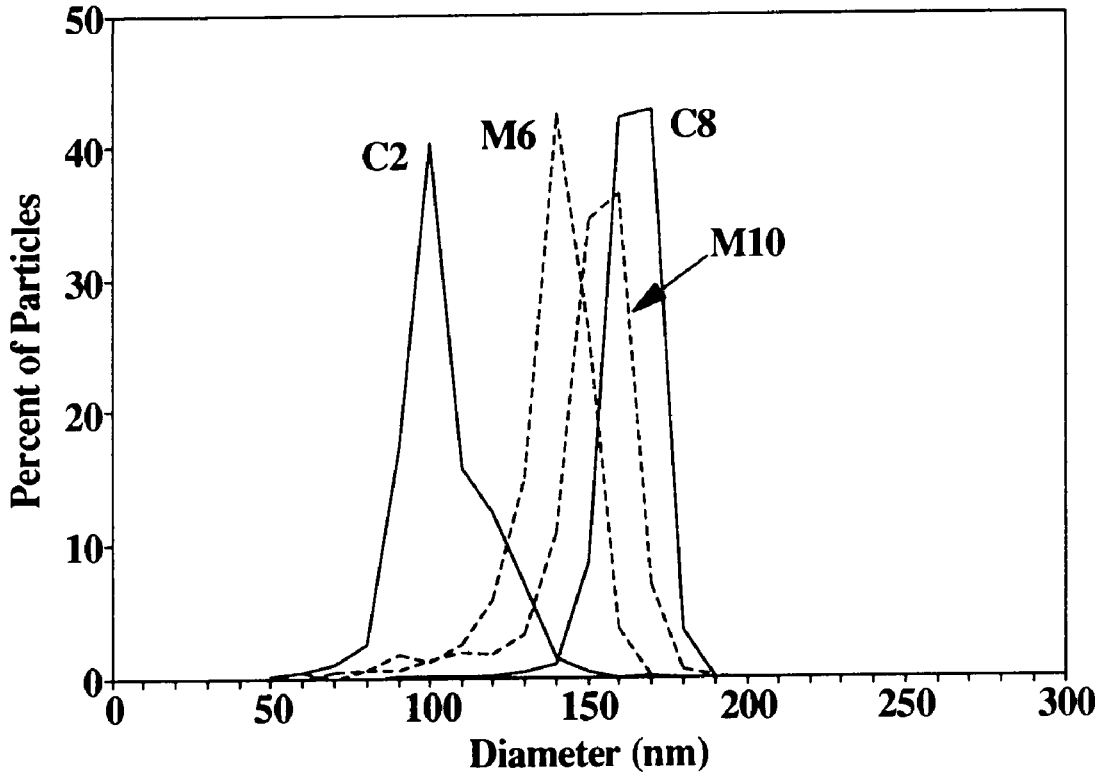

Figure 2-10: Particle size distributions for conventional emulsion polymerization of styrene: runs C2 (Microfluidizer, 10 mM SLS), C8 (Microfluidizer, 5 mM SLS); and miniemulsion polymerization of styrene: M6 (Microfluidizer, 10 mM SLS/30 mM CA), and M10 (Microfluidizer, 5 mM SLS/15 mM CA).

Table 2-3: Volume Average Diameter, Coefficient of Variation and Final Particle Concentration Obtained by Polymerization of Emulsions Prepared by Different Methods.

Run	D_v(nm)	S_n/D_n	N_p 10^{13}/cc
C2	115	0.13	26.8
C6	169	0.06	8.75
C7	168	0.05	9.34
C8	160	0.08	10.8
M6	134	0.12	18.4
M10	147	0.11	13.4
M11	168	0.14	9.36
M12	145	0.06	15.7
M13	271	0.18	2.5
M16	163	0.10	11.0
M17	163	0.10	11.0
M19	143	0.06	16.4
M21	344	0.30	1.1

kinetics due to higher number of droplets which resulted from more stable droplets. These results also show that the polymerization rates of miniemulsions (M6 and M10), prepared with varying surfactant (above and below the CMC) and co-surfactant levels, do not differ as much as those (C2 and C8) prepared without co-surfactant; this phenomena may not be true if the comparisons were carried out on either side of the CMC. The final particle numbers (sizes) are consistent with the kinetic results (Table 2-3); the faster polymerizations produced greater numbers of particles.

From the conversion-time data of Figure 2-9, the polymerization rates versus conversion were obtained as shown on Figure 2-11. These results

indicate that the polymerization rates of all the runs exhibit similar behavior with respect to conversion; the polymerization rates increase to a maximum at about 30% conversion followed by a decrease. No significant constant rate period is observed. This phenomenon has been reported previously[18] and would indicate that when nucleation is predominantly in the monomer droplets, it continues until all droplets disappear (by either nucleation or consumption by growing particles), thus no constant rate period is seen. This postulate is supported by results found in a study of semicontinuous miniemulsion polymerizations by Tang et al.[29], which showed that particle nucleation takes place whenever miniemulsion droplets are present in the reaction system. The polymerization rate continues to decrease until about 60% conversion when the gel effect, which brings about a decrease in the rate of termination inside a particle, causes the rate to increase. The polymerization rate continues to increase to about 85% conversion when the particles reach their glass transition point[30] bringing about a reduction in the propagation rate and thus reducing the polymerization rate.

2.3.2 Effect of the Degree of Aging of the Emulsion

Another set of experiments was carried out to evaluate the effect of emulsion stability on the polymerization kinetics. The results are shown in Figure 2-12. The emulsions used in these experiments were prepared using the Microfluidizer but without co-surfactant and they were polymerized after aging under varying conditions. These emulsions were relatively unstable without the co-surfactant, the droplets becoming larger with time due to their instability against diffusion degradation and instability against coagulation when the size difference between them are large. The emulsion in run C8 was initiated just after degassing (it was about 30 minutes from finishing homogenization to

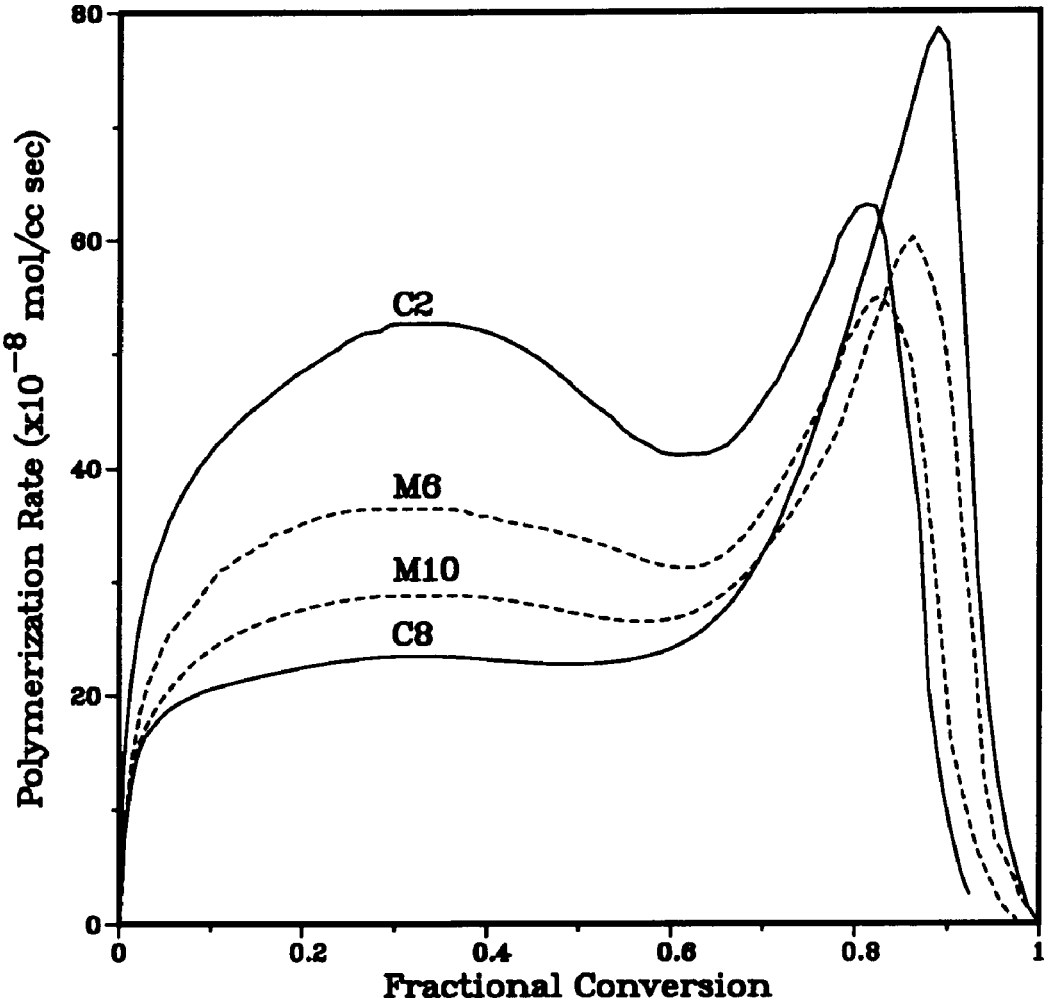

Figure 2-11: Polymerization rate versus conversion curves for conventional emulsion polymerization of styrene: runs C2 (Microfluidizer, 10 mM SLS), C8 (Microfluidizer, 5 mM SLS); and miniemulsion polymerization of styrene: M6 (Microfluidizer, 10 mM SLS/30 mM CA), and M10 (Microfluidizer, 5 mM SLS/15 mM CA).

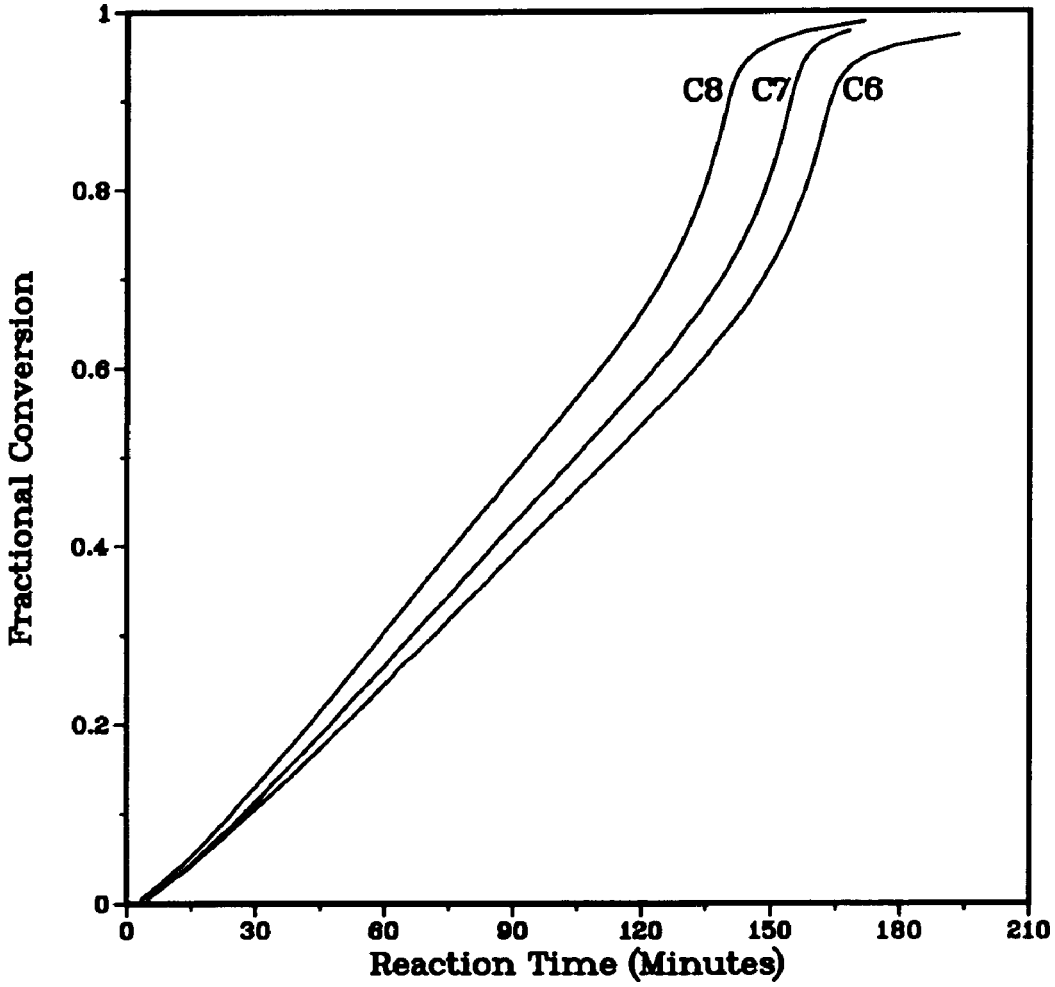

Figure 2-12: Conversion versus time curves for conventional emulsion polymerization of styrene: runs C8 (Microfluidizer, 5 mM SLS and no aging time), C7 (Microfluidizer, 5 mM SLS and one hour at 70°C) and C6 (Microfluidizer, 5 mM SLS and two hours at 25°C prior to polymerization).

injecting the initiator), whereas C7 was stirred at 70°C for one hour and C6 was left unstirred for two hours at room temperature before initiation. The results from Figure 2-12 show that the polymerization rate decreased with increased aging of the emulsion. These results are also consistent with the final particle numbers (Table 2-3).

A similar study was also carried out with the incorporation of cetyl alcohol and the results are shown in Figure 2-13. Both runs were prepared with 5 mM SLS, 15 mM cetyl alcohol and the Microfluidizer. The miniemulsion in run M16 was initiated after one hour unstirred at room temperature and the miniemulsion in run M17 was initiated after four hours unstirred at room temperature. The results show that the conversion-time behavior is identical between one to four hours of aging. This indicates the monomer droplets are not changing between one to four hours of aging and that cetyl alcohol increases the stability of the monomer droplets. These results are also consistent with the final particle number (Table 2-3). However, Miller et al.[31] have monitored the size of monomer droplets with time using the capillary hydrodynamic fractionation method and have shown that when a miniemulsion was prepared with cetyl alcohol and the sonifier, the droplet sizes increased with time up to about one and a half hours and leveled off after that. This is likely because the sonifier produces a wide distribution of droplet sizes and the monomer from the small droplets diffuses to the larger ones until the concentration of cetyl alcohol within the small droplets is high enough to substantially retard the diffusion of monomer and establish a pseudo-equilibrium state.

Another study was also carried out with hexadecane and the results are shown in Figure 2-14. Both runs were prepared with 5 mM SLS, 20 mM hexadecane and the Microfluidizer. The miniemulsion in run M12 was initiated

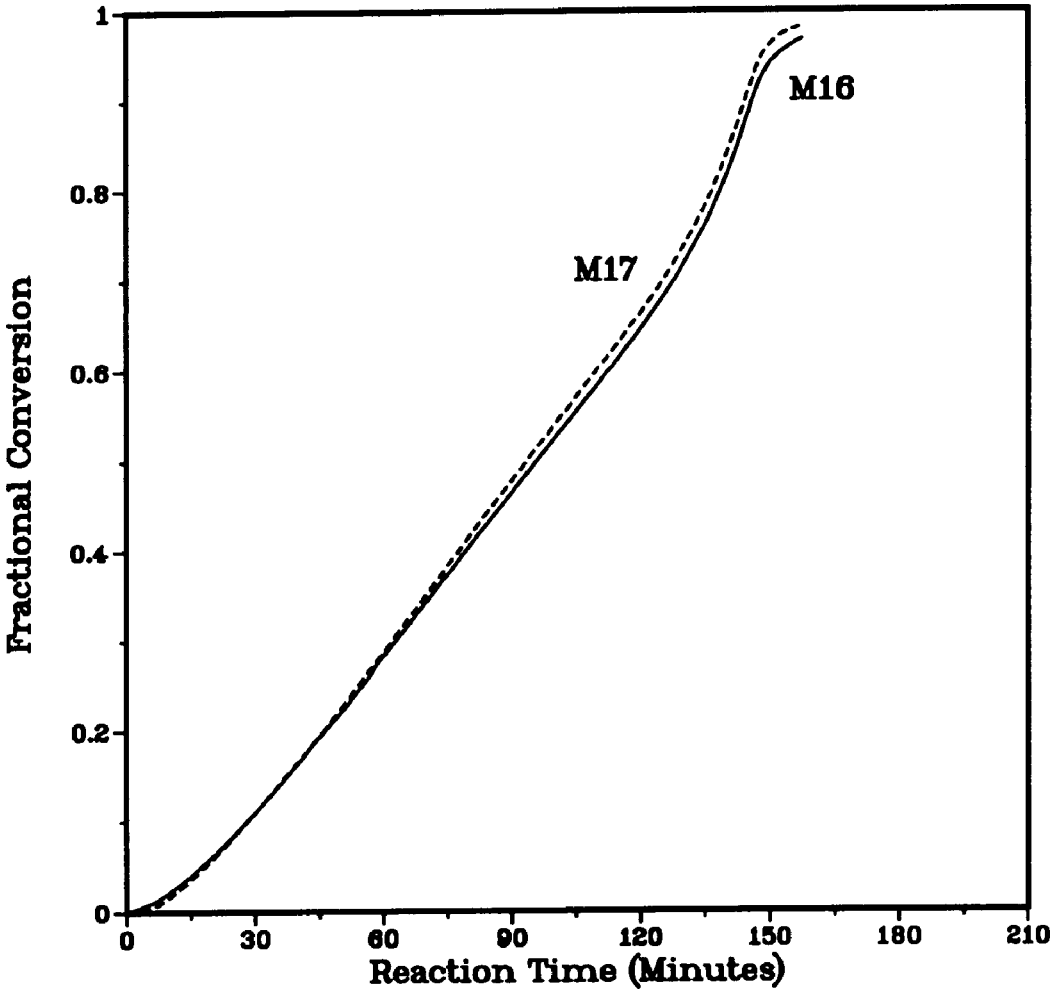

Figure 2-13: Conversion versus time curves for miniemulsion polymerization of styrene: runs M16 (Microfluidizer, 5 mM SLS, 15 mM CA and one hour of aging time), M17 (Microfluidizer, 5 mM SLS, 15 mM CA and four hours of aging time prior to polymerization).

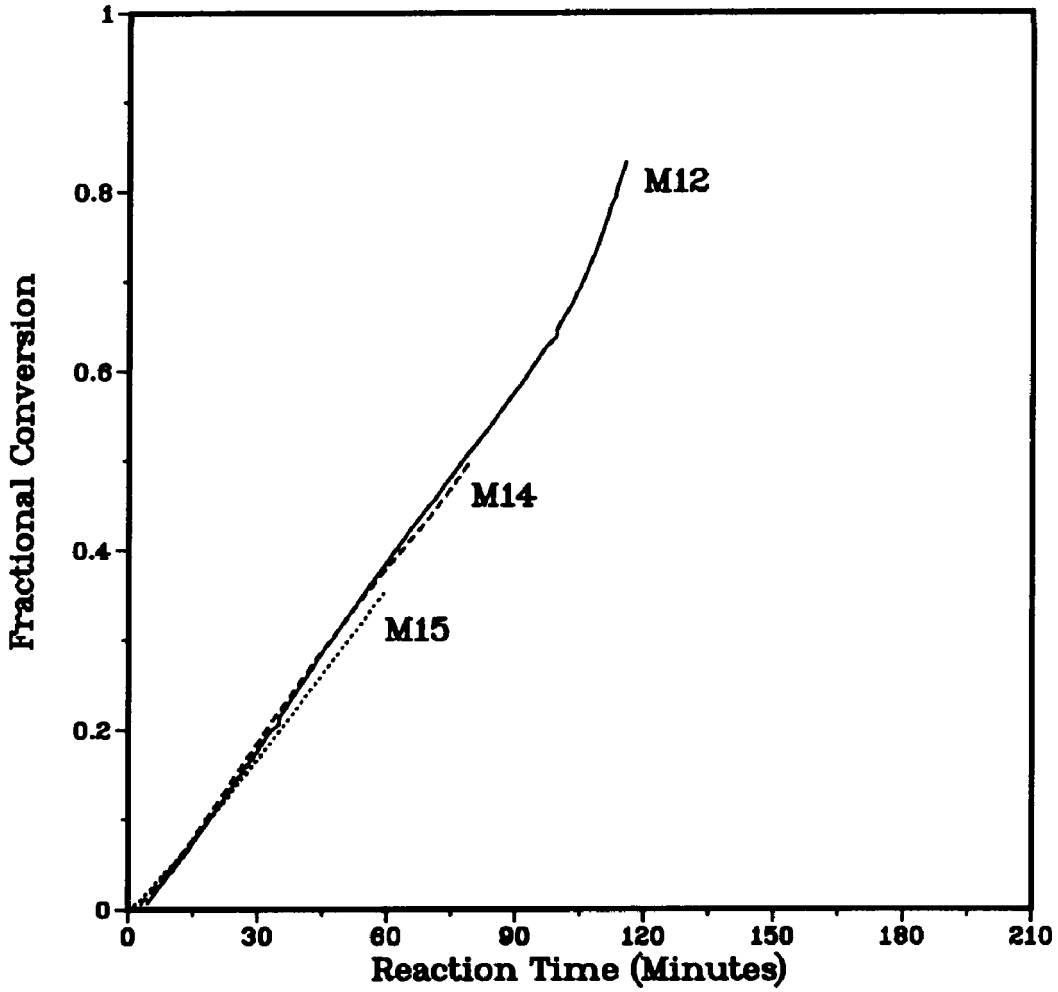

Figure 2-14: Conversion versus time curves for miniemulsion polymerization of styrene: runs M12 (Microfluidizer, 5 mM SLS, 20 mM HD and no aging time), M14 (Microfluidizer, 5 mM SLS, 20 mM HD and one hour of aging time) and M15 (Microfluidizer, 5 mM SLS, 20 mM HD and four hours of aging prior to polymerization).

right after degassing, the miniemulsion in run M14 was initiated after one hour unstirred at room temperature and the miniemulsion in run M15 was initiated after four hours unstirred at room temperature. The results show that the conversion-time behavior is similar between zero and four hours of aging. This indicates that hexadecane increases the stability of the monomer droplets.

2.3.3 Effect of Temperature of Preparation of the Emulsion

Different methods of preparing miniemulsions with the same recipe can also result in different kinetics and final particle concentrations. This can be seen from the results in Figure 2-15 in which miniemulsions were prepared using cetyl alcohol (see Figure 2-2) with the only difference being that M10 was prepared without cooling the gel phase. The styrene was added to the gel solution (sodium lauryl sulfate, cetyl alcohol and water) at 65°C before shearing with the Microfluidizer, whereas in run M11 the gel solution was cooled to room temperature and sonified to break up the gel phase before adding the styrene and followed by homogenization. The kinetics of run M10 were significantly faster than that of run M11. This indicates that the emulsion droplets of run M10 were smaller than those of run M11. This was likely because the size of the gel aggregate of the emulsion prepared at the higher temperature (M10) was smaller than that at room temperature (M11) which in turn resulted in lower viscosity allowing more effective homogenization. The final particle numbers are consistent with the kinetic results (Table 2-3). The corresponding particle size distributions (Figure 2-16) exhibit similar shapes and show a significant amount of small particles. This indicates that some particle nucleation occurs continuously during most of the polymerizations.

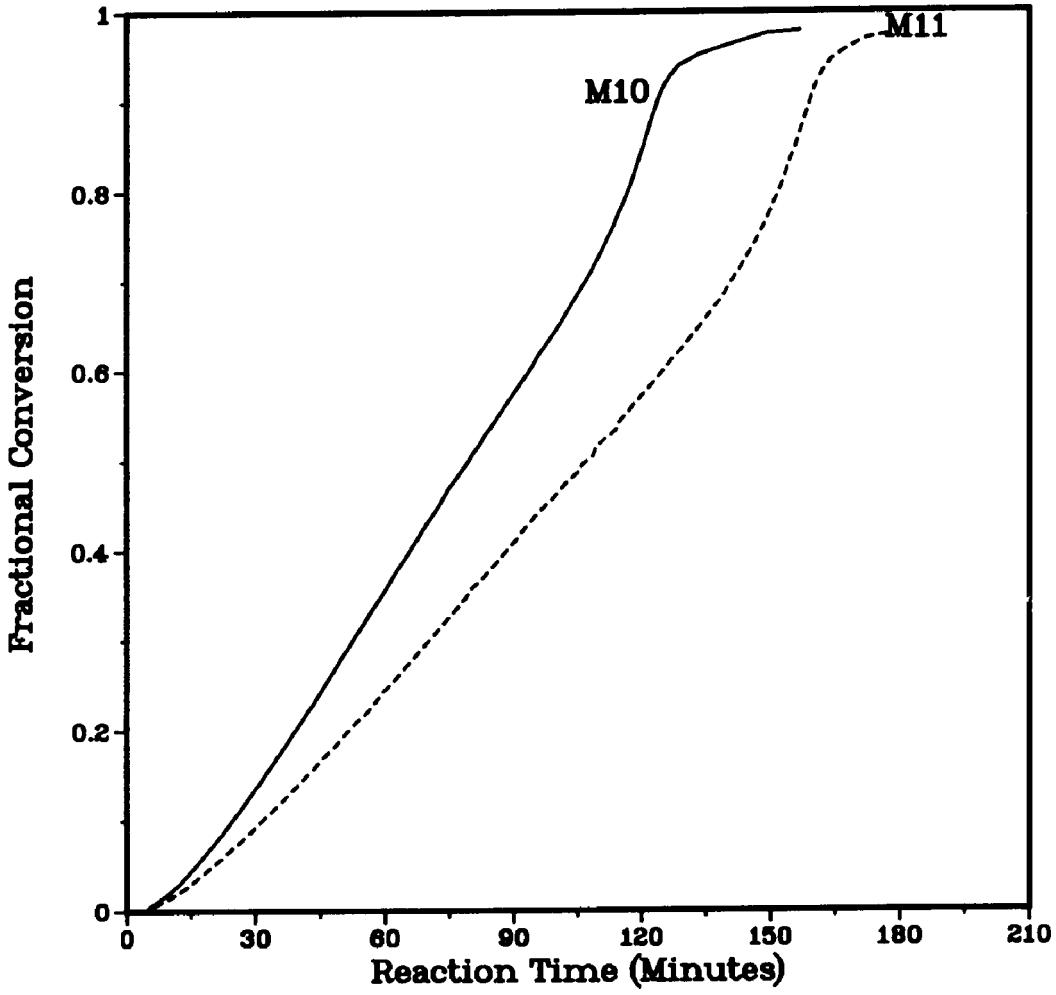

Figure 2-15: Conversion versus time curves for miniemulsion polymerization of styrene: runs M10 (Microfluidizer, 5 mM SLS/15 mM CA, styrene added to the gel phase at 65°C) and M11 (Microfluidizer, 5 mM SLS/15 mM CA, styrene added to the gel phase at 25°C).

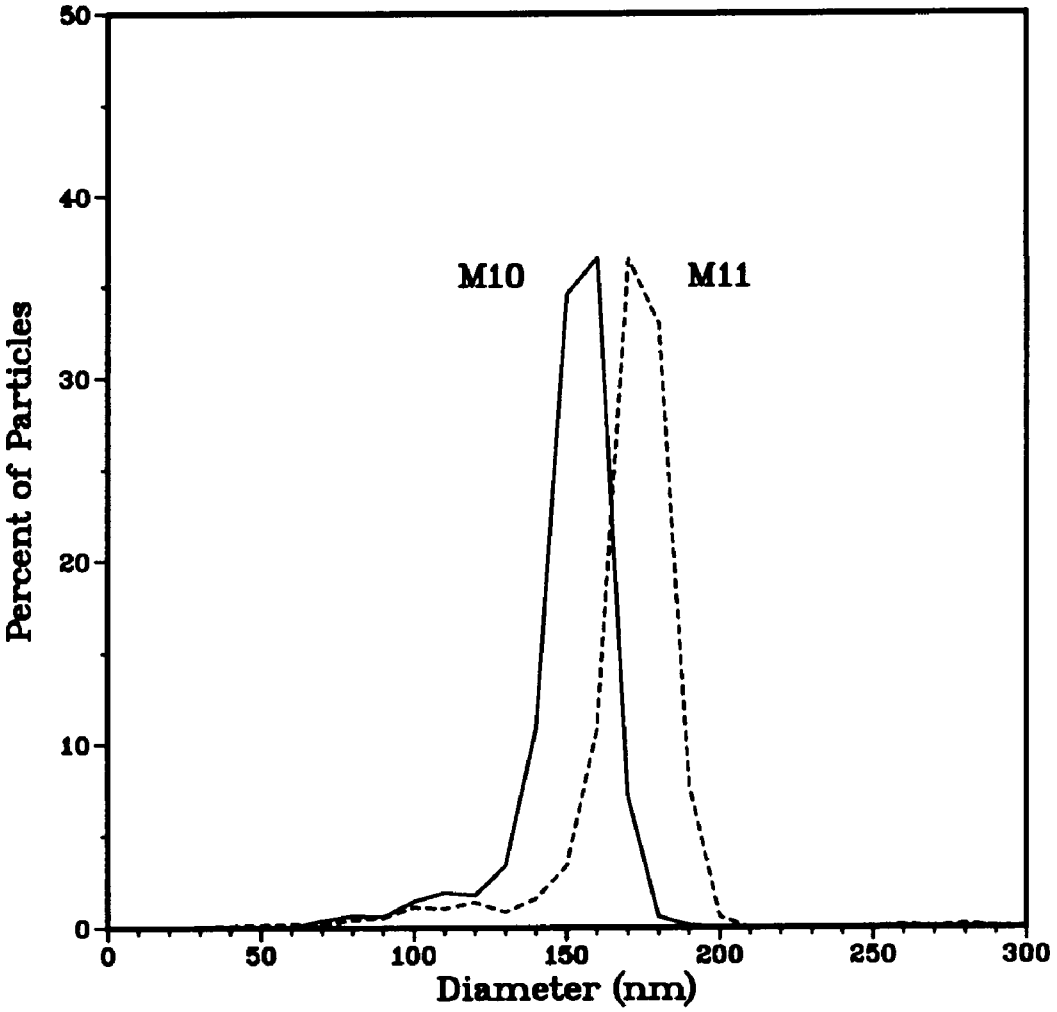

Figure 2-16: Particle size distributions for miniemulsion polymerization of styrene: runs M10 (Microfluidizer, 5 mM SLS/15 mM CA, styrene added to the gel phase at 65°C) and M11 (Microfluidizer, 5 mM SLS/15 mM CA, styrene added to the gel phase at 25°C).

2.3.4 Effect of Means of Homogenization

Another study was carried out to evaluate the effect of the type of homogenization on the polymerization kinetics and final particle size distribution. The results are shown in Figure 2-17 in which the only difference is that the emulsion in run M12 was homogenized using the Microfluidizer, run M13 by the sonifier and run M21 by the Omni mixer; all contained 5 mM sodium lauryl sulfate and 20 mM hexadecane. The polymerization rate in run M12 was much faster than that of run M13 which in turn was faster than in run M21. These results also agree with the final particle numbers (Table 2-3); the faster polymerization rate produces a larger number of particles. Figure 2-18 shows that the PSD of run M12 is narrower than that of run M13 and run M21 (which has a considerable amount of large particles) which is consistent with the claim that the Microfluidizer provides a greater and more uniform shear than the sonifier and the Omni mixer.

2.3.5 Effect of Co-Surfactants

The combination of cetyl alcohol and hexadecane was also used to prepare a miniemulsion. Water, sodium bicarbonate, sodium lauryl sulfate and cetyl alcohol were mixed at 65°C for two hours, cooled to room temperature to form the gel phase, and sonified to break up the gel phase. Hexadecane was added to styrene and this solution was mixed with the gel solution for 10 minutes before shearing with the Microfluidizer. The resulting conversion versus reaction time is shown in Figure 2-19 which indicates that the run using both cetyl alcohol and hexadecane had a faster reaction rate than those having only one type of surfactant. This also suggests that the ratio of SLS/CA of 1:3 and SLS/HD of 1:4 may not yet be the optimum ratios. This may be because these ratios were obtained by measuring the concentration of surfactant in the aqueous phase and

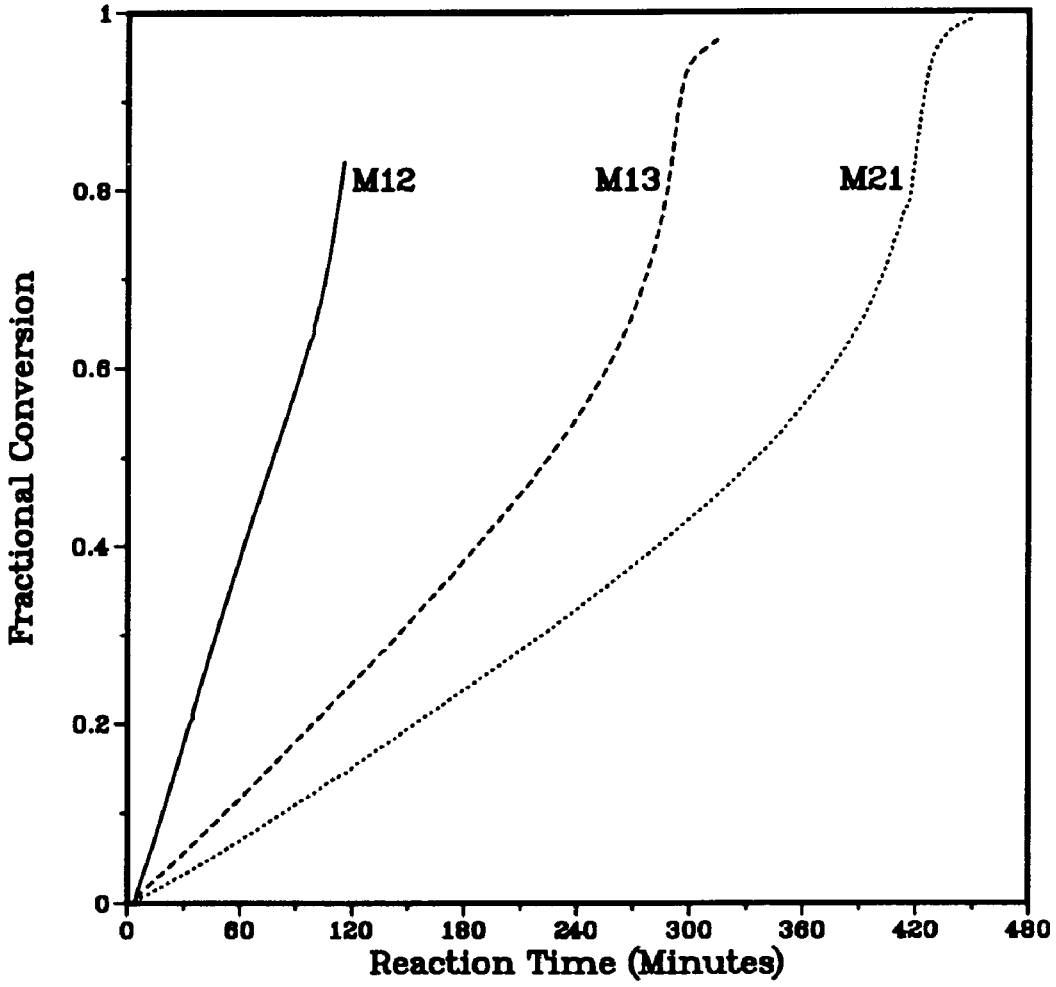

Figure 2-17: Conversion versus time curve for miniemulsion polymerization of styrene: runs M12 (homogenized with the microfluidizer), M13 (homogenized with the sonifier) and M21 (homogenized with the Omni mixer); all contain 5 mM SLS/20 mM HD.

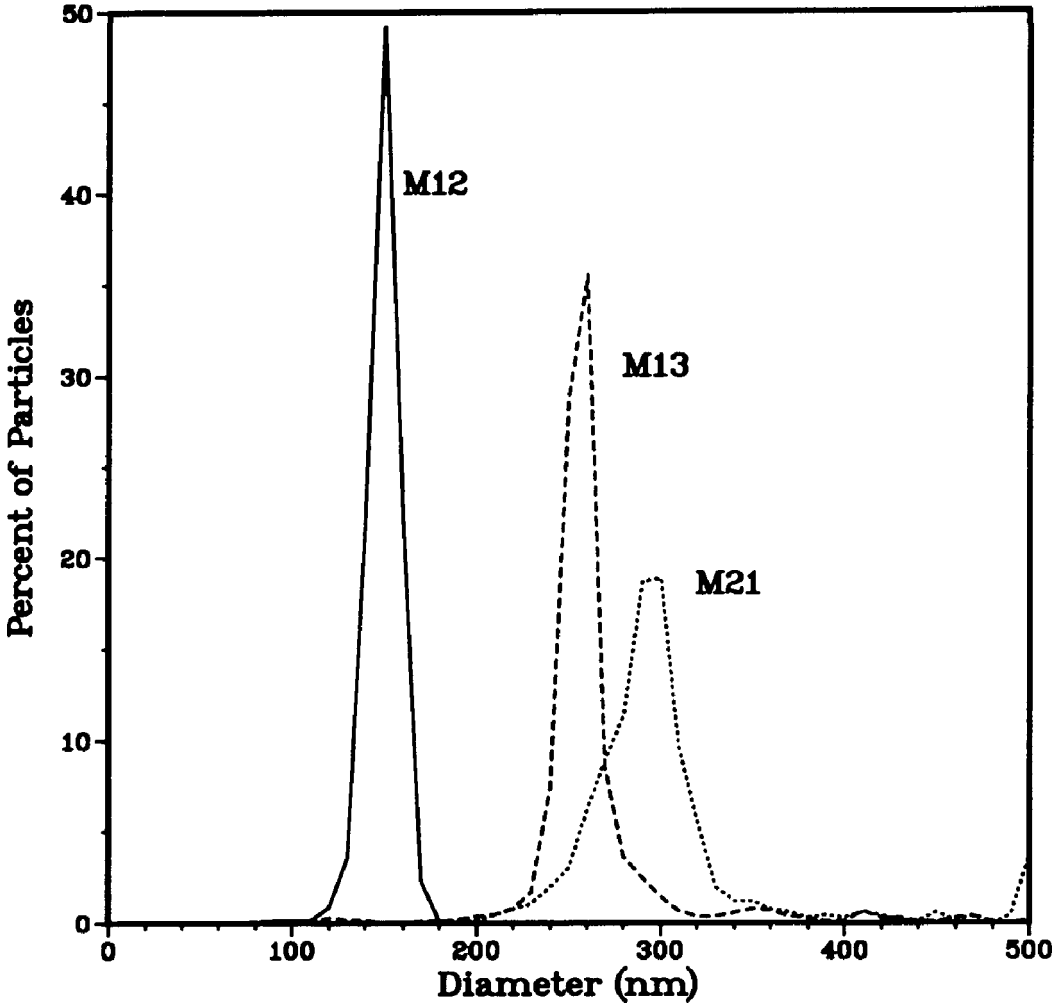

Figure 2-18: Particle size distributions for miniemulsion polymerization of styrene: runs M12 (Microfluidizer), M13 (sonifier) and M21 (Omni mixer); all contain 5 mM SLS/20 mM HD.

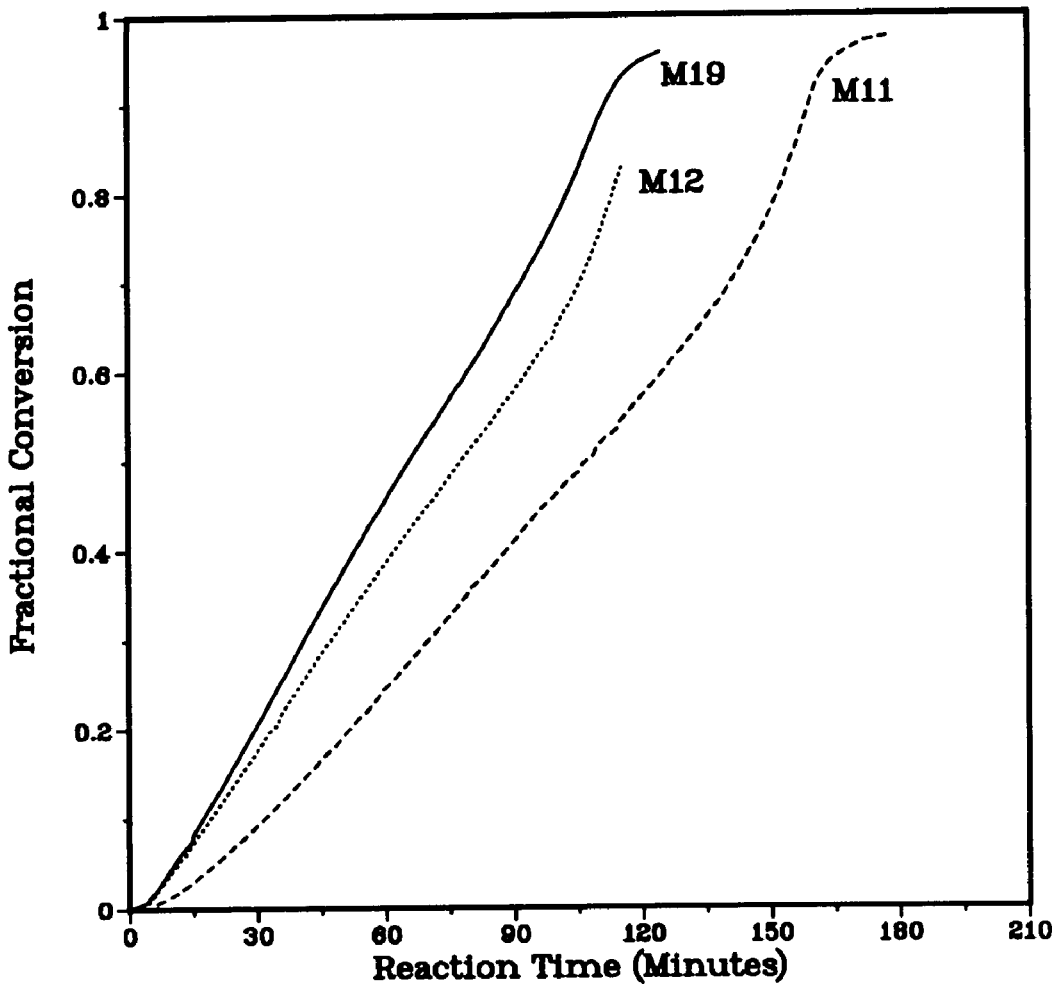

Figure 2-19: Conversion versus time curve for miniemulsion polymerization of styrene: runs M11 (5 mM SLS/15 mM CA), M12 (5 mM SLS/20 mM HD) and M19 (5 mM SLS, 15 mM CA and 20 mM HD); all homogenized with the Microfluidizer.

correlated the results to the droplet size[18, 27, 20]. A better answer should be obtained by measuring the droplet size directly, such as by capillary hydrodynamic fractionation.

2.3.6 Effect of Cetyl Alcohol on the Polymerization Kinetics

Further information on the polymerization kinetics may be obtained from the combined results illustrated in Figure 2-20. At conversions higher than about 30% all runs exhibit similar kinetics, but at lower conversions some differences can be noted. This region is magnified in Figure 2-21. The initial polymerization rates of the miniemulsions prepared with cetyl alcohol (M10 and M11) are slower than those prepared with hexadecane (M12) and those without co-surfactant (C6, C7 and C8). However, the rate in Run M10 increases and surpasses those of the "conventional" cases. The corresponding rate of polymerizations versus conversion are shown in Figure 2-22 which also exhibits the initial slow rate of the miniemulsions prepared with cetyl alcohol. This may indicate that particle nucleation is slowed by the presence of cetyl alcohol on the surface of the monomer droplets.

2.4 Summary

A comparative study was carried out to evaluate the effect of the variation in parameters important to the preparation of styrene emulsions on the polymerization kinetics and the resulting particle size distributions. The variables studied were the type of co-surfactant and the means of homogenization. The results show that when the concentration of SLS is above its cmc, the overall rate of the conventional polymerization is faster than that of the miniemulsion system. However, it is the opposite when the concentration of SLS is below its cmc. When the emulsion without a co-surfactant is allowed to

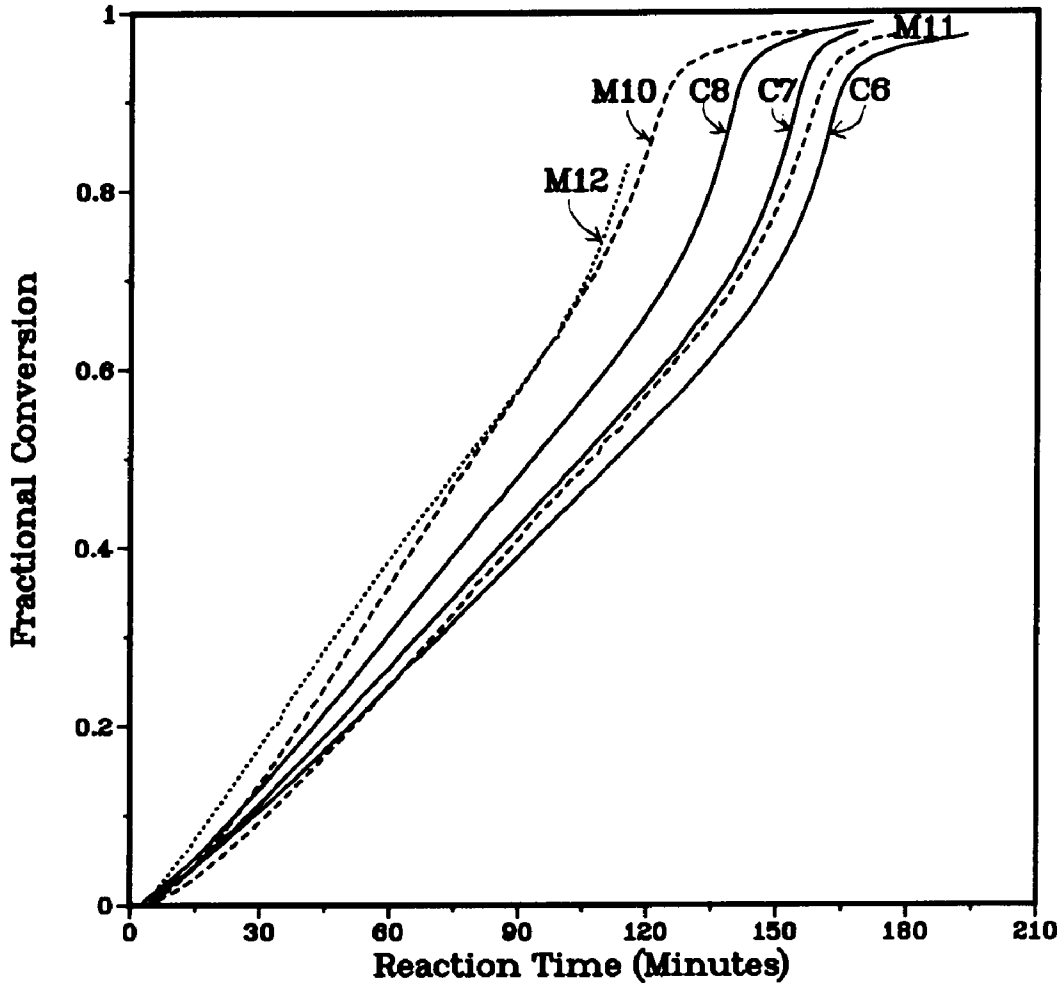

Figure 2-20: Conversion versus time curves for emulsion polymerization of styrene: runs C6, C7 and C8, "conventional" cases; M10 and M11, miniemulsions with cetyl alcohol; and M12, miniemulsion with hexadecane.

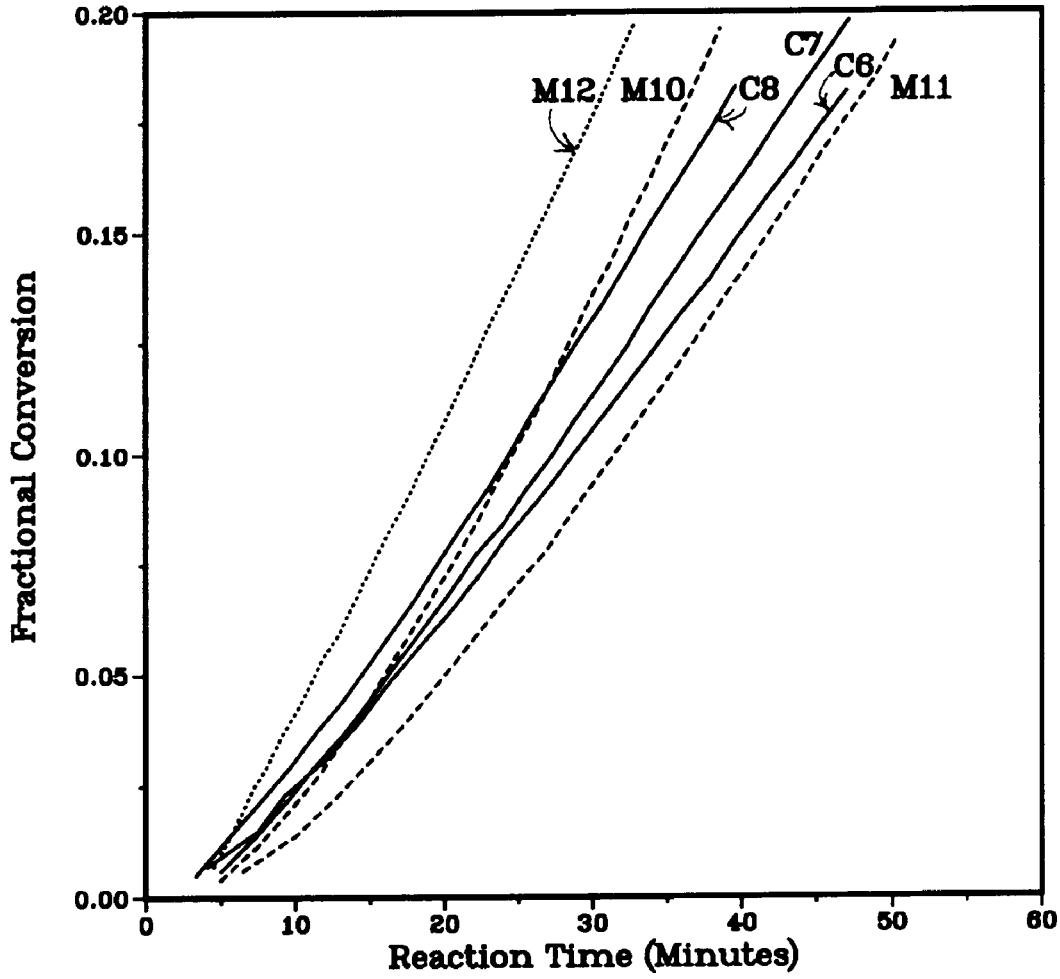

Figure 2-21: Conversion versus time curves magnified for emulsion polymerization of styrene: runs C6, C7 and C8, "conventional" cases; M10 and M11, miniemulsions with cetyl alcohol; and M12, miniemulsion with hexadecane.

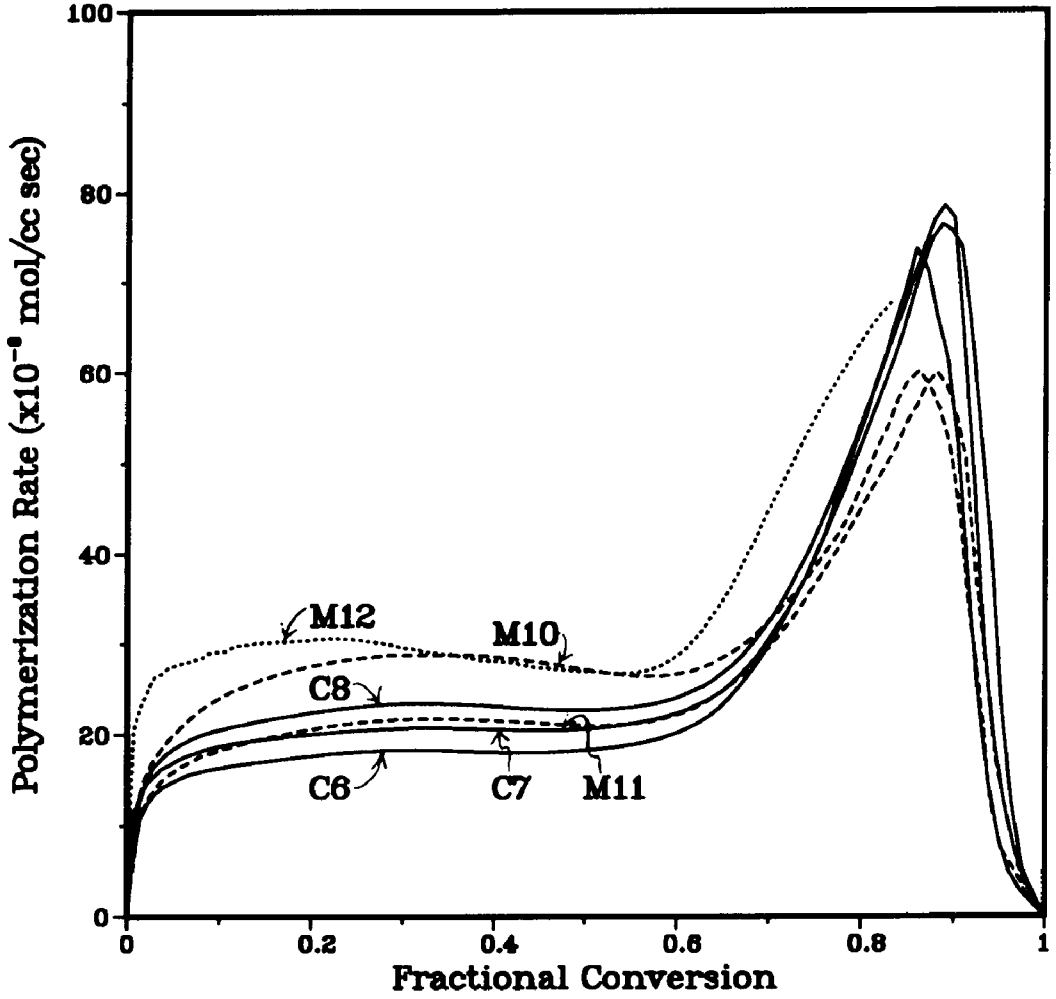

Figure 2-22: Polymerization rate versus conversion for emulsion polymerization of styrene: runs C6, C7 and C8, "conventional" cases; M10 and M11, miniemulsions with cetyl alcohol; and M12, miniemulsion with hexadecane.

age, thereby increasing the monomer droplet size, the polymerization rate was found to decrease with aging time (or with increasing droplet size). The miniemulsions prepared with cetyl alcohol or hexadecane were found to be unchanged within four hours of aging at room temperature. Different temperatures used in preparing cetyl alcohol miniemulsions with the same recipe can also result in different kinetics; the miniemulsion prepared with styrene added to the gel solution at 65°C had a faster reaction rate than the one prepared with styrene added to the gel solution at 25°C. The polymerization rates agree with the final particle size; the faster rates correspond to the smaller final particle size. These results indicate that, under the reported conditions, the Microfluidizer provides a greater and more uniform shear than the sonifier and the Omni mixer, thus resulting in smaller and more uniform final particle size distributions. The use of both cetyl alcohol and hexadecane was found to have a faster reaction rate than those having only one type of surfactant. The results also indicate that particle nucleation is slowed by the presence of cetyl alcohol on the surface of the monomer droplets.

2.5 References

1. C. N. Lewis and M. Randall, *"Thermodynamics and the Free Energy of Chemical Substances"*, McGraw-Hill Book Co., New York, 1923, p. 252.
2. W. I. Higuchi and J. Misra, *J. of Phar. Sci.*, **51**, 459 (1962).
3. Y. T. Choi, *Formation and Stabilization of Miniemulsions and Latexes*, Ph. D. Dissertation, Lehigh University, 1986.
4. E. G. Cockbain and T. S. McRoberts, *J. Colloid & Interface Sci.*, **8**, 440 (1953).
5. D. C. Blackley and A. C. S. Lawrence, *Discuss. Faraday Soc.*, **28**, 268 (1954).
6. P. Pithayanukul and N. Pipel, *J. Colloid & Interface Sci.*, **89**, 494 (1982).
7. F. M. Fowkes, *J. Phys. Chem.*, **67**, 1982(1963).
8. F. MacRitchie, *Nature (London)*, **170**, 1159 (1967).
9. R. D. Vold and K. L. Mittal, *J. Coll. Interface Sci.*, **38**, 451 (1972).
10. J. W. Vanderhoff, *J. Polym. Sci., Polym. Symp.*, **72**, 161 (1985).
11. J. Ugelstad, M. S. El-Aasser and J. W. Vanderhoff, *Polym. Lett.*, **11**, 503 (1973).
12. J. Ugelstad, F. K. Hansen and S. Lange, *Die Makromol. Chem.*, **175**, 507 (1974).
13. F. K. Hansen, E. Baumann Ofstad and J. Ugelstad, in *"Theory and Practice of Emulsion Polymerization"*, A. L. Smith, Ed., Academic Press, London, 1976, p. 13.
14. F. K. Hansen and J. Ugelstad, *J. Polym. Sci. Polym. Chem. Ed.*, **17**, 3069 (1979).
15. J. Ugelstad, P. C. Mork, K. Herder Kaggerud, T. Ellingsen and A. Berge, *Adv. Colloids Interface Sci.*, **13**, 101 (1980).
16. J. Ugelstad, T. Ellingsen and K. Herder Kaggerud, *Adv. in Organic Coating Sci. & Tech.*, Vol. 2, Technomic, Westport Connecticut, 1980, p.1.
17. B. J. Chamberlain, D. H. Napper and R. G. Gilbert, *J. Chem. Soc., Faraday Trans. I*, **78**, 591 (1982).
18. Y. T. Choi, M. S. El-Aasser, E. D. Sudol and J. W. Vanderhoff, *J . Polym. Sci., Polym. Chem. Ed.*, **23**, 2973 (1985).
19. J. Delgado, M. S. El-Aasser and J. W. Vanderhoff, *J. Polym. Sci., Polym. Chem. Ed.*, **24**, 861 (1986).
20. V. S. Rodriguez, *Interparticle Monomer Transport in Miniemulsion*

Copolymerization, Ph. D. Dissertation, Lehigh University, 1988.

21. R. J. Goetz, A. Khan and M. S. ElAasser, *J. Colloid Interface Sci.*, **137**, 395 (1990).

22. *Technical Bulletin on Microfluidizer*, Microfluidics Corporations, Newton, MA, 1989.

23. W. L. Grimm, T. I. Min, M. S. El-Aasser and J. W. Vanderhoff, *J. Colloid Interface Sci.*, **94**, 531 (1983).

24. W. L. Grimm, *The Use of Mixed-Emulsifier Systems in the Preparation and Stabilization of Emulsions and Latexes*, M. S. Thesis, Lehigh University, 1982.

25. M. S. El-Aasser, C. D. Lack, Y. T. Choi, T. I. Min, J. W. Vanderhoff and F. M. Fowkes, *Colloids Surfaces*, **12**, 79 (1984).

26. C. D. Lack, *Emulsion Formation and Stabilization with Mixed Emulsifier Liquid Crystals*, Ph. D. Dissertation, Lehigh University, 1985.

27. J. Delgado, *Miniemulsion Copolymerization of Vinyl Acetate and n-Butyl Acrylate*, Ph. D. Dissertation, Lehigh University, 1986.

28. E. D. Sudol, *Kinetics of Successive Seeding of Monodisperse Latex*, Ph. D. Dissertation, Lehigh University, 1983.

29. P. L. Tang, E. D. Sudol, M. E. Adams, J. M. Asua and M. S. El-Aasser, *J. Appl. Polym. Sci.*, **42**, 2019 (1991).

30. M. Ballard, R. G. Gilbert and D. H. Napper, *Macromolecules*, **17(3)**, 504 (1984).

31. C. M. Miller, J. Venkatesan, E. D. Sudol, C. Silebi and M. S. El-Aasser, unpublished data.

Chapter 3
Effect of Cetyl Alcohol on the Entry and Exit of Radicals in Emulsion Polymerization

3.1 Introduction

A common feature of miniemulsion polymerizations is the relatively slow nucleation stage of the reaction as indicated by the long rise to a rate maximum in the experimental conversion-time data[1, 2, 3, 4, 5, 6]. This phenomenon is particularly notable in systems using sodium lauryl sulfate (SLS) and cetyl alcohol (CA) as co-emulsifiers, as can be seen from the results of Chapter 2, and has been attributed to a reduced radical absorption rate possibly caused by the interfacial layer formed by the mixed emulsifier at the droplet-water interface[3]. It has been postulated that a reduced radical absorption rate into monomer droplets is due to the fact that the entering oligomer must first displace a surfactant molecule from the surface of the particle and the surfactant/monomer-rich surfaces have lower free energy than surfactant/polymer-rich ones, thus the entry into the former should be lower[2, 7]. Another possible cause for a reduced radical absorption rate is the lowering of the monomer concentration in the aqueous phase due to the presence of cetyl alcohol (by acting as a swelling promoter for the monomer droplets) thus slowing the polymer radical production in the aqueous phase (oligomeric radical growth is a function of monomer concentration in the aqueous phase). This has not been established conclusively, however, and more direct evidence is needed. Thus, the objective of this work is to study the effect of cetyl alcohol on the entry and exit of radicals in emulsion polymerization.

In order to obtain experimentally the entry (ρ) and exit (k) rate

coefficients, the particle concentration needs to be constant and known and thus seeded polymerizations employing a monodisperse latex are needed. Comparisons can be made between reaction systems containing cetyl alcohol and those without. Thus, seeded polymerizations will be carried out in a dilatometer to obtain the kinetics required for determining the free radical entry and exit rate coefficients.

The methodology of Gilbert and Napper[8], referred to as "Method 1", will be evaluated for determining the free radical entry and exit rate coefficients. These parameters are inferred from the slope and intercept of conversion-time data in which the rate of approach of the polymerization to steady-state is observed. Another approach involving the estimation of these kinetic rate parameters[9], referred to as "Method 2", will also be evaluated. This method describes the change in the distribution of radicals within the particles and the rate of polymerization just as in the previous approach. However, the latter method uses all the data points in the estimation. The two methods are expected to provide similar results. The two methods are described in some detail in section 3.3.

3.2 Experimental

3.2.1 Materials

Styrene (Polysciences) was distilled under reduced pressure (20 mm Hg) of nitrogen. The purified monomer was stored at $-2^{o}C$ for no more than four weeks before use. Potassium persulfate (FMC) was recrystallized from distilled-deionized water and then dried at room temperature under vacuum. Sodium lauryl sulfate, SLS, (BDH Chemicals), cetyl alcohol (CA), 98% (Aldrich) and azo-bis-isobutyronitrile, AIBN, (Du Pont) were used as recieved. The water was distilled and deionized (DDI).

Table 3-1: Recipe for the Seeded Polymerization.

Ingredient	Amount
DDI Water	20.4 g
Styrene	3.0 g
Polystyrene	2.2 g
Sodium Lauryl Sulfate	10 mM *
Cetyl Alcohol	0--30 mM *
Potassium Persulfate	0.013--1.33 mM *

* based on aqueous phase

3.2.2 The Polymerization Process

The recipe used in this study is shown on Table 3-1. The variables were the seed size (92 nm or 357 nm in diameter) and the concentrations of cetyl alcohol and initiator. The reaction temperature was 50°C to assure that the change in the concentration of initiator is negligible during the polymerization, and this condition is necessary for obtaining good results for the entry and exit rate coefficients.

The conditions for seeded polymerizations are described in Table 3-2. The polystyrene seed latex (LS 1039E and LS 1103A, Dow Chemical Company) was cleaned by serum replacement to remove surfactant and electrolyte. The particle sizes were determined by transmission electron microscopy. The LS 1093E seed was found to have a diameter of 92 nm with a coefficient of variation of 9% while the LS 1103A seed was found to be 357 nm in diameter with a

Table 3-2: Conditions of Seeded Polymerizations.

Run	Description
SCA1	1.33 mM $K_2S_2O_8$, 10 mM CA, 92 nm seed
SCA2	0.133 mM $K_2S_2O_8$, 10 mM CA, 92 nm seed
SCA3	0.0133 mM $K_2S_2O_8$, 30 mM CA, 92 nm seed
SCA4	0.665 mM $K_2S_2O_8$, 30 mM CA, 92 nm seed
SCA14	0.66 mM $K_2S_2O_8$, 30 mM CA, 357 nm seed
SCA15	1.33 mM $K_2S_2O_8$, 30 mM CA, 357 nm seed
SNO1	1.33 mM $K_2S_2O_8$, no CA, 92 nm seed
SNO2	0.133 mM $K_2S_2O_8$, no CA, 92 nm seed
SNO3	0.0133 mM $K_2S_2O_8$, no CA, 92 nm seed
SNO6	0.665 mM $K_2S_2O_8$, no CA, 92 nm seed
SNO9	0.66 mM $K_2S_2O_8$, no CA, 357 nm seed
SNO10	1.33 mM $K_2S_2O_8$, no CA, 357 nm seed

coefficient of variation of 2%. For experiments without cetyl alcohol, sodium lauryl sulfate was added back to the latex, followed by the addition of styrene with swelling taking place overnight with mixing. For experiments using cetyl alcohol: sodium lauryl sulfate, cetyl alcohol and water were mixed at 65°C for two hours to form the gel phase[5, 10], cooled to room temperature, and sonified to break up the gel phase. This aqueous gel phase was added to the clean latex and mixed overnight. The latex mixture was centrifuged and the serum was analyzed for cetyl alcohol in the aqueous phase. This serum was added to ethanol before injecting into a gas chromatograph and the results were compared to a standard curve of known cetyl alcohol concentration in ethanol (see Appendix B). No trace of cetyl alcohol was detected by gas chromatography indicating that most of the cetyl alcohol is adsorbed onto or into the polymer particles. Styrene was then added to the latex mixture followed by overnight swelling with mixing.

Dilatometry was applied to monitor the conversion-time behavior of the polymerization. After the emulsion was degassed at a pressure of about 20 mm Hg for 20 minutes using an aspirator, it was loaded into the 25 cc flask and the capillary was quickly inserted to avoid entrapment of air between the flask and the capillary. It took about 15 minutes for the level of the mixture to stay constant. The bath was controlled at a temperature of 50 ± 0.02°C. To start the polymerization an initiator solution, at 50°C, was injected into the dilatometer with a micro-syringe connected to a small polyethylene tube.

The fractional conversion, x, was calculated based on additive volumes of monomer and polymer as:

$$x = \frac{\Delta V}{g_m^o (1/\rho_s - 1/\rho_{ps})} \tag{3.1}$$

where ΔV is the change in volume of the reaction mixture, g_m^o the initial mass of

monomer, ρ_s and ρ_{ps} the densities of styrene and polystyrene, respectively.

3.3 Determination of the Entry and Exit Rate Coefficients

3.3.1 Method 1

This method[8] is applicable to seeded systems in which the number of particles is constant throughout the reaction and no more than one free radical occupies a particle at any time (zero-one system). A narrow particle size distribution is also necessary. In a conventional emulsion polymerization, the rate of fractional conversion of monomer to polymer (dx/dt) is expressed as:

$$\frac{dx}{dt}=\frac{k_p C_m^p \bar{n} N_p}{M_m^o N_A} \tag{3.2}$$

where k_p is the propagation rate constant, C_m^p the concentration of monomer in the polymer particles, $\bar{n}$ the average number of radicals per particle, N_p the number of particles per unit volume of continuous phase, M_m^o the initial number of moles of monomer per unit volume of continuous phase, and N_A Avogadro's number.

In Interval II, C_m^p and N_p remain constant, thus Equation (3.2) can be expressed as:

$$\frac{dx}{dt}=B\bar{n} \quad where \quad B=\frac{k_p C_m^p N_p}{M_m^o N_A} \tag{3.3}$$

During Interval III, C_m^p varies with conversion and the general kinetic equation describing Interval III is:

$$-\frac{dC_m^p}{dt}=k_p C_m^p [R^{\cdot}] \tag{3.4}$$

where the average concentration of radicals within the particles, $[R^{\cdot}]$, is given by:

$$[R^{\cdot}]=\frac{\bar{n}}{N_A V_s} \tag{3.5}$$

and where V_s is the swollen volume of a latex particle. Equation (3.4) then becomes:

$$-\frac{dC_m^p}{dt}=\frac{k_p C_m^p \bar{n}}{N_A V_s} \tag{3.6}$$

In Interval III, the fractional conversion is:

$$x=1-\frac{C_m^p}{C_m^o} \tag{3.7}$$

where C_m^o is the initial concentration of monomer in the particles. The combination of Equation (3.6) and Equation (3.7) results in

$$-\frac{dln(1-x)}{dt}=\frac{k_p}{N_A V_s}\bar{n} \tag{3.8}$$

Thus any analysis of Interval II data will also hold for Interval III, except that x is replaced by $-ln(1-x)$ and B becomes $k_p/N_A V_s$.

For the zero-one system, the Smith-Ewart Equations can be written as

$$\frac{dN_0}{dt}=-\rho N_0+(\rho+k)N_1 \tag{3.9}$$

and

$$\frac{dN_1}{dt}=\rho N_0-(\rho+k)N_1 \tag{3.10}$$

where N_o is the number of particles containing no radical and N_1 the number of particles containing one radical, ρ is the pseudo-first order rate coefficient of radical absorption by the particles, and k is the rate coefficient for radical desorption from the particles. Equation (3.10) can be solved with the initial conditions t=0 and $\bar{n}$=0 to yield:

$$N_1=\omega-\omega exp(-\lambda t) \tag{3.11}$$

where

$$\lambda=2\rho+k \quad and \quad \omega=\rho/\lambda \tag{3.12}$$

The integration of Equation (3.3) with the initial condition that at t=0, $x(t)$=0 yields:

$$x(t)=\frac{B}{\lambda}[\omega\lambda t-\omega(1-exp(-\lambda t)) \tag{3.13}$$

At long times Equation (3.13) is linear and can therefore be written in the form of:

$$x(t)=b+at \tag{3.14}$$

where b is the intercept at time t=0 and a is the slope of a conversion-time curve. At long times, Equations (3.13) and (3.14) can be solved for ρ and k directly as:

$$\rho=-\frac{a^2}{Bb} \tag{3.15}$$

and

$$k=-\frac{a(B-2a)}{Bb} \tag{3.16}$$

The rate of radical absorption in Equation (3.15) does not include the possibility of heterotermination of radicals in the aqueous phase, nor re-entry of radicals that have exited from the particles. When these events are taken into account, the entry rate coefficient can be written as a function of the fate parameter, α, which ranges from −1 (heterotermination is dominant) to 1 (re-entry of radicals is dominant). However, for the purpose of this work α will be considered to be 0 since it has been shown that for the styrene system that α is 0 or −1 and these are generally not distinguishable[11].

3.3.2 Method 2

This method was adapted from the work of Asua et al.[12] to estimate the entry and exit rate coefficients in a seeded zero-one system. Again, the rate of fractional conversion of monomer to polymer is expressed as in Equation (3.2). In the Interval III, C_m^p can be written as:

$$C_m^p = \frac{g_m^o(1-x)}{[g_m^o(1-x)]/d_m + [g_p^o + g_m^o x]/d_p} \frac{1}{M_o} \tag{3.17}$$

where g_m^o is the initial mass of monomer, g_p^o the initial mass of polymer, d_m the density of monomer, d_p the density of polymer and M_o the molecular weight of monomer. The population balance for particles containing one radical is written as:

$$\frac{dN_1}{dt} = \rho(N_p - 2N_1) - kN_1 \tag{3.18}$$

Equations (3.2) and (3.18) can be written as:

$$\frac{dS}{dt} = F(t, S, Y, K) \tag{3.19}$$

where S is the vector of the state variables, Y the vector of independent variables, and K the vector of adjustable parameters, where:

$$S = \{x, N_1\} \tag{3.20}$$

and

$$K = \{k, \rho\} \tag{3.21}$$

The residual sum of squares is expressed as:

$$Sum = \sum_{i=1}^{G} \left[(x_e - x_c^h) - \left(\frac{\partial[x_c]}{\partial[S]}\right)^h \left(\frac{\partial[S]}{\partial[K]}\right)^h \Delta K^{h+1} \right]^2 \tag{3.22}$$

where G is the number of experimental points, x_e the experimental conversion, x_c^h the conversion predicted by the model with a particular set of parameters, h. Equation (3.22) is linear in ΔK^{h+1} and minimizing the *Sum* with respect to ΔK^{h+1} gives:

$$\Delta K^{h+1} = [H^h]^{-1} \sum_{i=1}^{G} [J^h]_i^T (x_e - x_c^h)_i \tag{3.23}$$

where:

$$H^h = \sum_{i=1}^{G} [J^h]_i^T [J^h]_i \tag{3.24}$$

and

$$J_i = \left(\frac{\partial[x_c]}{\partial[S]}\right)_i^h \left(\frac{\partial[S]}{\partial[K]}\right)_i^h \tag{3.25}$$

in which the superscript T stands for the transposed matrix.

In order to calculate $\partial[S]/\partial[K]$, both sides of Equation (3.19) are differentiated with respect to K giving:

$$\frac{\partial[dS/dt]}{\partial[K]} = \frac{\partial[F]}{\partial[K]} + \frac{\partial[F]}{\partial[S]}\frac{\partial[S]}{\partial[K]} \tag{3.26}$$

Interchanging the order of differentiation yields:

$$\frac{d(\partial[S]/\partial[K])}{dt} = \frac{\partial[F]}{\partial[K]} + \frac{\partial[F]}{\partial[S]}\frac{\partial[S]}{\partial[K]} \tag{3.27}$$

Based on these equations, an algorithm for parameter estimation in stiff differential equations has been developed. The algorithm is started with some initial value K, Equations (3.2), (3.18) and (3.27) are integrated, J_i and $(x_e - x_c^h)_i$ at each experimental conversion are calculated. ΔK^{h+1} is calculated followed by the new values of the parameters

$$K^{h+1} = K^h + \Delta K^{h+1} \tag{3.28}$$

The algorithm is repeated until convergence is reached.

3.4 Results and Discussion

One requirement to calculate the entry and exit rate coefficients is that the number of particles remains constant throughout the polymerization. Thus the final particle size distributions must be examined for the gain or loss of particles through new nucleation or coagulation, respectively. Typical results are shown in Figure 3-1 which indicate that significant amounts of particles were not formed or lost during the polymerization. To calculate the entry and exit rate coefficients by Method 1, $-ln(1-x)$ was plotted against reaction time as shown in Figure 3-2 along with the conversion-time data. Because of the small differences between these results, a repeatability study was carried out and the

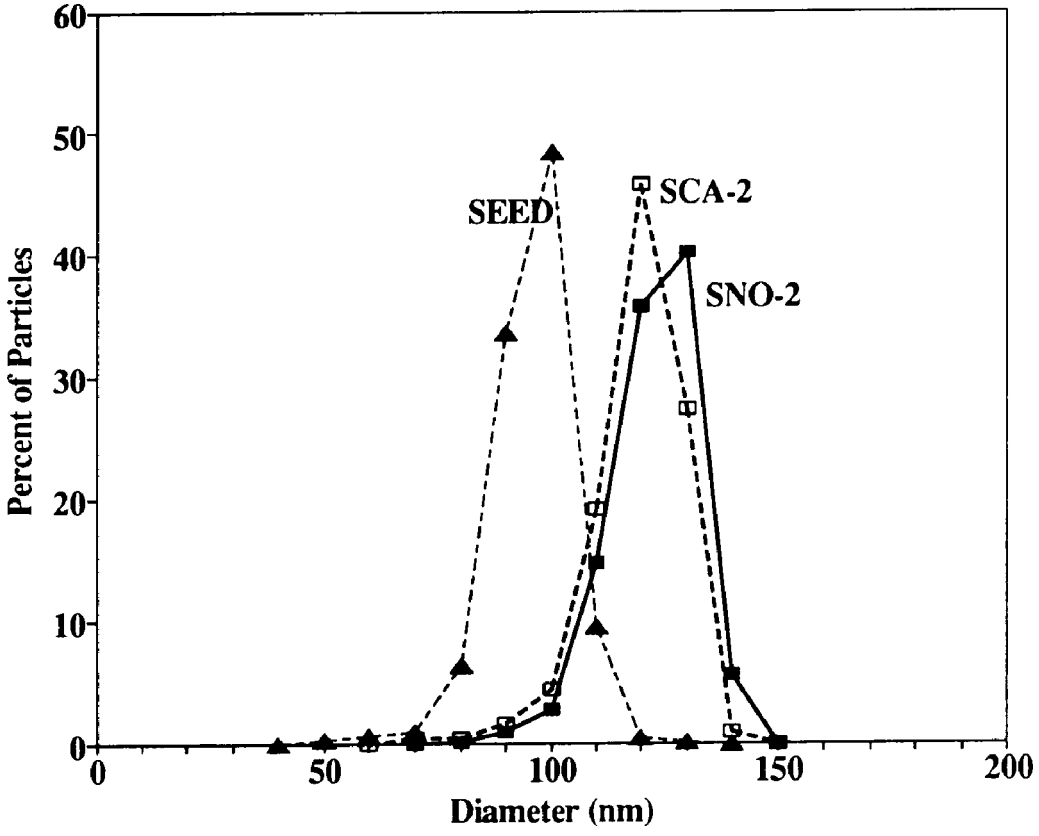

Figure 3-1: Particle size distributions for the 92 nm polystyrene seed particles and the final latex particles after seeded emulsion polymerization of run SNO2 (0.13 mM $K_2S_2O_8$ and no CA) and SCA2 (0.13 mM $K_2S_2O_8$ and 10 mM CA).

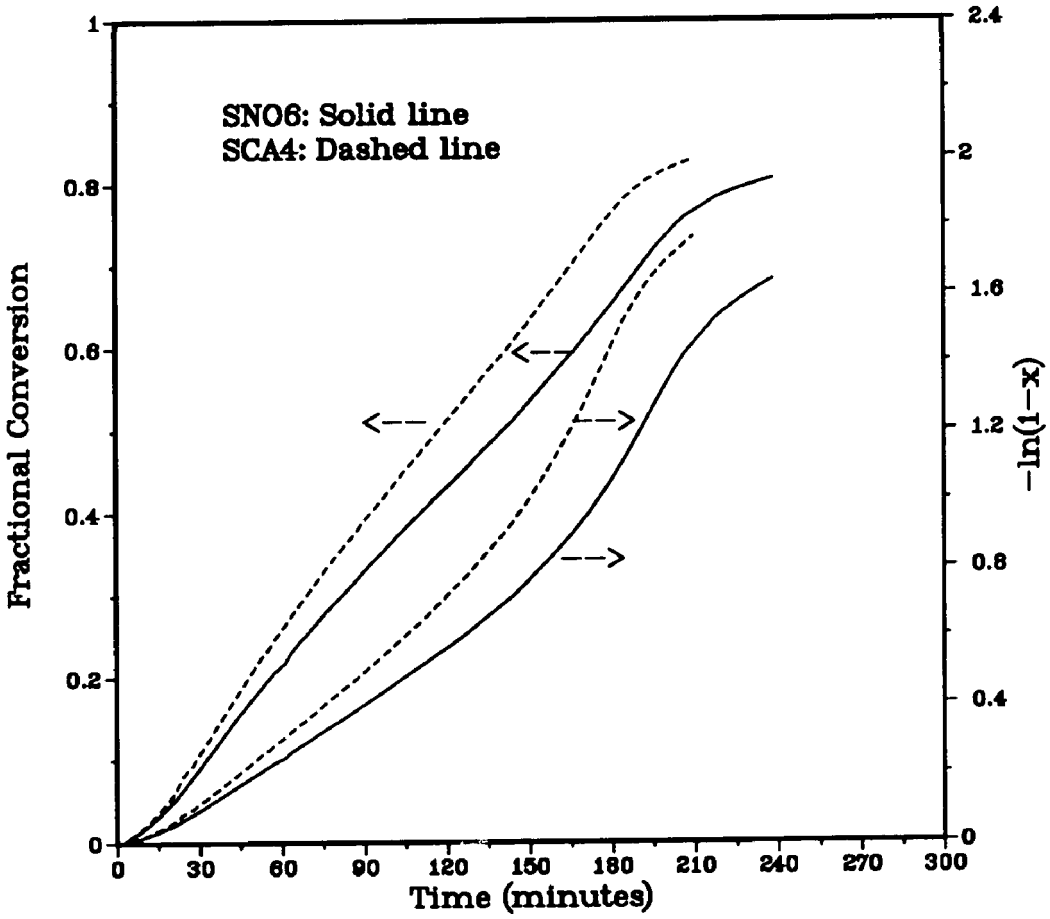

Figure 3-2: Conversion and $-ln(1-x)$ versus time curves for seeded emulsion polymerization of polystyrene seed/styrene monomer: runs SNO6 (0.66 mM $K_2S_2O_8$, no CA and 92 nm seed); and SCA4 (0.66 mM $K_2S_2O_8$, 30 mM CA and 92 nm seed).

results are shown in Figure 3-3. These indicate that the reproducibility is good and the polymerization rate in a seeded system increases when cetyl alcohol is present. This is contrary to the idea that cetyl alcohol hinders the entry of radicals into the monomer-swollen particles by forming a complex at the oil-water interface. An increased polymerization rate with the presence of cetyl alcohol is also seen at other levels of initiator in the concentration range of 0.013 mM to 1.33 mM based on the aqueous phase as shown by the results presented in Figure 3-4.

The linear (steady-state) portions of the $-ln(1-x)$ curves were used to extract ρ and k for each experiment using Method 1. For example, in Figure 3-2, the curves from 40 to 100 minutes were used to obtain the slopes (a) and intercepts (b) and from these the entry and exit rate coefficients were determined (Equations (3.15) and (3.16)). The plot of the average number of radicals per particle versus time, in Figure 3-5, verifies that these systems are zero-one at least through the linear portion of the $-ln(1-x)$ versus time curve. Method 2 uses all the data (from t=0 through the steady-state region e.g., for the curves in Figure 3-5 through 100 minutes) obtained for a set of fractional conversion-time curves (at various initiator concentrations) to determine ρ and k. The data from Figure 3-3 were used to calculate the entry (ρ) and exit (k) rate coefficients. The results of the calculations using Method 1 are $\rho = (3.65 \pm 0.18) \times 10^{-4}$/s and $k = (0.68 \pm 0.05) \times 10^{-3}$/s for the runs using cetyl alcohol, and $\rho = (2.66 \pm 0.26) \times 10^{-4}$/s and $k = (0.74 \pm 0.04) \times 10^{-3}$/s for the runs without cetyl alcohol. The results of Method 2 estimations are $\rho = (3.38 \pm 0.19) \times 10^{-4}$/s and $k = (0.97 \pm 0.09) \times 10^{-3}$/s for the runs with cetyl alcohol, and $\rho = (2.42 \pm 0.28) \times 10^{-4}$/s and $k = (0.89 \pm 0.09) \times 10^{-3}$/s for the runs without cetyl alcohol. They results indicate that the two methods provide similar solutions. The results also suggest that the entry rate coefficient for the case with cetyl alcohol is larger

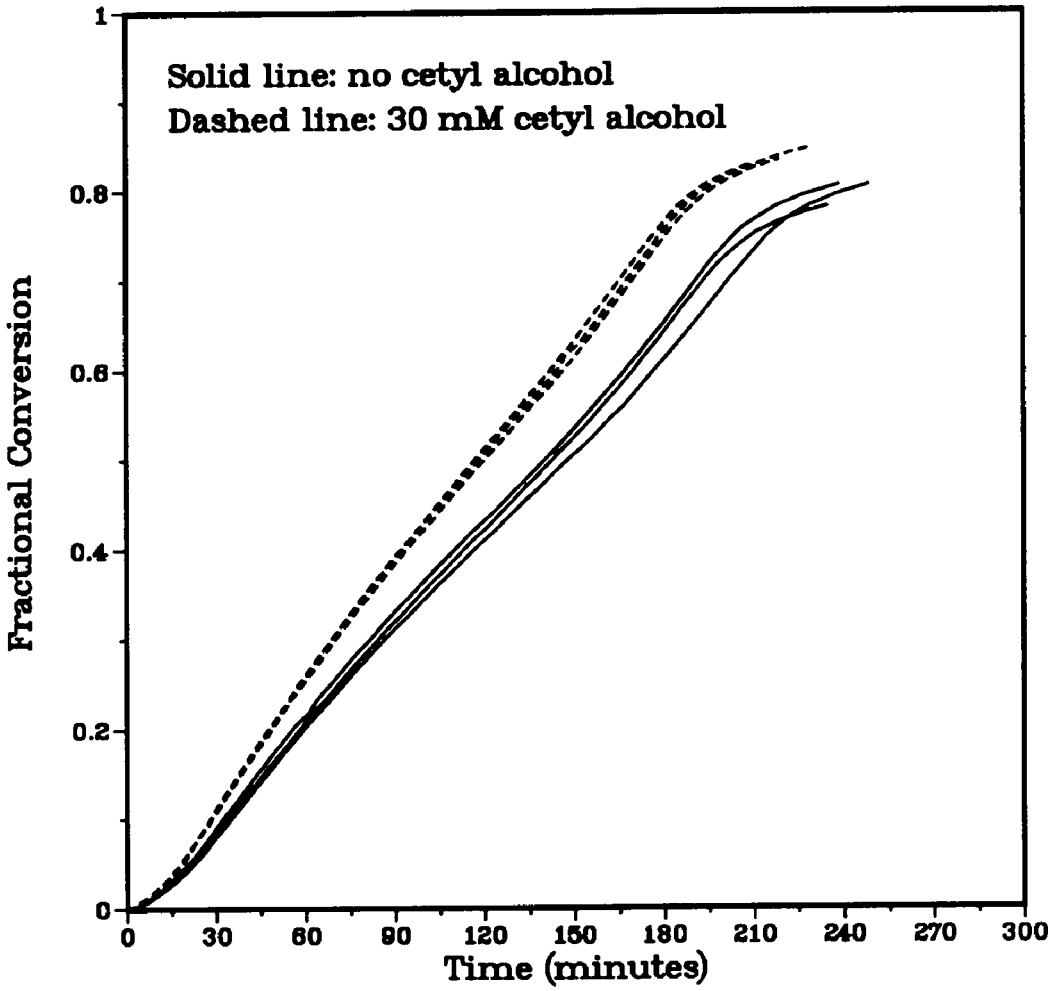

Figure 3-3: Repeatability of conversion versus time curves for seeded emulsion polymerizations of polystyrene/styrene system with initiator concentration of 0.66 mM and 92 nm seed; solid curves obtained with no CA, dashed curves with 30 mM CA.

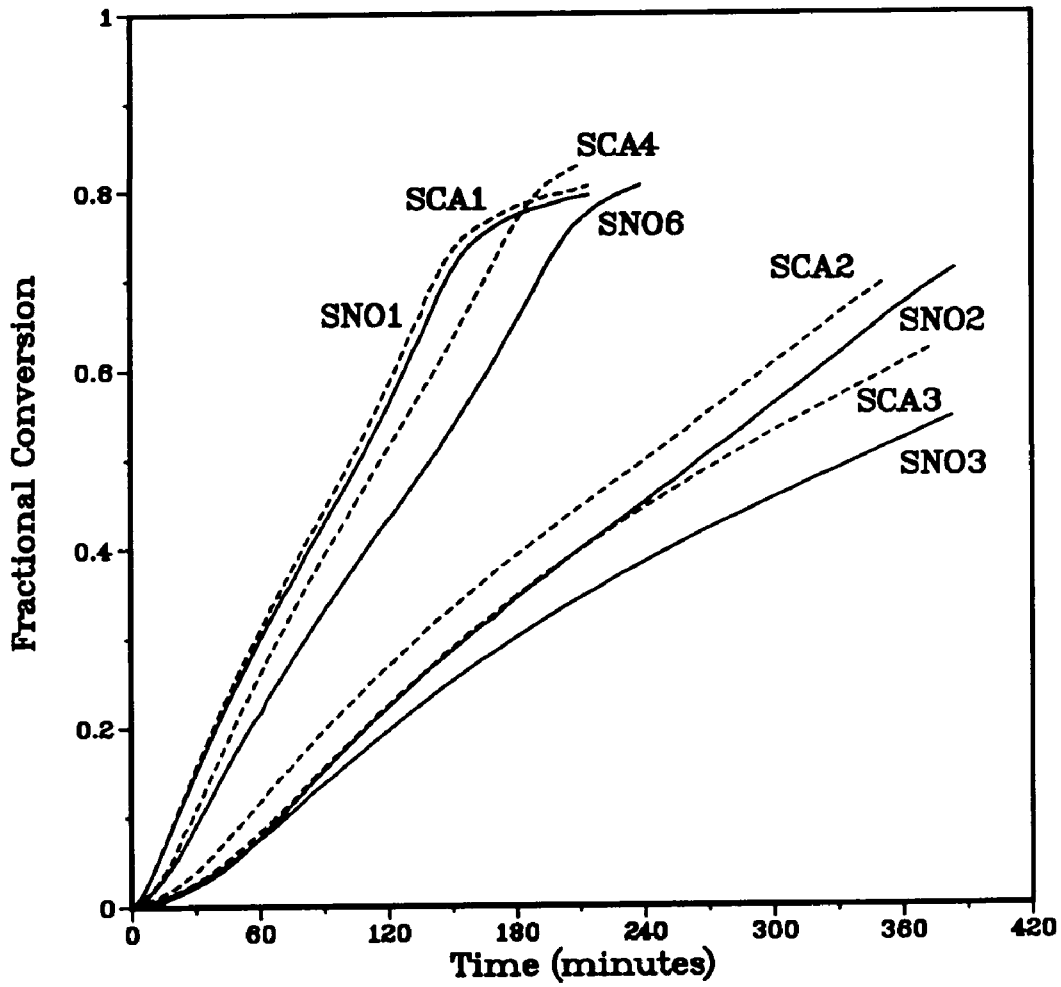

Figure 3-4: Conversion versus time curves for seeded emulsion polymerization of polystyrene/styrene system: runs SCA1 (1.33 mM $K_2S_2O_8$ and 10 mM CA), SNO1 (1.33 mM $K_2S_2O_8$ and no CA), SCA4 (0.66 mM $K_2S_2O_8$ and 30 mM CA), SNO6 (0.66 mM $K_2S_2O_8$ and no CA), SCA2 (0.13 mM $K_2S_2O_8$ and 10 mM CA), SNO2(0.13 mM $K_2S_2O_8$ and no CA), SCA3 (0.013 mM $K_2S_2O_8$ and 30 mM CA) and SNO3 (0.013 mM $K_2S_2O_8$ and no CA); all with 92 nm seed, dashed lines obtained with CA and solid lines without CA.

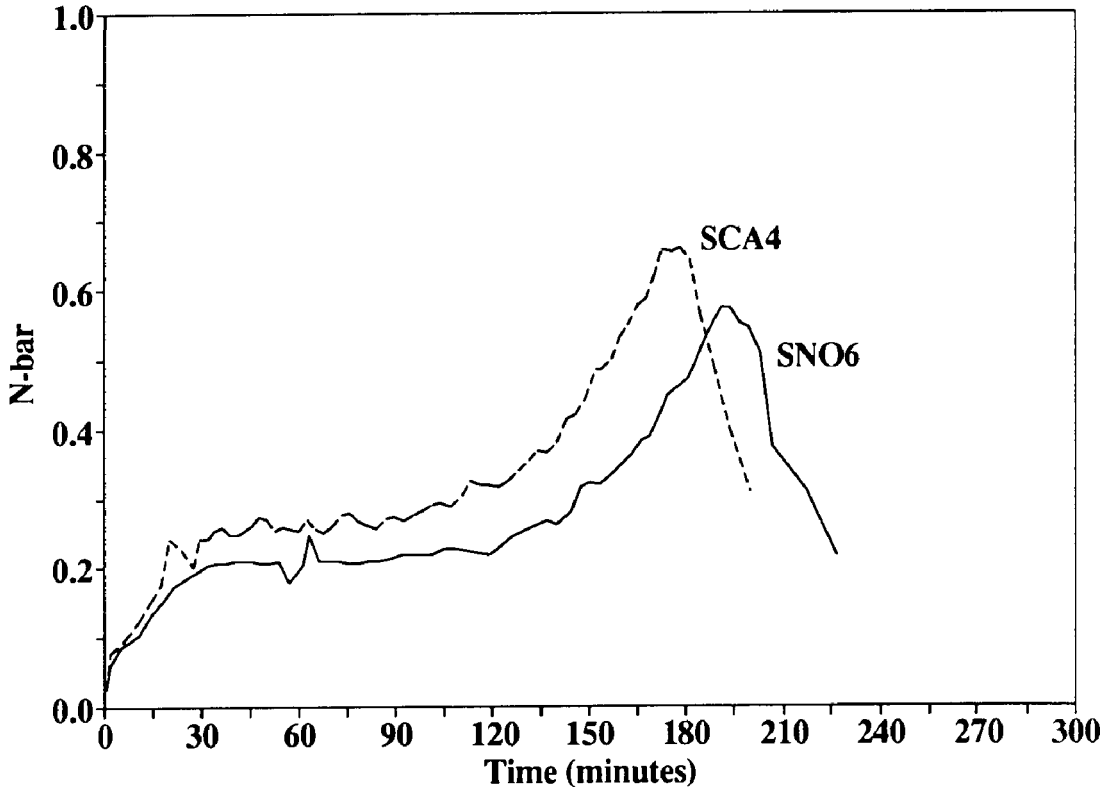

Figure 3-5: Average number of radicals per particle versus time curves for seeded emulsion polymerization of polystyrene/styrene system: runs SNO6 (0.66 mM $K_2S_2O_8$, no CA and 92 nm seed); and SCA4 (0.66 mM $K_2S_2O_8$, 30 mM CA and 92 nm seed).

than that of the case without cetyl alcohol, and the difference in the exit rate coefficients is not distinguishable.

Table 3-3 shows the entry (rows 6 and 11) and exit (rows 7 and 12) rate coefficients obtained by the two methods, respectively, for experiments at different initiator and cetyl alcohol concentrations. The results of the two methods are in relative agreement, although they have slightly different values. The entry rate coefficients are consistent with the rates of polymerization; larger values of the entry rate coefficient correspond to faster polymerizations. The exit rate coefficient seems to be smaller for the systems containing cetyl alcohol on (or in) the particles for a given initiator concentration (with the exception of the results obtained using 0.13 mM initiator which is likely to be due to the large difference in the entry rate coefficients which in turn causes a large difference in the calculated values of the exit rate coefficients). The exit rate coefficient decreases systematically with decreasing initiator concentration, in both series with and without cetyl alcohol. This, however, is contrary to the theory that the exit rate coefficient is independent of the initiator concentration[8]. Table 3-3 also presents results for the entry rate coefficient (rows 9 and 14) at a fixed value of the exit rate coefficient of 2.1×10^{-3}/s, which was calculated using the method of Asua et al.[9]. The results indicate that for a given initiator concentration, the presence of cetyl alcohol increases the entry rate of radicals into the particles.

The data in Figure 3-4 were used to estimate the second order entry rate coefficient for radicals into the particles (k_a^p) and the exit rate coefficient (k). The estimation using the sets of experiments containing cetyl alcohol gives $k_a^p = 1.4 \times 10^6 dm^3 mol^{-1} s^{-1}$ and $k = 6.7 \times 10^{-3}\ s^{-1}$, and the estimation using the sets of experiments without cetyl alcohol gives $k_a^p = 6.2 \times 10^6 dm^3 mol^{-1} s^{-1}$ and $k = 17.0 \times 10^{-3}\ s^{-1}$. Although this data alone is insufficient to draw any good conclusion,

Table 3-3: Conditions and Results for the Study of the Effect of Cetyl Alcohol on the Entry and Exit of Radicals in Seeded Emulsion Polymerization.

Run	Row	SCA1	SNO1	SCA4	SNO6	SCA2	SNO2	SCA3	SNO3
[I],mM	2	1.33	1.33	0.665	0.665	0.133	0.133	0.013	0.013
CA,mM	3	10	--	30	--	10	--	30	--
$\bar{n}$	4	0.280	0.268	0.262	0.213	0.130	0.119	0.118	0.098
METHOD 1									
$\rho, 10^{-4}/s$	6	9.03	9.02	3.54	2.95	1.08	.612	.638	.593
$k, 10^{-3}/s$	7	1.41	1.56	.639	.794	.613	.393	.411	.484
Fixing $k = 2.1 \times 10^{-3}/s$									
$\rho, 10^{-4}/s$	9	13.6	12.0	11.5	7.81	3.69	3.27	3.26	2.58
METHOD 2									
$\rho, 10^{-4}/s$	11	9.74	10.0	3.16	2.72	.883	.403	.496	.497
$k, 10^{-3}/s$	12	2.61	2.86	.865	.981	.542	.195	.317	.426
Fixing $k = 2.1 \times 10^{-3}/s$									
$\rho, 10^{-4}/s$	14	8.34	7.97	5.50	4.59	2.34	1.78	1.82	1.66
Fixing ρ									
$\rho, 10^{-4}/s$	16	7.97	7.97	4.59	4.59	1.78	1.78	1.66	1.66
$k, 10^{-3}/s$	17	1.98	2.1	1.61	2.1	1.5	2.1	1.87	2.1
Percent difference									
$\%\Delta k$	19	6	--	23	--	29	--	11	--

the results might suggest that both the entry and exit of radicals are slowed by the presence of cetyl alcohol.

From the above results, the effect of cetyl alcohol on the entry and exit of radicals cannot be separated. Radical desorption events are expected to be important because of the small particle size of the seed (≈ 100 nm). Experiments with larger particle size (> 350 nm) can be utilized to minimize the kinetic importance of radical desorption and provide more definitive information concerning the effect of cetyl alcohol on the entry and exit of radicals in seeded systems. However, the calculation of ρ and k may not be possible for this system since the average number of radical per particle is likely to exceed 0.5. Nonetheless, from the conversion versus time data, one can qualitatively examine the effect of cetyl alcohol on radical entry into polymer particles.

Comparison of the kinetics of experiments with cetyl alcohol and those without were also carried out using the 357 nm seed in order to study the effect of cetyl alcohol on radical absorption. Final particle size distributions were also determined and the results showed that no particles were formed or lost during the polymerization. Figure 3-6 shows the conversion-time results which indicate that the polymerization rate was the same (at a given initiator concentration) regardless of whether cetyl alcohol was present in the system. Figure 3-7, which shows the average number of radicals per particle versus time results for the set of experiments at the initiator concentration of 1.33 mM, confirms that exit is not important in these experiments (e.g., $\bar{n}$ is much greater than 0.5). These results along with the results from the 92 nm seed would indicate that cetyl alcohol does not effect the entry of radicals but may only effect the exit of radicals from the particles (for the small size seed system). This would be true if cetyl alcohol acts as a chain transfer agent and in its

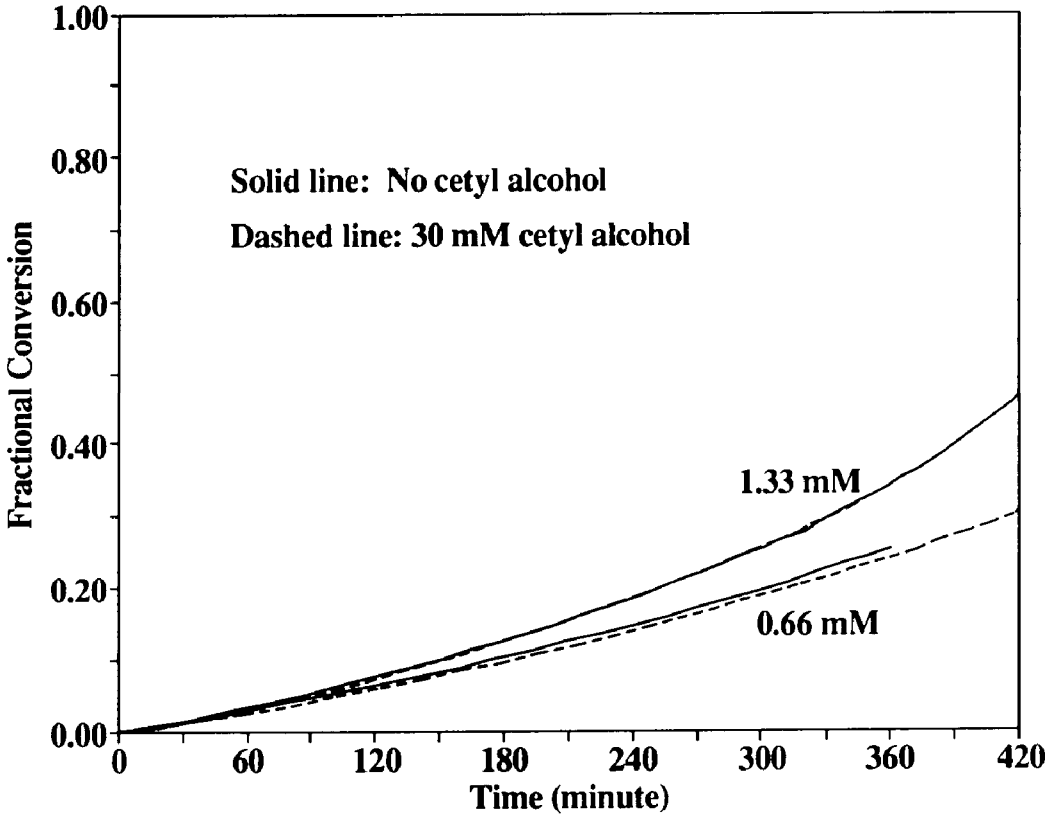

Figure 3-6: Conversion versus time curves for seeded emulsion polymerization of polystyrene/styrene system obtained using a 357 nm seed; 1.33 mM and 0.66 mM of $K_2S_2O_8$; dashed lines obtained with CA, solid lines without CA.

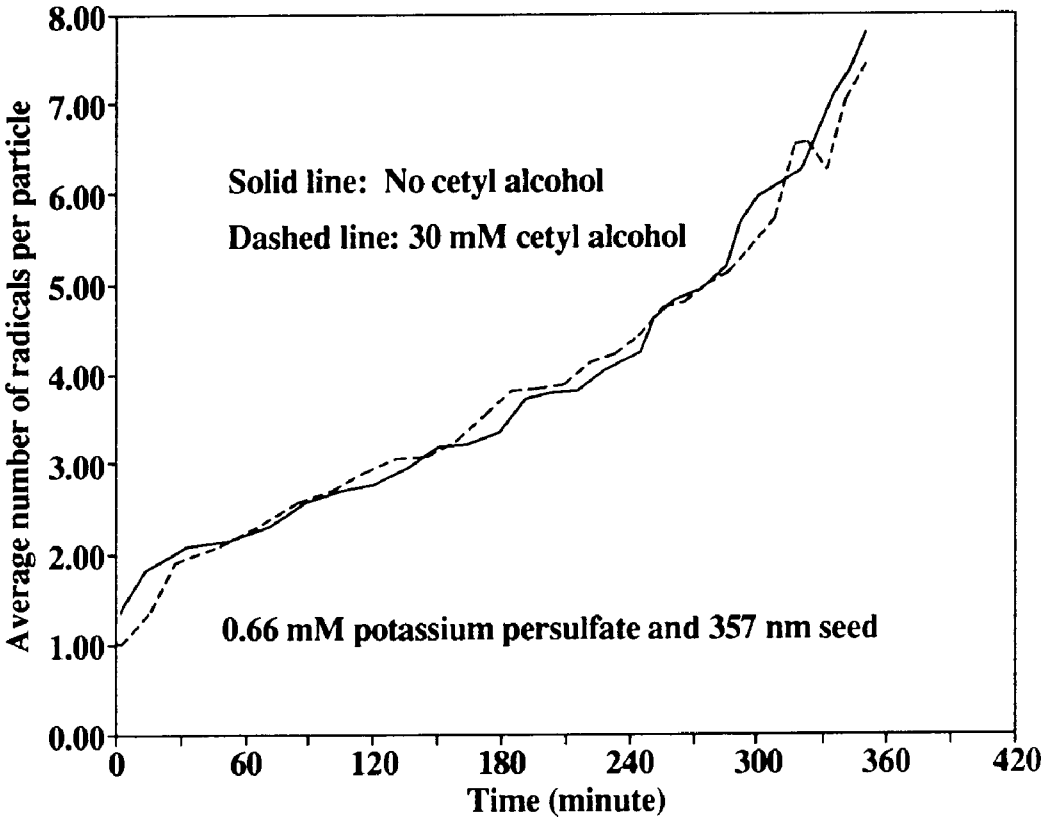

Figure 3-7: Average number of radicals per particle versus time curves for seeded emulsion polymerization of polystyrene/styrene system obtained using a 357 nm seed and 1.33 mM of $K_2S_2O_8$; dashed lines obtained with CA, solid lines without CA.

radical form it is less likely to desorb than a single unit monomer radical (radical exit in emulsion polymerization generally refers to a single unit monomer[9, 13, 14]).

Experiments were carried out to determine the chain transfer constant for cetyl alcohol by carrying out bulk polymerizations of styrene at 50°C with different cetyl alcohol concentrations[15]. AIBN was used as initiator and the conversion was held to less than five percent. The number average molecular weight was determined by gel permeation chromatography from which the number-average degree of polymerization, X_n, was obtained. The slope of $1/X_n$ versus the ratio of cetyl alcohol concentration to styrene concentration represents the value of the chain transfer constant for cetyl alcohol. The results of these experiments are shown in Figure 3-8 from which the chain transfer constant for cetyl alcohol, C_s, was determined to be 11×10^{-4} which is more than one order of magnitude larger than chain transfer to styrene monomer at 50°C[16] ($0.35 - 0.78 \times 10^{-4}$). From these results, we can fix the value of the entry rate coefficient to examine the effect of cetyl alcohol on exit. The entry rate coefficients (ρ) for experiments without cetyl alcohol were calculated by fixing the value of the exit rate coefficient ($k = 2.1 \times 10^{-3}$/s) as before and the results were used to estimate k for those experiments with cetyl alcohol. Thus, the difference in k for each set of experiments at a particular initiator concentration was calculated. These results are shown in rows 16, 17 and 19 of Table 3-3, which indicate that the effect of cetyl alcohol on exit is more important at low initiator concentrations (with the exception of the initiator level of 0.0133 mM which is close to the level of thermal initiation of styrene at 50°C). These results are consistent with the finding that radical exit is more important at low initiator concentrations[17].

The results from the above experiments suggest that when a cosurfactant

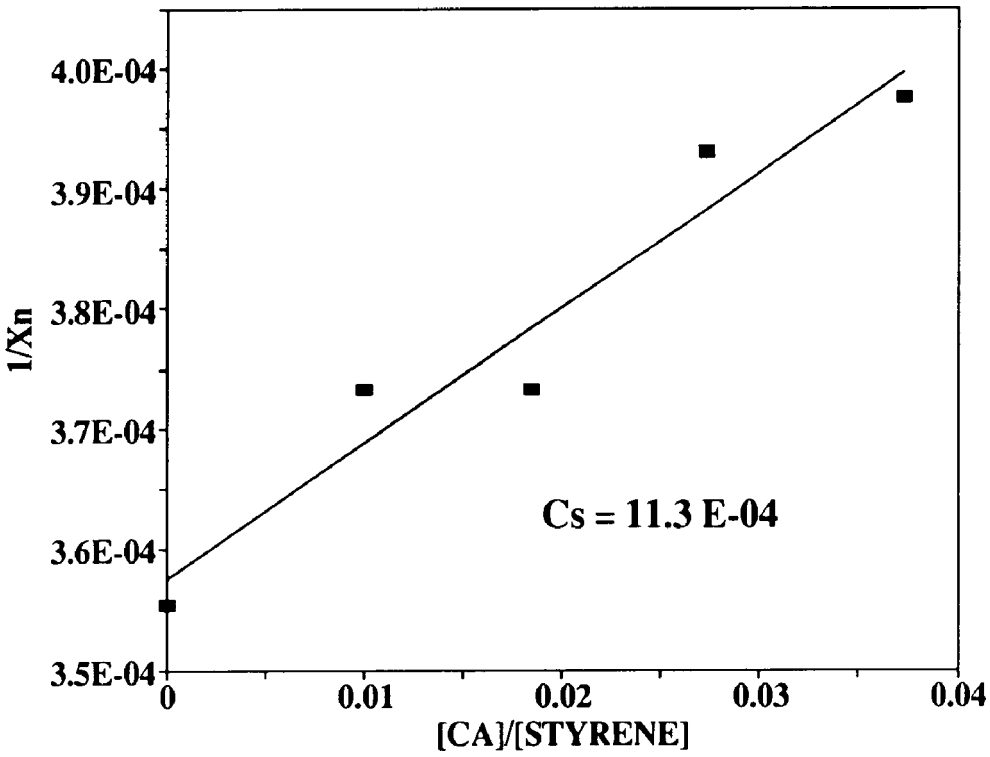

Figure 3-8: Ratio of cetyl alcohol concentration to styrene concentration versus one over the number-average degree of polymerization using AIBN at 50°C.

(such as cetyl alcohol) is used in miniemulsion polymerization, it may affect the exit of radicals from the swollen polymer particles if it has a higher chain transfer constant than that of the monomer. The results also suggest that when a miniemulsion droplet becomes a polymer particle, the polymerization behavior is similar to conventional polymer particles and the difference in the entry rate coefficients for droplets and particles is likely due to the difference in their physico-chemical nature. This may be explained by the postulate of Gilbert et al.[2, 7] that the entering oligomer must first displace a surfactant molecule from the surface of the particle and the surfactant/monomer-rich surfaces have lower free energy than surfactant/polymer-rich ones, thus the entry into the former should be lower. However, the entry rate coefficient for monomer droplets have not been determined experimentally due to their instability and the difficulty of controlling the number of droplets during the reaction. Figure 2-19 of Chapter 2 indicates that the reduced entry rate of radicals into droplets may be seen at less than one percent conversion and the type of co-surfactant may affect the magnitude of the entry rate coefficient for droplets. Perhaps, a method of high swelling, at least 100 to 1 monomer to polymer ratio, of the seed should be developed, or direct emulsification of high ratio of monomer to polymer solution in order to have a better chance to obtain the entry rate coefficient of radicals into the monomer droplets.

3.5 Summary and Conclusions

The effect of cetyl alcohol on the entry and exit rate coefficients was studied using seeded emulsion polymerization. Two methods were employed to determine these coefficients and were found to be in relative agreement. It was found that cetyl alcohol increases the polymerization rate in a seeded system. The presence of cetyl alcohol was found not to affect entry but instead to affect

exit by acting as a chain transfer agent competing with monomer and decreasing the exit of monomeric radicals. The chain transfer constant to cetyl alcohol was found to be more than an order of magnitude greater than that of styrene. The effect of cetyl alcohol on the kinetics of seeded emulsion polymerization was found to increase in importance with decreasing initiator concentration. These results also suggest that when a miniemulsion droplet becomes a polymer particle, the polymerization behavior is similar to conventional polymer particles and that the difference in the entry rate coefficients for droplets and particles is likely due to the difference in their physico-chemical nature.

3.6 References

1. F. K. Hansen and J. Ugelstad, *J. Polym. Sci. Polym. Chem. Ed.*, **17**, 3069 (1979).

2. B. J. Chamberlain, D. H. Napper and R. G. Gilbert, *J. Chem. Soc., Faraday Trans. I*, **78**, 591 (1982).

3. Y. T. Choi, M. S. El-Aasser, E. D. Sudol and J. W. Vanderhoff, *J . Polym. Sci., Polym. Chem. Ed.*, **23**, 2973 (1985).

4. J. Delgado, M. S. El-Aasser, C. A. Silebi and J. W. Vanderhoff, *J. Polym. Sci. Polym. Chem. Ed.*, **28**, 777 (1990).

5. V. S. Rodriguez, *Interparticle Monomer Transport in Miniemulsion Copolymerization*, Ph. D. Dissertation, Lehigh University, 1988.

6. P. L. Tang, E. D. Sudol, C. A. Silebi and M. S. El-Aasser, accepted by *J. Appl. Polym. Sci.*.

7. D. F. Wood, B. C. Y. Whang, D. H. Napper, R. G. Gilbert and G. Lichti, *J. Polym. Sci. Polym. Chem. Ed.*, **21**, 985 (1983).

8. R. G. Gilbert and D. H. Napper, *Rev. Macromol. Chem. Phys.*, **C23**(1), 127 (1983).

9. J. M. Asua, E. D. Sudol and M. S. El-Aasser, *J. Polym. Sci., Polym. Chem. Ed.*, **27**, 3903 (1989).

10. R. J. Goetz, A. Khan and M. S. ElAasser, *J. Colloid Interface Sci.*, **137**, 395 (1990).

11. B. C. Y. Whang, D. H. Napper, M. J. Ballard, R. G. Gilbert and G. Lichti, *J. Chem. Soc., Faraday Trans. I*, **78**, 1117 (1982).

12. J. M. Asua, M. E. Adams and E. D. Sudol, *J. Polym. Sci., Polym. Chem. Ed.*, b(39), 1183 (1990).

13. F. K. Hansen and J. Ugelstad, *Makromol. Chem.*, **180**, 2423 (1979).

14. M. Nomura, in *"Emulsion Polymerization"*, Irja Piirma, Ed., Acadamic Press, New York, 1982, p. 191.

15. E. A. Collins, J. Bares and F. W. Billmeyer, Jr., *"Experiments in Polymer Science"*, Wiley-interscience, New York, 1973, pp. 333-337.

16. *"Polymer Handbook"*, 2nd. Ed., J. Brandrup and H. Immergent, Ed., Wiley Interscience, New York, 1975.

17. B. S. Hawkett, R. G. Gilbert and D. H. Napper, *J. C. S. Faraday I*, **76**, 1323 (1980).

Chapter 4
Mathematical Modeling of Miniemulsion Polymerization

4.1 Introduction

A mathematical model that can reconstruct the reaction profile of an emulsion polymerization is valuable in confirming, elucidating or predicting the various mechanisms in the polymerization. Although the kinetics of emulsion polymerization have been studied extensively, many mechanistic aspects of the emulsion polymerization process still remain unclear, especially the particle nucleation mechanism.

Particle nucleation is very important because it governs the number of particles present in the reaction system and thus the rate of polymerization. Three possible nucleation loci have been suggested and widely discussed in the literature: monomer-swollen micelles, aqueous phase and monomer droplets. Only monomer-droplet nucleation will be discussed here because it is the dominant nucleation mechanism in miniemulsion polymerization[1].

The first mathematical model for the miniemulsion polymerization of styrene was developed by Chamberlain et al.[2] This model was based on the mathematical treatment by Hawkett et al.[3] for seeded emulsion polymerization. It was assumed that polymer particles were formed only upon the entry of free radicals into the monomer droplets and each entry event resulted in a polymer particle. The rate of particle formation was expressed as a first-order radical entry into monomer droplets:

$$\frac{dN_p}{dt}=\rho_D N_d \tag{4.1}$$

where ρ_D is the first order entry rate coefficient for radicals into the monomer

droplets, N_d the number of monomer droplets, and N_p the number of polymer particles. It was assumed that the entry rate coefficient for radicals into the monomer droplets decreased with the decreasing surface area of monomer droplets and was expressed as:

$$\rho_D = \rho \left[\frac{V_D(t)}{V_D(0)} \right]^{2/3} \tag{4.2}$$

Where $V_D(t)$ and $V_D(0)$ are the volumes of a droplet at times t and zero respectively, and ρ the first order entry rate coefficient for radicals into the polymer particles, which was used as an adjustable parameter.

For ease of mathematical computation, the monomer droplet and particle size distributions were assumed to be monodisperse. The uninitiated monomer droplets were assumed to act as monomer reservoirs supplying monomer to the polymer particles. Thus the concentration of monomer in the polymer particles, while monomer droplets were present in the reaction system, was assumed to be the equilibrium value of Interval II (6.2 mol/liter). It was demonstrated by Delgado[4] that when the monomer droplets exist in the system, the equilibrium concentrations in the presence of small amount of water-insoluble compounds are lower than the equilibrium concentration in the absence of small amount of water-insoluble compounds; thus, while monomer droplets still exist, the concentration of monomer in the polymer particles is not the equilibrium value of Interval II in conventional emulsion polymerization.

Chamberlain et al.[2] assumed that monomer droplets disappear only by diffusion of monomer to the polymer particles. Monomer droplet disappearance was derived as a function of conversion with the resulting prediction that they disappear around 30 percent conversion. However, Delgado[4] showed that the presence of water-insoluble compounds, fatty alcohol or long-chain alkane, prevents the complete disappearance of monomer droplets by molecular

diffusion of monomer. The results from Chamberlain et al.[2], Choi et al.[5, 6], Delgado[4] and Rodriguez[7] suggest that monomer droplets do disappear at a certain point during the polymerization, but it is likely that this disappearance is due to a coagulation process between droplets and particles[8]. Chamberlain's work showed that the rate coefficient for radical entry into the monomer droplets was an order of magnitude less than the value determined for the seeded emulsion polymerization of styrene in order to fit the experimental data.

Choi[6] modified Chamberlain's model by deriving the rate of radical entry into monomer droplets and polymer particles from an aqueous phase radical balance and found that the model predicted faster rates of polymerization than those found experimentally for low initiator concentrations.

The scope of this chapter is to present a general framework to model the kinetics of miniemulsion polymerization of styrene. The predicted results will be compared to the experimental data obtained by Choi et al.[5, 6], because these data contain sets of conversion-time data over a wide range of initiator concentrations (0.13 to 2.66 mM). The population balance will be based on the Smith-Ewart equation[9]; the calculation of the desorption rate coefficient for radicals from the polymer particles will be taken from Asua et al.[10]; equilibrium swelling thermodynamics[11, 12] will be employed to calculate the concentrations of each component in each phase; monomer droplet nucleation as presented by Chamberlain et al.[2] will be applied; and coagulation of particles and droplets based on the DLVO theory[13] and the Muller equation[14] will be examined.

4.2 Modeling Framework

The rate of change of fractional conversion in an emulsion polymerization is expressed as:

$$\frac{dx}{dt}=\frac{k_p C_m^p \bar{n} N_p}{M_m^o N_A} \tag{4.3}$$

where k_p is the rate coefficient for radical propagation, C_m^p the monomer concentration in the polymer particles, $\bar{n}$ the average number of radicals per particle, N_p the number of particles per unit volume of the continuous phase, M_m^o the initial moles of monomer per unit volume of the continuous phase, and N_A Avogadro's number. The average number of radicals per particle is defined as:

$$\bar{n}=\frac{\sum_{n=0}^{\infty} nN_n}{\sum_{n=0}^{\infty} N_n} \tag{4.4}$$

where N_n is the number of particles containing n radicals. Therefore, it is necessary to know the concentration of monomer in the polymer particles and the number of particles containing a given number of radicals to predict the experimental data.

4.2.1 Population Balances

The population balance of the number of particles containing n radicals was expressed by Smith and Ewart[9] as:

$$\begin{aligned}\frac{dN_n}{dt}=&\rho(N_{n-1}-N_n)+k[(n+1)N_{n+1}-nN_n]\\&+c[(n+2)(n+1)N_{n+2}-n(n-1)N_n]\end{aligned} \tag{4.5}$$

where ρ is the first-order entry rate coefficient for radicals into the polymer particles, k the desorption rate coefficient for radicals from the polymer particles, and c the bimolecular termination rate coefficient for free radicals in a particle. The first-order rate coefficient for radical entry into particles can be

expressed as:

$$\rho = k_a^p C_R^w \tag{4.6}$$

in which k_a^p is the second-order entry rate coefficient for radicals into the polymer particles and C_R^w the concentration of radicals in the aqueous phase in molecular units.

Monomer droplets are assumed to disappear by nucleation and coagulation with polymer particles, thus the rate of monomer droplet disappearance can be written as:

$$\frac{dN_d}{dt} = -k_a^d C_R^w N_d - k_c N_d N_p \tag{4.7}$$

where N_d is the number of monomer droplets, k_a^d the second-order rate coefficient for radical entry into monomer droplets, and k_c the coagulation coefficient for polymer particles and droplets. The coagulation between droplets is neglected in this study because of the assumption of monodisperse droplets and that coagulation is more important when the size difference between the droplets are large[14]. The rate of change of the number of particles containing one radical is expressed as:

$$\frac{dN_1}{dt} = k_a^p C_R^w (N_0 - N_1) + k(2N_2 - N_1) + k_a^d C_R^w N_d \tag{4.8}$$

The rate of change of the concentration of radicals in the aqueous phase can be written in terms of the generation of primary radicals by initiator decomposition, desorption of radicals from the particles, absorption of radicals by the particles and droplets, and termination of radicals in the aqueous phase:

$$\frac{dC_R^w}{dt} = 2fk_I C_I + \frac{k_d \phi_w N_1}{N_A} + \frac{2k_d \phi_w N_2}{N_A} - \frac{(k_a^d N_d + k_a^p N_p) C_R^w \phi_w}{N_A} - 2k_{tw} (C_R^w)^2 \tag{4.9}$$

where f is the initiator efficiency factor, k_I the rate constant for initiator decomposition, C_I the initiator concentration, ϕ_w the volume fraction of water in the aqueous phase, and k_{tw} the radical termination rate constant in the aqueous

phase.

4.2.2 Equilibrium Concentrations

The equilibrium concentration of each component in each phase can be determined from the equilibrium swelling thermodynamics. This treatment for polymer particles was initially developed by Morton et al.[15] and was subsequently used and modified by many investigators. Ugelstad et al.[11] used the thermodynamic treatment to study the effect of low molecular weight and low water solubility compounds in the particles on the swelling capability of the polymer particles. Tseng et al.[16] treated thermodynamically the effect of the presence of a small amount of water in the latex particles on their swelling capability. Guillot[17], Delgado[12] and Rodriguez[18, 8] applied the thermodynamic treatment to obtain the comonomer distribution during an emulsion polymerization process.

The equilibrium swelling thermodynamics is based on the idea that the equilibrium condition is attained when the partial molar free energies of mixing of monomer in all phases are the same. The equilibrium condition can be expressed as:

Monomer droplets—aqueous phase

$$\left(\frac{\overline{\Delta G}}{RT}\right)_i^d = \left(\frac{\overline{\Delta G}}{RT}\right)_i^a \tag{4.10}$$

Polymer particles—aqueous phase

$$\left(\frac{\overline{\Delta G}}{RT}\right)_i^p = \left(\frac{\overline{\Delta G}}{RT}\right)_i^a \tag{4.11}$$

where $\overline{\Delta G}$ is the change in the Gibbs free energy, R the gas constant, T the temperature; a stands for aqueous phase, d for droplets, p for particles and i for a component.

The partial molar free energy of mixing of a component i in phase q is given by the Flory-Huggins lattice theory of polymer solutions[19], with the addition of an interfacial energy term for spherical phases[15], and was expressed by Ugelstad et al.[11] as:

$$\left(\frac{\overline{\Delta G}}{RT}\right)_i^q = \ln\phi_{i,q} + \sum_{j=1,j\neq i}^{n}(1-m_{ij})\phi_{j,q} + \sum_{j=1,j\neq i}^{n}\chi_{ij}\phi_{j,q}^2$$

$$+ \sum_{j=1,j\neq i}^{n-1}\sum_{k=j+1,\neq i}^{n}\phi_{j,q}\phi_{k,q}(\chi_{ij}+\chi_{ik}-\chi_{jk}m_{ij}) + \frac{2\gamma\overline{V}_i}{rRT} \qquad (4.12)$$

where $\phi_{i,q}$ is the volume fraction of component i in phase q, m_{ij} the ratio of the equivalent number of molecular segments between i and j (usually expressed as the ratio of molar volumes of i and j), χ_{ij} the Flory-Huggins interaction parameter, γ the interfacial tension, $\overline{V}_i$ the molar volume of component i, and r the radius of the phase. Thus the partial molar energy of monomer in each phase can be expressed as:

i. <u>monomer droplets</u>:

$$\left(\frac{\overline{\Delta G}}{RT}\right)_m^d = \ln\phi_{m,d} + (1-m_{mc})\phi_{c,d} + \chi_{mc}\phi_{c,d}^2 + \frac{2\gamma_d\overline{V}_m}{r_dRT} \qquad (4.13)$$

ii. <u>aqueous phase</u>:

$$\left(\frac{\overline{\Delta G}}{RT}\right)_m^a = \ln\phi_{m,w} + (1-m_{mw})\phi_{w,a} + \chi_{mw}\phi_{w,a}^2 \qquad (4.14)$$

iii. <u>monomer-polymer particles</u>:

$$\left(\frac{\overline{\Delta G}}{RT}\right)_m^p = \ln\phi_{m,p} + (1-m_{mc})\phi_{c,p} + (1-m_{mp})\phi_{p,p} + \chi_{mc}\phi_{c,p}^2 +$$

$$\chi_{mp}\phi_{p,p}^2 + \phi_{c,p}\phi_{p,p}(\chi_{mc}+\chi_{mp}-\chi_{cp}m_{mc}) + \frac{2\gamma_p\overline{V}_m}{r_pRT} \qquad (4.15)$$

Material balance for each phase:

Material balance for the droplets

$$\phi_{m,d}+\phi_{c,d}=1 \tag{4.16}$$

Material balance for the aqueous phase

$$\phi_{m,a}+\phi_{w,a}=1 \tag{4.17}$$

Material balance for the polymer particles

$$\phi_{m,p}+\phi_{c,p}+\phi_{p,p}=1 \tag{4.18}$$

Material balance for the components:

Material balance for monomer

$$M_m^o\overline{V}_m(1-x)=\phi_{m,p}V_p+\phi_{m,d}V_d+\phi_{m,a}V_a \tag{4.19}$$

Material balance for cetyl alcohol

$$M_c^o\overline{V}_c=\phi_{c,d}V_c+\phi_{c,p}V_p \tag{4.20}$$

Material balance for water

$$M_w^o\overline{V}_w=\phi_{w,a}V_a \tag{4.21}$$

Material balance for polymer

$$M_m^o\overline{V}_m x=\phi_{p,p}V_p \tag{4.22}$$

where M_i^o is the initial moles of component i, x the fractional conversion and V_q the volume of phase q.

The solution to the above set of equations will provide the volume fraction of every component in the three phases and the average radius of droplets and particles as a function of conversion. The equilibrium concentrations can be expressed as:

$$C_{ei,q}=\phi_{i,q}/\overline{V}_i \tag{4.23}$$

4.2.3 Entry Rate Coefficient

There are four radical entry models which have been proposed for emulsion polymerization: collisional entry[20, 21], diffusive entry[22, 23], colloidal entry[24] and propagational entry[25]. In the collisional model, radicals enter the polymer particles by collision of oligomeric radicals with polymer particles and the rate of entry is determined by the collisional frequency between them. The entry rate is predicted to be proportional to the square of the particle radius. The diffusive model assumes that radical entry into the polymer particles is controlled by the rate of radical diffusion in the aqueous phase and predicts the entry rate to be proportional to the particle radius. The colloidal entry model assumes that the entering unit is a small colloidal precursor particle which may be a single polymer chain of sufficiently high degree of polymerization or an aggregate of smaller polymer chains formed in the aqueous phase. This model predicts that the entry rate is proportional to the particle radius. The propagational model proposes that the growth of the free radicals in the aqueous phase to a critical degree of polymerization is the rate-determining step for free-radical entry into the polymer particles, at which the entry of the free radicals into the polymer particles is instantaneous. This model predicts that the entry rate is independent of the particle radius. All of these models show that the second-order entry rate coefficient for radicals into polymer particles, k_a^p, is a function of the number of particles.

The second-order entry rate coefficient for radicals into polystyrene/styrene particles, k_a^p, was found experimentally by Penboss et al.[26] to be in the range of $5x10^5$ to $5x10^6$ $dm^3mol^{-1}s^{-1}$. The collisional model predicts k_a^p to be in the range of 10^{15} to 10^{16} $dm^3mol^{-1}s^{-1}$ and the diffusive model in the range of 10^9 to 10^{10} $dm^3mol^{-1}s^{-1}$. Asua et al.[27] used kinetic parameter estimation of experimental data to evaluate these proposed models and

concluded that the propagational model gave the best fit to the experimental data with k_a^p equal to 1.25×10^6 $dm^3 mol^{-1} s^{-1}$.

In this work, the adjustable parameter which will be used is the second-order entry rate coefficient for radicals into monomer droplets and polymer particles. The second-order entry rate coefficient for monomer droplets, k_a^d, is very difficult to determine experimentally, because of the difficulty of determining their number during a reaction. However, it was demonstrated that the second-order entry rate coefficient for monomer droplets is about an order of magnitude smaller than that of the polymer particles[2, 6]. In this work, the second-order entry rate coefficient for droplets is assumed to be a constant fraction of that of the particles.

4.2.4 Desorption Rate Coefficient

The desorption rate coefficient for radicals from the particles was first derived theoretically by Nomura et al.[28, 29] using both stochastic and deterministic approaches. It was assumed that only single-unit monomeric radicals desorb from the polymer particles and the reaction of the desorbed monomeric radicals in the aqueous phase was negligible. This theory was refined by Asua et al.[10] by taking into account the reaction of the desorbed monomeric radicals in the aqueous phase. The desorption rate coefficient was derived as:

$$k = \frac{k_{fm} C_m^p K_o}{\beta K_o + k_p C_m^p} \tag{4.24}$$

where k_{fm} is the monomer chain transfer constant, K_o the rate of diffusion of monomeric radicals out of the particles, and β the probability that the desorbed monomeric radicals react in the aqueous phase by either propagation or termination and is given as:

$$\beta = \frac{k_p C_m^w + k_{tw} C_R^w}{k_p C_m^w + k_{tw} C_R^w + (k_a^d N_d + k_a^p N_p)\phi_w / N_A} \tag{4.25}$$

where C_m^w is the concentration of monomer in the aqueous phase.

The rate of diffusion of monomeric radicals out of the particles was derived by Nomura[29] by assuming a diffusion mechanism and no resistance at the interface and was expressed as:

$$K_o = \frac{12 D_w / m_d d_p^2}{1 + 2 D_w / m_d D_p} \tag{4.26}$$

where D_w and D_p are the diffusion coefficients of monomeric radicals in the aqueous phase and in the polymer particles, respectively, m_d the partition coefficient of monomeric radicals between the particles and the aqueous phase, and d_p the diameter of the particles. The value of D_p is dependent on the monomer concentration in the particles. Experimental values of D_p obtained by Ferry et al.[30] as a function of of the volume fraction of polymer in the particles ($\phi_{p,p}$) were fitted with a polynomial as:

$$D_p = 4.0x10^{-5} + 1.5x10^{-5}\phi_{p,p} - 4.6x10^{-3}\phi_{p,p}^2 + 6.8x10^{-2}\phi_{p,p}^3 - 0.56\phi_{p,p}^4 + 2.7\phi_{p,p}^5 - 8.0\phi_{p,p}^6 + 0.14\phi_{p,p}^7 - 0.13\phi_{p,p}^8 + 5.3\phi_{p,p}^9 \tag{4.27}$$

4.2.5 Coagulation Coefficient for Droplets and Particles

The studies of miniemulsion polymerizations by Chamberlain et al.[2], Choi et al.[5, 6], Delgado[4] and Rodriguez[7] suggest that monomer droplets do disappear at a certain point in the polymerization. Chamberlain et al. assumed that monomer droplets disappear only by diffusion of monomer to the polymer particles. However, Delgado[4] showed that the presence of water-insoluble compounds, fatty alcohols or long-chain alkanes, in the droplets prevents the complete disappearance of monomer droplets by molecular diffusion of monomer. There, the disappearance of the monomer droplets is likely to be due

to the coagulation between droplets and particles[4, 7], and this becomes more important when the size difference between them becomes large[14]. Therefore in this work the coagulation of particles and droplets based on the DLVO theory[13] and the Muller Equation[14], will be applied to explain the disappearance of monomer droplets during the polymerization.

The coagulation coefficient for particles and droplets can be calculated based on the Muller Equation[14]:

$$k_c = V_t\left(\frac{2r_p k_B T}{3r_d \mu W_{dp}}\right)\left(1+\frac{r_d}{r_p}\right)^2 \tag{4.28}$$

where V_t is the total volume of the system, r_p and r_d are the radii of particle and droplet, respectively, k_B the Boltzmann constant, μ the viscosity of the medium and W_{dp} the Fuchs stability ratio[31].

The stability ratio W_{dp} can be written as[32, 33]:

$$W_{dp} = 2\int_2^{\infty}\left(\frac{e^{(\Phi_T(s)/k_B T)}}{s^2}\right)ds \tag{4.29}$$

where Φ_T is the total potential energy and s the ratio of the center-to-center distance to the average of the radii. This ratio can be estimated from the relationship[13]:

$$W_{dp} \approx \left(\frac{r_d + r_p}{2\kappa r_d r_p}\right) e^{(\Phi_{T\,max}/k_B T)} \tag{4.30}$$

where κ^{-1} is the thickness of the double layer and $\Phi_{T\,max}$ the height of the energy barrier to coagulation. The value of $\Phi_{T\,max}$ can be obtained from DLVO theory[34] as the maximum relative to s in the interparticle potential function:

$$\Phi_{T\,max} = {}^{max}_{s}(\Phi_T(s)) = {}^{max}_{s}(\Phi_A(s) + \Phi_R(s)) \tag{4.31}$$

where Φ_A is the van der Waals attractive potential and Φ_R the electrostatic repulsive energy.

The van der Waals attractive potential energy was derived by Hamaker[35] as:

$$\Phi_A = \frac{-A}{6}\left[\frac{2r_d r_p}{R_{dp}^2-(r_d+r_p)^2}+\frac{2r_d r_p}{R_{dp}^2-(r_d-r_p)^2}+ln\left(\frac{R_{dp}^2-(r_d+r_p)^2}{R_{dp}^2-(r_d-r_p)^2}\right)\right] \tag{4.32}$$

where A is the Hamaker constant and R_{dp} the center-to-center distance between droplet and particle which can be expressed as a function of s:

$$R_{dp} = \frac{(r_d+r_p)s}{2} \tag{4.33}$$

The calculation of the electrostatic repulsive energy is complex. For particles whose radii are not greatly different and where the double layer thickness is small compared to the particle size ($\kappa r > 5$), Φ_R can be calculated by using the expression developed by Hogg et al.[36]:

$$\Phi_R = \frac{\varepsilon r_d r_p(\zeta_d^2+\zeta_p^2)}{4(r_d+r_p)}\left[\frac{2\zeta_d\zeta_p}{(\zeta_d^2+\zeta_p^2)}ln\left(\frac{1+e^{-\kappa L_{dp}}}{1-e^{-\kappa L_{dp}}}\right)+ln(1-e^{-2\kappa L_{dp}})\right] \tag{4.34}$$

where ζ_d and ζ_p are the zeta potentials for droplets and particles, respectively, and L_{dp} the surface separation between droplet and particle which can be expressed as:

$$L_{dp} = R_{dp}-(r_d+r_p) \tag{4.35}$$

The zeta potential can be calculated as[37]:

$$\zeta_i = \left(\frac{2k_BT}{z_+e_L}\right)ln\left(\frac{e^{\lambda_4}+1}{e^{\lambda_4}-1}\right) \tag{4.36}$$

where z_+ is the valency of a cation, e_L the electronic charge, and λ_4 is defined as:

$$\lambda_4 = \kappa\delta + ln\left(\frac{e^{\lambda_5}+1}{e^{\lambda_5}-1}\right) \tag{4.37}$$

where δ is the Stern layer thickness and λ_5 is:

$$\lambda_5 = \frac{z_+e_L\psi_{oi}}{2k_BT} \tag{4.38}$$

in which ψ_{oi} is the surface potential of droplet or particle.

The inverse electrical double layer thickness is calculated from:

$$\kappa = (8\pi e_L^2 N_A I_e/\varepsilon k_B T)^{1/2} \tag{4.39}$$

in which the permitivity of the dispersion medium is defined as:

$$\varepsilon = 4\pi\varepsilon_o\varepsilon_r \tag{4.40}$$

where ε_o is the permitivity of vacuum and ε_r the dielectric constant, and the ionic strength is calculated as:

$$I_e \equiv \frac{1}{2}\sum_j (C_{+jw}z_{+jw}^2 + C_{-jw}z_{-jw}^2) \tag{4.41}$$

where C is the concentration and z the valancy, the subscripts $+jw$ and $-jw$ stand for positive ion of component j and negative ion of component j in water, respectively.

It was demonstrated by Goetz[38] that the zeta potential of droplets is much smaller than that of polymer particles, thus the Debye-Huckel[13] (low potential) formula will be used to calculate the surface potential of the droplets:

$$\psi_{od} = \frac{4\pi r_d \sigma_{vd}}{\varepsilon(1+\kappa r_d)} \tag{4.42}$$

where σ_{vd} is the surface charge density for the droplets, and the Gouy-Chapman[13] (high potential) formula is used to calculate the surface potential of the particles:

$$\psi_{op} = \left(\frac{2k_BT}{z_+e_L}\right) sinh^{-1}\left(\frac{2\pi e_L z_+ \sigma_{vp}}{\varepsilon k_B T \kappa}\right) \tag{4.43}$$

where σ_{vp} is the surface charge density for the particles.

The surface charge density σ_{vi} is assumed to be derived from the contributions of both surfactant and initiator:

$$\sigma_{vi} = \sigma_{si} + \sigma_{Ii} \tag{4.44}$$

The ionic end group contribution, σ_{Ii}, was calculated using the method of Ottewill[32] and assuming that a fraction ω of the initiator end groups is on the surface of the particles. This is expressed as:

$$\sigma_{Ip} = \frac{2\rho_p e_L N_A r_p \omega}{3M_n} \tag{4.45}$$

where ρ_p is the density of the polymer and M_n the number average molecular weight of the polymer.

The surfactant contribution can be calculated[33] by assuming that the adsorption of surfactant follows the multicomponent Langmuir isotherm for the surface coverage, θ. Thus the particle and droplet surface coverage by surfactant can be expressed as:

$$\sigma_{si}=\frac{z_{+}e_{L}\theta_{si}}{a_{si}'} \tag{4.46}$$

where a_{si}' is the area occupied by a surfactant molecule. The surface coverages for particle and droplet are expressed as:

$$\theta_{sd}=\frac{b_{sd}C_{sw}}{(1+b_{sd}C_{sw}+b_{sp}C_{sw})} \tag{4.47}$$

and

$$\theta_{sp}=\frac{b_{sp}C_{sw}}{(1+b_{sd}C_{sw}+b_{sp}C_{sw})} \tag{4.48}$$

where b_{si} is the Langmuir isotherm constant and C_{sw} the concentration of surfactant in the aqueous phase, which can be obtained from a mass balance as:

$$C_{sw}=\frac{C_{st}V_{t}-(A_{d}\theta_{sd}/a_{sd}'N_{A})-(A_{p}\theta_{sp}/a_{sp}'N_{A})}{V_{w}} \tag{4.49}$$

where C_{st} is the total concentration of surfactant in the reactor, V_t the total volume of the reaction mixture, A_d and A_p are the total surface areas of the droplets and particles, respectively, and V_w the volume of the aqueous phase.

From these equations, the coagulation coefficient for droplets and particles can be calculated depending on the size and number of the droplets and particles.

4.2.6 Simulation algorithm

The mathematical simulation will be divided into many elementary events that can be treated as mathematically independent. Figure 4-1 shows the simulation algorithm used in the modeling. Before the initiator is added, the monomer droplets and the aqueous phase are in equilibrium. The concentrations of the components in each phase is calculated by solving a set of non-linear equations describing the thermodynamic equilibrium between droplets and the aqueous phase (Equations (4.10) to (4.22)). When the polymerization starts by adding initiator, the process is divided into a sequence of small time intervals (dt) during which particle nucleation from monomer droplets, polymerization inside the particles and transport of components occur simultaneously. At the beginning of each time interval, the coagulation coefficient between monomer droplets and polymer particles is estimated (Equations (4.28) to (4.49)), the equilibrium concentrations in the different phases are calculated (Equations (4.10) to (4.22)), and thus these calculated parameters are input to the system of differential equations describing nucleation, population balances and material balances (Equations (4.3) to (4.9) and (4.24) to (4.26)). All simulation were performed on the Cyber 850 mainframe computer. IMSL MATH/LIBRARY version 1.1 Fortran subroutines were used. Subroutine IVPAG, based on the Gear method, was used to solve the initial-value ordinary differential equations; subroutine NEQNF, using the finite difference Jacobian, was used to solve the nonlinear equations of the thermodynamic model.

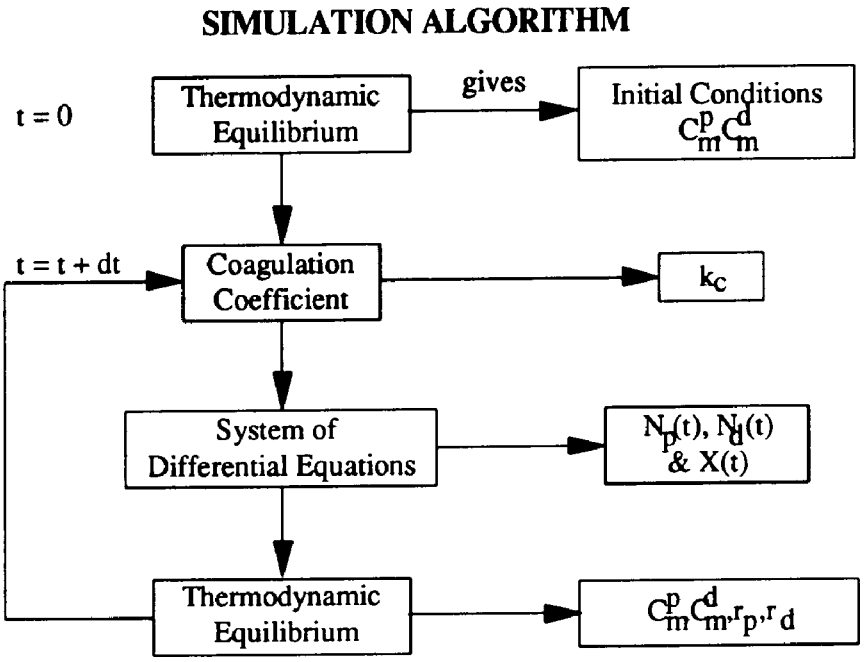

Figure 4-1: Simulation algorithm for the kinetics of styrene miniemulsion polymerization.

4.3 Results and Discussion

The simulated results will be compared to the experimental data obtained by Choi[6] on the polymerization of styrene miniemulsions for a wide range of initiator concentrations. The recipe consists of 25 ml of water, 8 ml of styrene, 10 mM sodium lauryl sulfate, 30 mM cetyl alcohol, 2.66 mM $NaHCO_3$ and 0.13 to 2.66 mM $K_2S_2O_8$. This model will concentrate on the nucleation stage and not attempt to predict the high conversion region of the polymerization (the gel effect). Monomer droplet nucleation is the only mechanism considered in this simulation, because the concentration of surfactant in the aqueous phase is about two orders of magnitude below the cmc (a typical value of surfactant concentration in the aqueous phase was calculated by the model to be 0.07 mM). It is assumed that once a monomer droplet captures a radical, it instantly becomes a polymer particle. The miniemulsion droplets are considered to be monodisperse droplets of 80 nm in diameter (based on Choi's[6] experimental work).

It is likely that at the beginning of the reaction, coagulation is not important due to the large droplet size which has higher surface potential energy. As the polymerization proceeds, monomer from the uninitiated droplets diffuses to the growing polymer particles until the monomer droplets become so small that coagulation between droplets and particles becomes important. Thus, the final number of particles is determined by nucleation in the monomer droplets and coagulation of droplets and particles. The only adjustable parameter used is the second order entry rate coefficient for radical into the polymer particles (for initiator concentration less than 2.66 mM); other parameters are shown in Table 4-1. The Flory-Huggins interaction parameters for the hexadecane system obtained by Rodriguez[7] were used for the cetyl alcohol system in this work. The area occupied by a surfactant molecule on a

Table 4-1: Parameters used in the Simulations.

Symbol	Value	Reference
m_{mc}	= 0.41	$\overline{V}_m/\overline{V}_c$
m_{mp}	= 7.0 x 10^{-5}	$\overline{V}_m/\overline{V}_p$
m_{mw}	= 1.28	39
χ_{mc}	= 1.69	7
χ_{mp}	= 0.35	7
χ_{mw}	= 7.97	39
χ_{cp}	= 5.4	7
γ_p	= 6 x 10^{-5} J dm^{-2}	7
γ_d	= 3 x 10^{-5} J dm^{-2}	7
a_{sp}'	= 43 $Å^2$molecule^{-1}	40
b_{sp}	= 2400 dm^3 mol^{-1}	40
a_{sd}'	= 60 $Å^2$molecule^{-1}	This Work
b_{sd}	= 620 dm^3 mol^{-1}	This work
A	= 6.5 x 10^{-21} J	32
δ	= 1.41 x 10^{-9} dm	41
ε_r	= 70	42
μ	= 4.042 x 10^{-3} kg dm^{-1} s^{-1}	43
ω	= 1	44
f	= 1	6
k_a^p	= 1.25 X 10^6 dm^3 mol^{-1} s^{-1}	27
k_d^d/k_a^p	= 0.07	This work
k_p	= 425.6 dm^3 mol^{-1} s^{-1}	45
c	= 1 s^{-1}	2
k_{tw}	= 3.7 x 10^9 dm^3 mol^{-1} s^{-1}	25
k_I	= 2.4 x 10^{-5} s^{-1}	45
k_{fm}	= 1.0 x 10^{-3} dm^3 mol^{-1} s^{-1}	This work
D_w	= 1.2 x 10^{-7} dm^2 s^{-1}	46

droplet (a_{sd}') was estimated based on the area occupied by a surfactant molecule on a particle (a_{sp}') with the assumption that the surfactant molecules on the surface of the droplets is reduced by 25% by the presence of cetyl alcohol. The Langmuir isotherm constant for droplets (b_{sd}) was based on the value found for polymethyl methacrylate[47] which has a similar value for the area occupied by a surfactant molecule for droplets. The monomer chain transfer constant (k_{fm}) used in this study is based on the value used by Asua et al.[10] and the results from Chapter 3 that cetyl alcohol decreases the exit of radicals from the polymer particles.

4.3.1 Magnitude of the Second Order Entry Rate Coefficient for Radicals into Monomer Droplets

The results in Chapter 2 showed that the rate of polymerization is a strong function of the stability of the droplets (or the number of droplets) and Chapter 3 showed that the presence of cetyl alcohol does not slow the entry of radicals into the polymer particles. The difference between the entry rate into the droplets and the particles is probably due the difference in their nature. It was demonstrated by Chamberlain et al.[2] and Choi[6] through mathematical modelling efforts that the rate coefficient for radicals entry into the monomer droplets was an order of magnitude less than the values determined for the seeded emulsion polymerization of styrene. However, it is very difficult to determine experimentally the rate coefficient for radical entry into the monomer droplets because of their instability and the difficulty in controlling the number of droplets during the reaction.

An attempt was made to investigate the entry rate of radicals into the monmer droplets by carrying out seeded polymerizations with various monomer/polymer swelling ratios; the recipe is shown in Table 4-2. The

Table 4-2: Recipe for Seeded Polymerization at Different Monomer to Polymer Swelling Ratios.

Ingredient	Amount
DDI Water	39.4 g
Styrene	0.54 -- 20.0 g
Polystyrene (92 nm)	0.4 g
Sodium Lauryl Sulfate	10 mM *
Cetyl Alcohol	30 mM *
Potassium Persulfate	1.33 or 2.66 mM *

* based on aqueous phase

concentration of particles (based on the aqueous phase) is the same for all experiments. The variables are the amount of styrene (or swelling ratio) and the initiator concentration. The method of swelling the polymer seed with cetyl alcohol was described in Chapter 3. Sodium lauryl sulfate, cetyl alcohol and water were mixed at 65°C for two hours to form the gel phase[7, 48], cooled to room temperature, and sonified to break up the gel phase. This aqueous gel phase was added to the clean latex and mixed overnight. Styrene was then added to the latex mixture followed by overnight swelling with mixing. No monomer layer was observed after swelling which indicated that the majority of monomer was with the swollen polymer particles. Dilatometry was used to monitor the conversion-time behavior of the polymerization. The reactions were carried out at 50°C.

Monomer/polymer swelling ratios (by weight) of up to 50 to 1 were

achieved. The final particle size for Run SCA11 (monomer/polymer swelling ratio of 50 to 1) was determined by TEM to be 296 nm in diameter with a coefficient of variation of 8% which is smaller than the 9% of the seed. These results indicate that no significant amounts of new particles were formed during the polymerization. The conversion-time data of these experiments are shown in Figure 4-2. The conversion was calculated in terms of grams of polymer formed per liter of the aqueous phase versus time so that comparisons could be carried out on an equal basis (the same number of particles based on the aqueous phase). Runs SCA9, SCA8, SCA7, SCA11 and SCA13 have monomer/polymer swelling ratios by weight of 1.36, 10, 15, 50 and 50 to 1, respectively. All runs had an initial initiator concentration of 1.33 mM (potassium persulfate) except for run SCA11 which had 2.66 mM. For the experiments at the same intiator concentration, the rate of polymerization (indicated by the slope of the conversion-time curve) increases with increasing swelling ratio up to a ratio of 15:1. In these experiments, the rate of polymerization is proportional to the product of the concentration of monomer in the particles and the average number of radicals per particle. The lower polymerization rate in Run SCA9 is due to the smaller particle size (resulting from the low swelling ratio) leading to a higher rate of radical desorption.

However, it is interesting that when the swelling ratio increases from 15:1 to 50:1, the rate of polymerization decreases; even doubling the amount of initiator (Run SCA11) produces a polymerization rate which is still slower than that with the 15:1 swelling ratio. This is because the average number of radicals per particle is decreased when the swelling ratio increases from 15:1 to 50:1 (Figure 4-3). This is not caused by radical desorption, since the higher swelling ratio one should result in a larger particle size and thus a lower desorption rate. The internal viscosity in these cases does not affect the

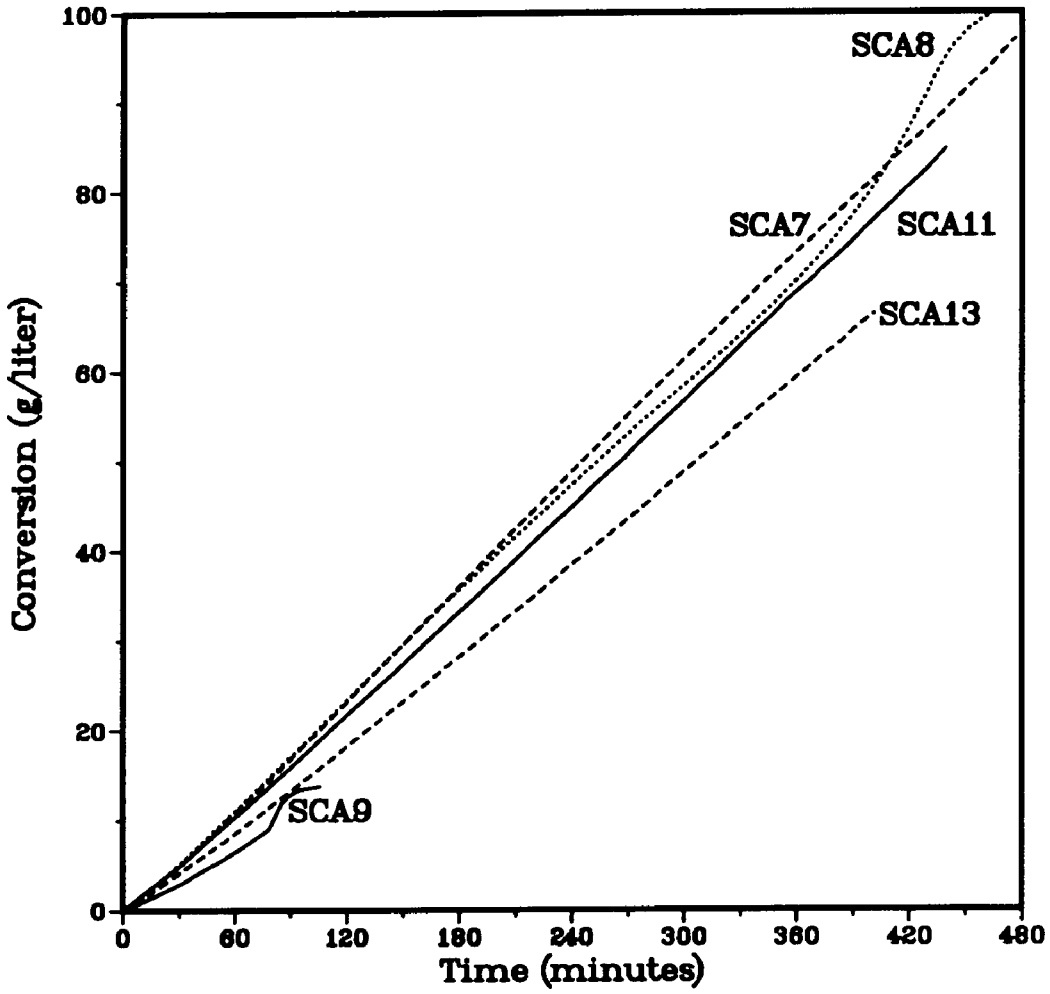

Figure 4-2: Conversion versus time for the seeded emulsion polymerizations of polystyrene/styrene at different monomer to polymer swelling ratio; SCA9: 1.36 to 1 ratio and 1.33 mM [I]; SCA8: 10 to 1 ratio and 1.33 mM [I]; SCA7: 15 to 1 ratio and 1.33 mM [I]; SCA13: 50 to 1 ratio and 1.33 mM [I]; and SCA11: 50 to 1 ratio and 2.66 mM [I].

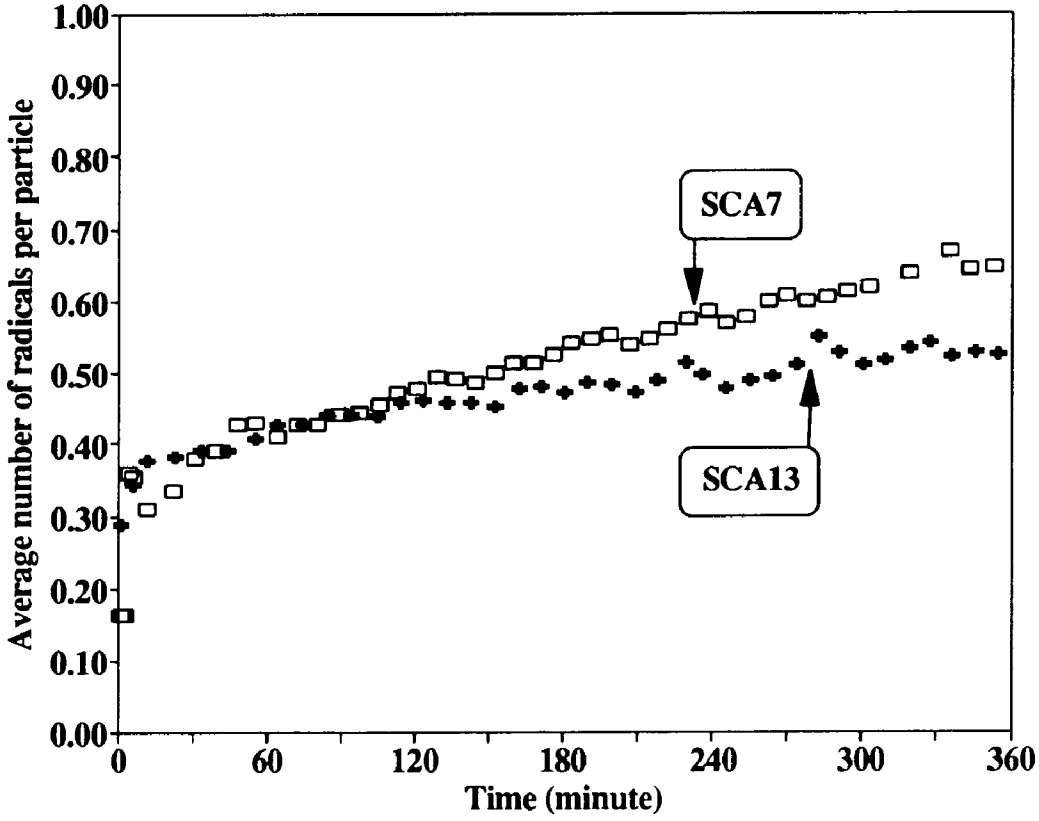

Figure 4-3: Average number of radicals per particle versus time for the seeded emulsion polymerizations of polystyrene/styrene monomer system at different monomer to polymer swelling ratio; SCA7: 15 to 1 ratio and 1.33 mM [I], and SCA13: 50 to 1 ratio and 1.33 mM [I].

diffusion of monomeric radicals due to the high concentration of monomer in the particles[30]. In other words, the low average number of radicals per particle for the high swelling experiment is due to the slow entry of radicals. These experiments also suggest that when the swelling ratio is high enough that the polymer particles exhibit a behavior closer to that of the monomer droplets, that is a reduced entry rate.

The parameter estimation method in chapter 3 was used to estimate the second order entry rate coefficient for radicals into the particles (k_a^p) and the exit rate coefficient for radicals from the particles (k) for runs SCA7 and SCA13 using data of up to 120 minutes where $\bar{n} < 0.5$ (Figure 4-3). This estimation from a single experiment may not yield accurate results, but the relative values of the results from runs SCA7 and SCA13 could provide useful information. For run SCA7, the following values were obtained: $k_a^p = 2.2 \times 10^6$ dm^3 mol^{-1} s^{-1} and $k = 4.9 \times 10^{-4}$ s^{-1}; and for run SCA13, $k_a^p = 1.4 \times 10^6$ dm^3 mol^{-1} s^{-1} and $k = 2.0 \times 10^{-4}$ s^{-1}. The differences between the values of k_a^p for runs SCA7 and SCA13 is about 40%, and these values are close to that found by Asua et al.[27] Still, at this high swelling ratio, the polymer concentration in the particles is about two percent, and it was suggested in Chapter 2 that the reduced entry rate of radicals into droplets may be better seen at less that one percent conversion. Although these experiments can not determine the absolute value of the entry rate coefficient for radicals into the monomer droplets due to the presence of at least 2% polymer in the particles, it suggests that the entry rate coefficient for radicals into the monomer droplets is much smaller than that of the particles.

A simulation was carried out to evaluate the magnitude of the entry rate coefficient of radicals into monomer droplets, containing cetyl alcohol, by assuming that the entry rate coefficient for radicals into droplets and particles are the same. The best fit of the experimental data was found when the value of

8 x 10^4 dm^3 mol^{-1} s^{-1} was used and the results are shown in Figure 4-4. Initially, the simulated data are able to keep up with the experimental ones due to the nucleation of particles from monomer droplets. However, at higher conversions when the rate of particle nucleation decreases due to the decreasing number of monomer droplets, the simulated polymerization rate is much slower than the experimental one. This is because a lower value of the entry rate coefficient into the particles (which is the same as that of the droplets) was necessary to fit the initial data when nucleation is more important, and at higher conversion when polymerization within the particles is more important, the simulation predicts a much lower number. Besides, the value of the entry rate coefficient for particles of 8 x 10^4 dm^3 mol^{-1} s^{-1} is about an order of magnitude lower than the lower limit of the experimental data by Penboss et al.[26]. Therefore, in all subsequent simulations the entry rate coefficient into monomer droplets was used as a constant fraction of that of the particles (for example, k_a^d / k_a^p of 0.07). This value was obtained by fitting Choi's experimental data obtained for an initiator concentration of 2.66 mM.

4.3.2 The Fate of Monomer Droplets

It was demonstrated by Choi[6] that not all monomer droplets become particles; only a fraction of the droplets (approximately 0.2) become particles and this fraction increases with increasing initiator concentration. Chamberlain et al.[2] assumed that monomer droplets disappear only by diffusion of monomer to the growing polymer particles. They derived an expression for the monomer droplets disappearance as a function of conversion and predicted that the droplets disappear around 30 percent conversion. However, Delgado[4] showed that the presence of water-insoluble compounds (fatty alcohol or long-chain alkane) in the droplets prevents the complete disappearance of monomer

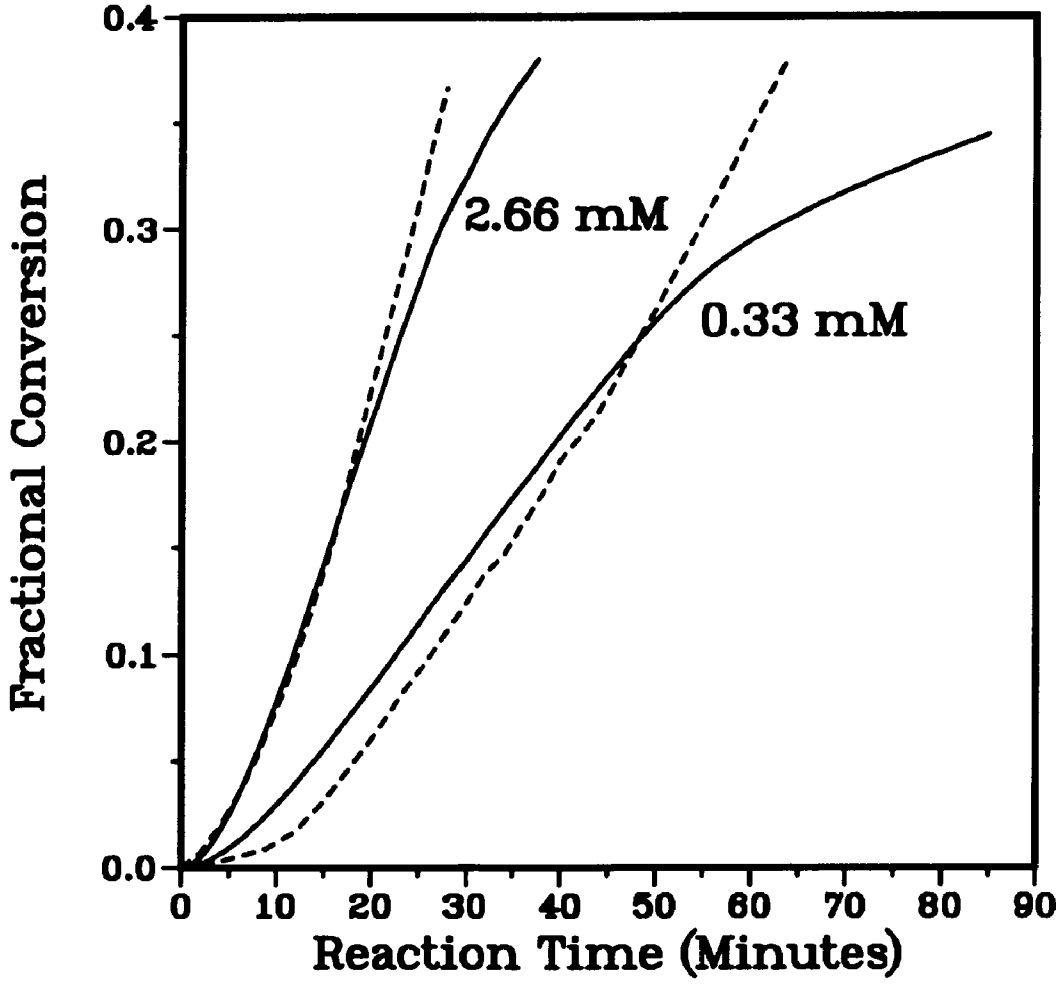

Figure 4-4: Conversion versus time simulations for miniemulsion polymerization of styrene using $k_a^d = k_p^d = 8 \times 10^4$ dm^3 mol^{-1} s^{-1} at different initiator concentrations (2.66 and 0.33 mM); dashed lines: Choi's experimental data[6], solid lines: simulation.

droplets by molecular diffusion of monomer. The results from Chamberlain et al.[2], Choi et al.[5, 6], Delgado[4] and Rodriguez[7] suggest that monomer droplets do disappear at a certain point in the polymerization, but it is likely that this disappearance is due to coagulation between droplets and particles. The coagulation between particles themselves should be negligible due to their large size (≈ 70 nm in diameter) and high surface charge density. When the size of the droplets becomes small enough by diffusion of monomer to the polymer particles, they become unstable toward polymer particles. With the assumption of monodisperse droplets, the coagulation between droplets can be neglected due to their similar size. This may not be valid if monomer droplets have a wide size distribution. However, Choi[6] used the Microfluidizer to prepare the miniemulsions which are likely to have narrow droplet size distributions (as indicated from the results in Chapter 2), and thus the assumption of monodisperse droplets is reasonable for this study.

In an attempt to distinguish between the different kinetic transitions during an emulsion polymerization, Choi[6] plotted his experimental data as the rate of polymerization versus conversion as reproduced in Figure 4-5. Initially, the rate of polymerization increases to about 35% conversion followed by a decrease. The initial increasing rate was attributed to the nucleation of particles from monomer droplets (Interval I) and the decreasing region the cessation of nucleation with the polymerization consuming the remaining monomer in the particles (Interval III). However, this may not be true for miniemulsion polymerization; a decreasing rate of polymerization may exist even when monomer droplets are still present in the system. This is contrary to conventional systems in which the polymerization rate is relatively constant while monomer droplets are still present in the system (Interval II). This phenomenon is caused by the presence of a compound such as cetyl alcohol or

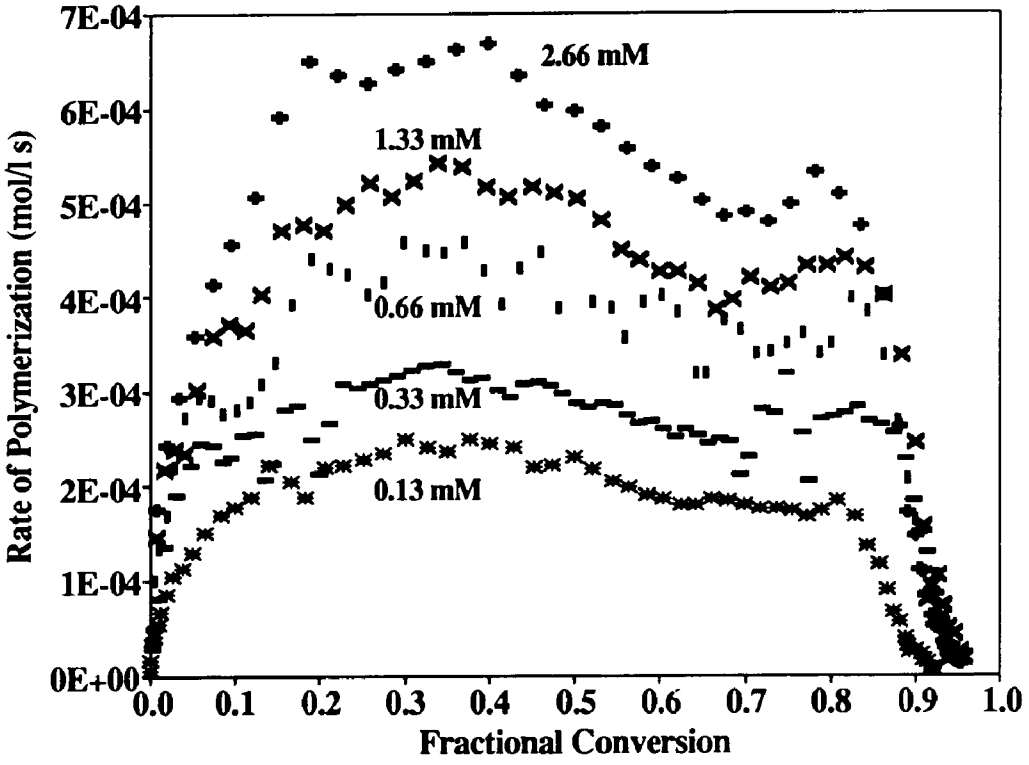

Figure 4-5: Rate of polymerization versus fractional conversion for miniemulsion polymerization of styrene from Choi's experimental results at different potassium persulfate initiator concentrations[6].

hexadecane with low molecular weight and low water solubility in the monomer droplets that causes the concentration of monomer in the polymer particles to be less than the conventional equilbrium value of 6.2 mol dm^{-3}. Figure 4-6 shows a typical monomer concentration profiles. Before the polymerization starts the concentration is above 6.2 mol dm^{-3} due to the absence of polymer. When polymerization begins, the concentration of monomer within the polymer particles is below the conventional equilibrium concentration even during the nucleation period. With the presence of cetyl alcohol in the monomer droplets, the concentration of monomer in the aqueous phase is about half of the solubility of monomer at 70°C[49]. Therefore, the droplets may not disappear by 30% conversion, but may disappear at a higher conversion or may not disappear at all during the reaction. This can be better understood by carrying out a simulation assuming that no droplets disappear during the polymerization (or coagulation constant, k_c, is zero).

The results of the simulation assuming no droplets disappear during the polymerization is shown in Figure 4-7 in which the rate of polymerization is plotted versus conversion for an initiator level of 2.66 mM. The model predictions are good for the data in the increasing rate period, but in the decreasing rate region the rate of polymerization is predicted to be higher than the experimental data ($0.4 < x < 0.6$). This indicates that the model predicts a high number of particles nucleated. The corresponding evolution of particles and droplets as a fraction of the initial number of droplets is shown in Figure 4-8. The results show that when the coagulation coefficient is assumed to be zero ($k_c = 0$), the final number of particles is close to the initial number of droplets (more than 80% of the initial droplets) which is about twice as much as the experimental number of particles (0.68×10^{18} dm^{-3}). The prediction of the number of particles is closer to the experimental data when the monomer

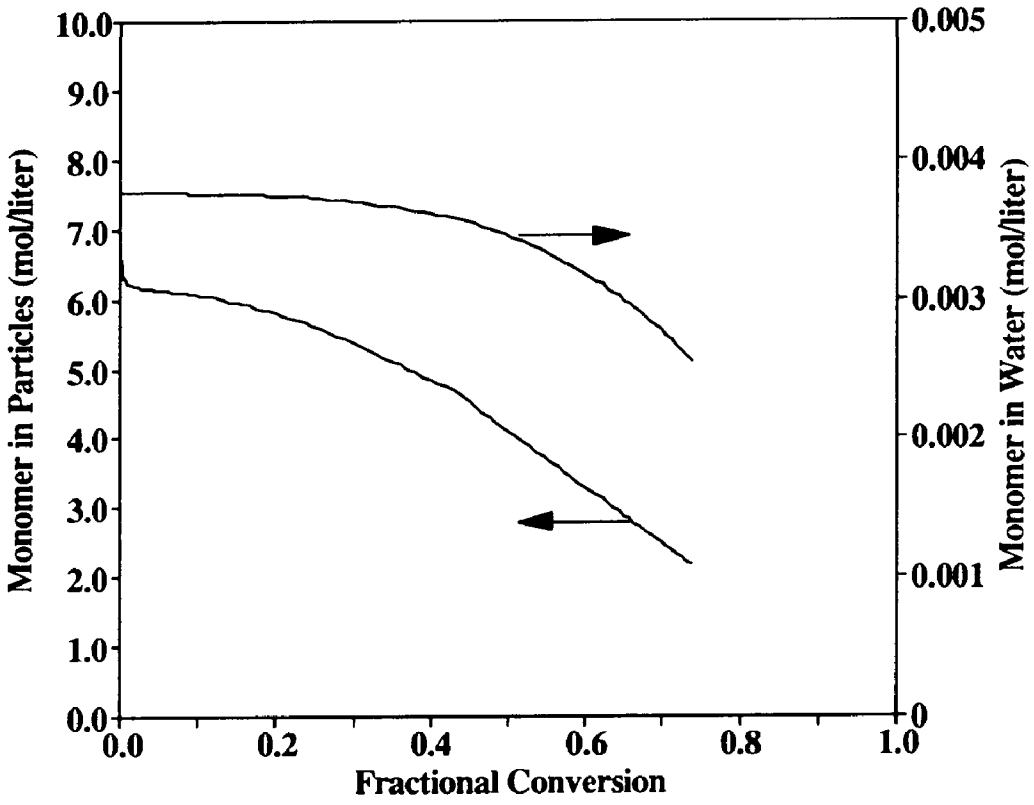

Figure 4-6: Concentration of styrene in the particles and in the aqueous phase versus fractional conversion from simulation of miniemulsion polymerization of styrene with initiator concentraion of 2.66 mM

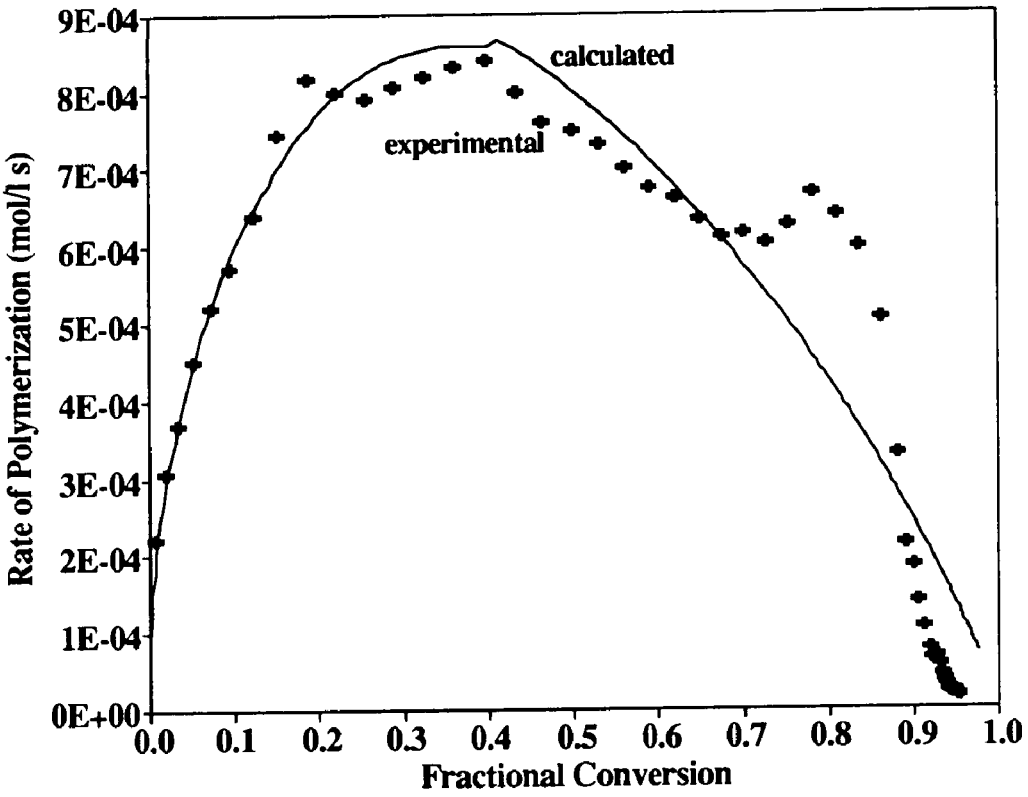

Figure 4-7: Comparison of simulated and Choi's experimental data for miniemulsion polymerization of styrene (2.66 mM potassium persulfate); simulation assumes droplets do not disappear.

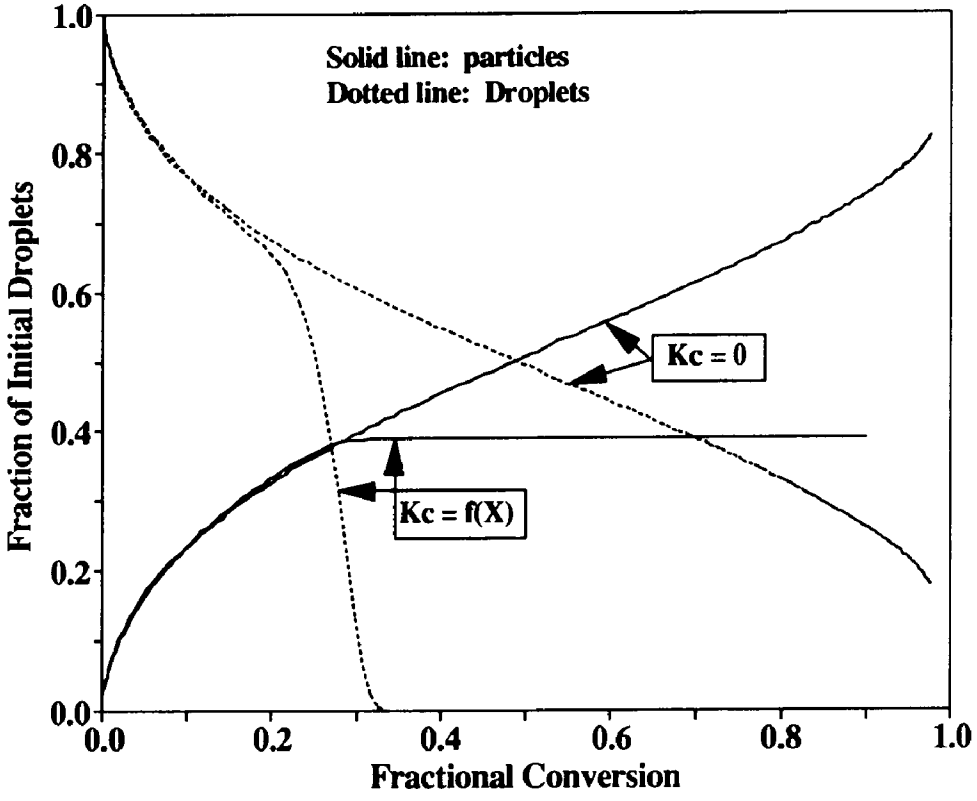

Figure 4-8: Evolution of particles and droplets as a fraction of the initial droplets with conversion from simulation of miniemulsion polymerization of styrene at 2.66 mM potassium persulfate for no droplet disappearance ($k_c = 0$) and droplet disappear at about 30% conversion($k_c = 10^{-15}exp[40(x - 0.43)]$); solid lines: number of particles as a fraction of the initial number of droplets and dotted lines: number of droplets as fraction of the initial droplets.

droplets are assumed to disappear at about 30% conversion (at which k_c = 1 x 10^{-17} dm^{-3} s^{-1}). These results suggest that the monomer droplets disappear sometime during the reaction and this is likely to take place in the conversion range from 30 to 60%.

The above results suggest that coagulation is unimportant initially and becomes more important as the conversion increases. Thus a simple empirical expression for the coagulation coefficient as an exponentially increasing function of conversion was written as:

$$k_c = 10^{-15} exp[40(x-0.43)] \tag{4.50}$$

The value of 0.43, in the above equation, results in monomer droplets disappearing at about 34% conversion. This correlation predicts that at low conversion coagulation is not important, and its importance increases with conversion until a conversion of about 34% is reached at which the collisions between the droplets and particles result in coagulation. This expression was incorporated into the model to predict the experimental data and the results are shown in Figure 4-9 which shows conversion-time curves for a wide range of initiator concentrations. At higher initiator concentrations, the predictions are close to the experimental data but become worse at lower initiator concentrations. This is likely because the second order entry rate coefficient for particles is a function of the number of particles leading to higher values for higher numbers of particles present in the system[20, 21, 22, 23, 24]. Therefore, as the concentration of initiator is decreased, the number of particles nucleated also decreases and thus the second order entry rate coefficient for particles decreases with the initiator concentration. The model predicts the experimental data better when a decreasing value of the second order entry rate coefficient for particles (k_a^p) with decreasing initiator was used. The results are shown in Figure 4-10 using k_a^p in the range of 1.25 x 10^6 -- 0.73 x 10^6 dm^3 mol^{-1} s^{-1} for

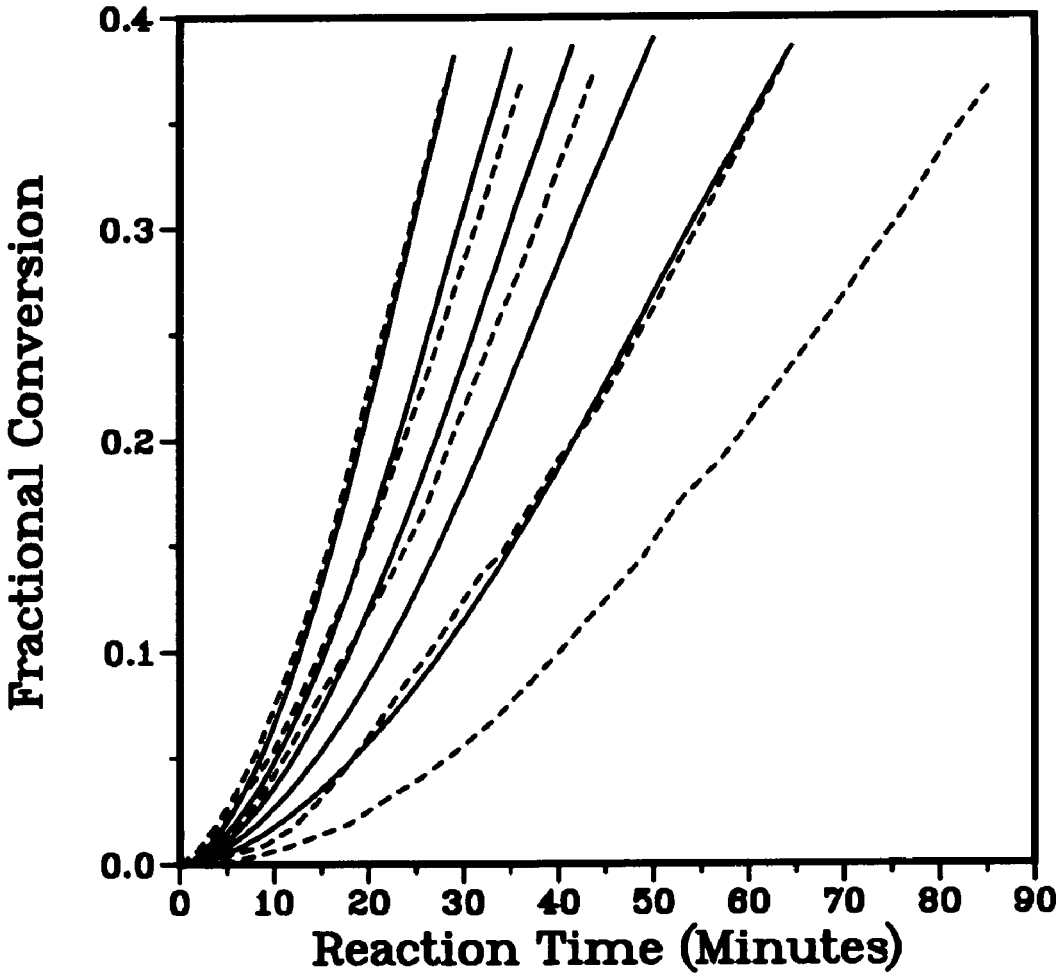

Figure 4-9: Comparison of simulated versus experimental conversion histories for the miniemulsion polymerization of styrene using various initiator concentrations (2.66, 1.33, 0.66, 0.33 and 0.13 mM potassium persulfate, respectively from left to right); simulation assumes the coagulation coefficient between droplets and particles is a function of conversion (Equation (4.50)); dashed lines: Choi's experimental data, solid lines: simulations.

initiator concentration in the range of 2.66 -- 0.13 mM.

These results can be examined further by plotting the rate of polymerization versus conversion as shown in Figure 4-11. These results indicate that when the monomer droplets are assumed to disappear around 34% conversion, the predicted rate of polymerization is much slower than that found experimentally. In order for the predictions to be closer to the experimental data, nucleation has to continue beyond 34% conversion. The model predictions are much better when it is assumed that the monomer droplets disappear around 55% conversion as shown on Figure 4-12. These simulations suggest that coagulation between droplets and particles becomes more important with increasing conversion or when the monomer droplets are small enough to be unstable toward the polymer particles. Thus the DLVO theory[13] and the Muller Equation[14] may be applied to study the stability of the monomer droplets during the polymerization.

4.3.3 Applying the DLVO Theory and the Muller Equation to Study the Stability of Monomer Droplets

The DLVO theory[13] was used by Ugelstad and Hansen[50] to explain the coagulation of polymer particles and the precipitating oligomers in homogeneous nucleation, and by Gilbert and Napper et al.[24, 41, 51] to explain the coagulation between stable particles and precursor particles in coagulative nucleation theory. The DLVO theory and the Muller Equation can also be applied to predict the stability of monomer droplets during miniemulsion polymerization. The Muller Equation predicts that coagulation becomes more important when the difference in size between the particles and droplets increases.

The DLVO theory was used to calculate the maximum total potential energy, the height of the energy barrier to coagulation, and the results at

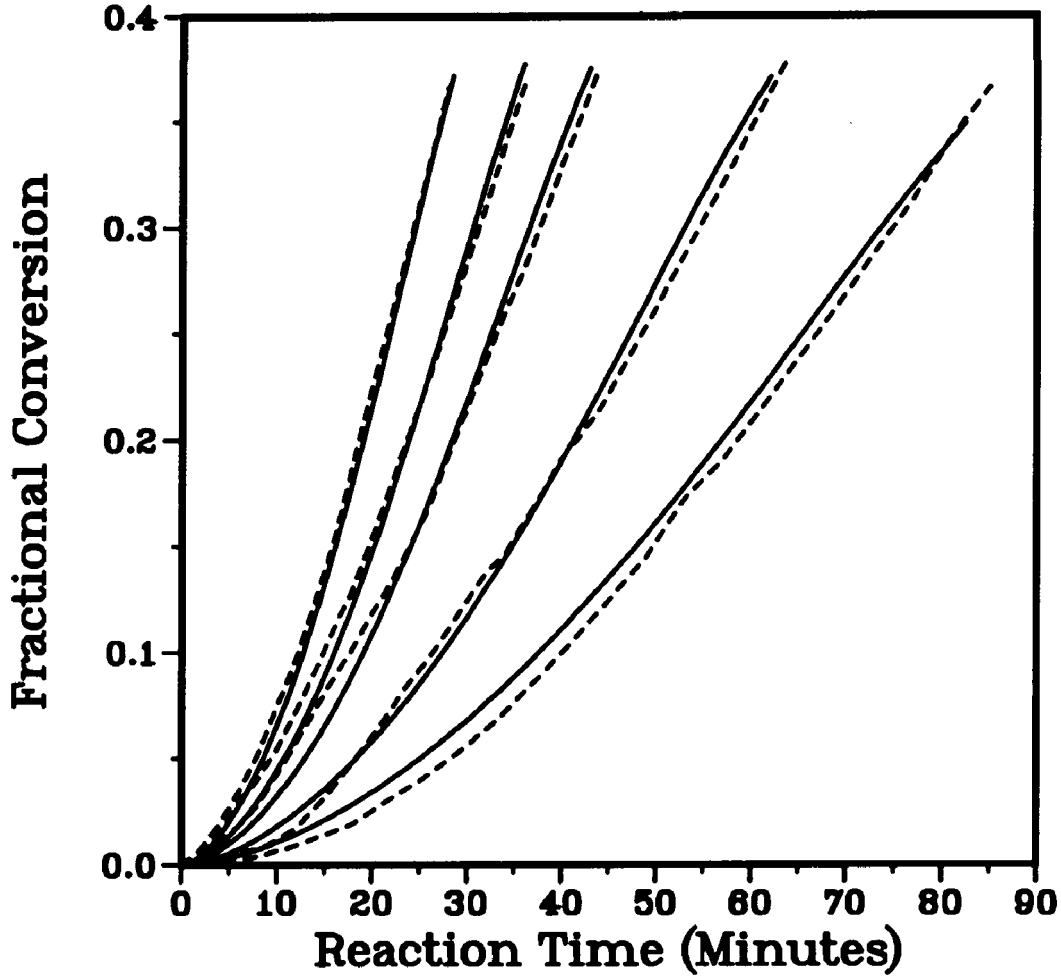

Figure 4-10: Comparison of simulated versus experimental conversion histories for the miniemulsion polymerization of styrene using various initiator concentrations (decreasing from left to right); simulation assumes the coagulation coefficient between droplets and particles is a function of conversion (Equation (4.50)) and adjusting k_a^p with initiator concentration: 1.25 x 10^6 dm^3 mol^{-1} s^{-1} for 2.66 mM [I], 1.12 x 10^6 dm^3 mol^{-1} s^{-1} for 1.33 mM [I], 1.10 x 10^6 dm^3 mol^{-1} s^{-1} for 0.66 mM [I], 0.81 x 10^6 dm^3 mol^{-1} s^{-1} for 0.33 mM [I], 0.73 x 10^6 dm^3 mol^{-1} s^{-1} for 0.13 mM [I]; dashed lines: Choi's experimental data, solid lines: simulations.

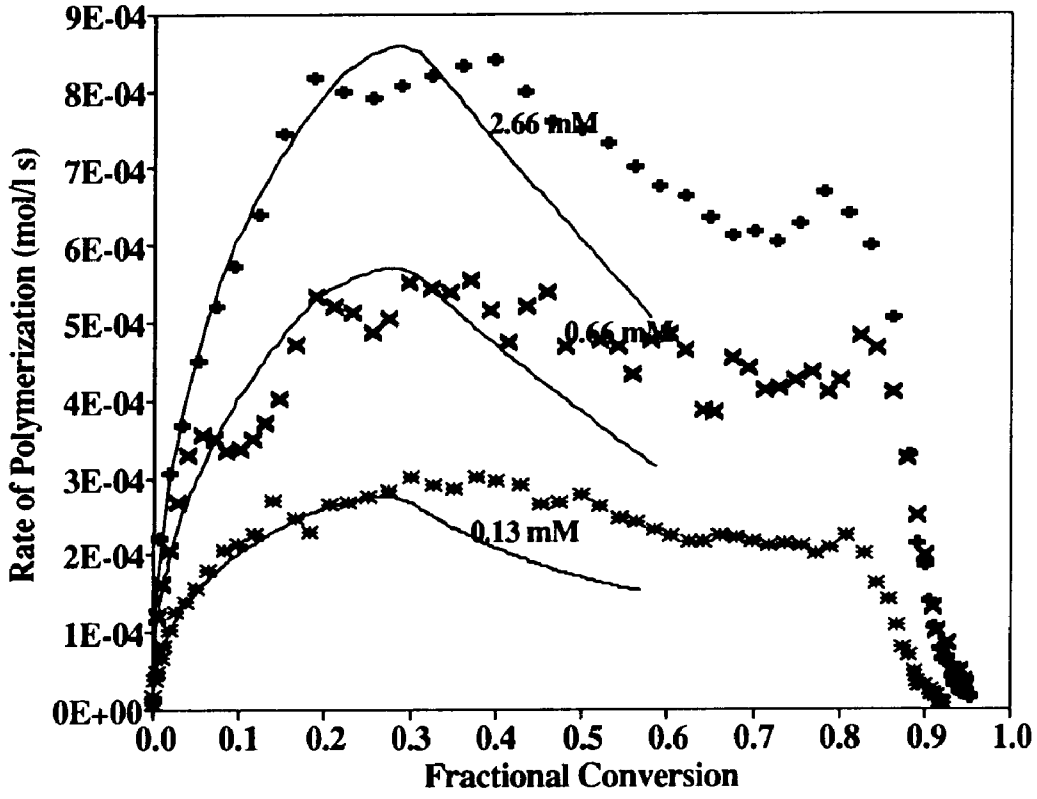

Figure 4-11: Rate of polymerization of styrene miniemulsion versus fractional conversion from simulation by assuming the coagulation coefficient as a function of conversion using Equation (4.50) and adjusting k_a^p with initiator concentration: 1.25 x 10^5 dm^3 mol^{-1} s^{-1} for 2.66 mM [I], 1.10 x 10^5 dm^3 mol^{-1} s^{-1} for 0.66 mM [I], 0.73 x 10^5 dm^3 mol^{-1} s^{-1} for 0.13 mM [I]; dashed lines: Choi's experimental data, solid lines: simulations.

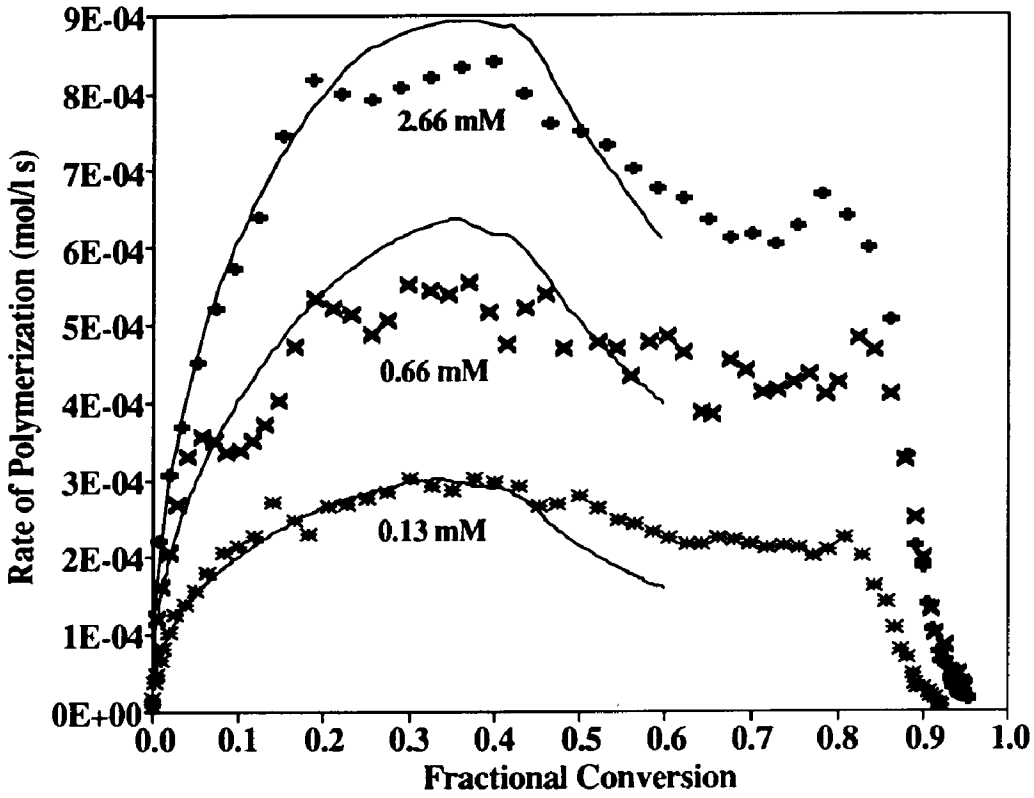

Figure 4-12: Rate of polymerization of styrene miniemulsion versus fractional conversion from simulation by assuming the coagulation coefficient as a function of conversion, using $k_c = 10^{-15}exp[40(x - 0.60)]$ and adjusting k_a^p with initiator concentration: 1.25 x 10^5 dm^3 mol^{-1} s^{-1} for 2.66 mM [I], 1.10 x 10^5 dm^3 mol^{-1} s^{-1} for 0.66 mM [I], 0.73 x 10^5 dm^3 mol^{-1} s^{-1} for 0.13 mM [I]; dashed lines: experimental data, Solid lines: simulations.

different initiator levels (causing the difference in ionic strength) are shown in Figure 4-13 in which the total potential energy is plotted versus the surface separation between droplet and particle. The total energy increases with decreasing initiator concentration as expected. The maximum potential energy is needed to calculate the stability ratio and thus the coagulation coefficient. The results are shown in Figure 4-14 which show that the coagulation coefficient varies by five orders of magnitude with initiator concentration in the range of 0.13 mM to 2.66 mM. These calculations were incorporated into the model for comparison to the experimental data and the results are shown in Figure 4-15. The results show that, when using a constant value of the second order entry rate coefficient of 1.25×10^6 dm^3 mol^{-1} s^{-1}, the model predictions are better at high initiator concentrations and become poorer at the lower initiator concentrations. When adjusting the second order entry rate coefficient with initiator concentration (k_a^p in the range of 1.25×10^6 -- 0.73×10^6 dm^3 mol^{-1} s^{-1} for initiator concentration in the range of 2.66 -- 0.13 mM), the model is better able to simulate the experimental data (Figure 4-16).

Closer examination of the data can be made by plotting the rate of polymerization versus conversion and the results are shown in Figure 4-17. These results indicate that the monomer droplets disappear at an earlier conversion for the highest initiator concentration, or the model seems too sensitive to the ionic strength of the system. The equation by Hogg et al.[36] (Equation (4.34)) was shown by Feeney et al.[41] to depend greatly on the ionic strength. This equation was derived by solving analytically the Poisson-Boltzmann Equation simplified by considering one dimension. Barouch and Matijevic[52, 53] demonstrated that, upon solving the Poisson-Boltzmann Equation numerically in two dimensions, the maximum total potential energy does not vary very much within the range of ionic strength in this study.

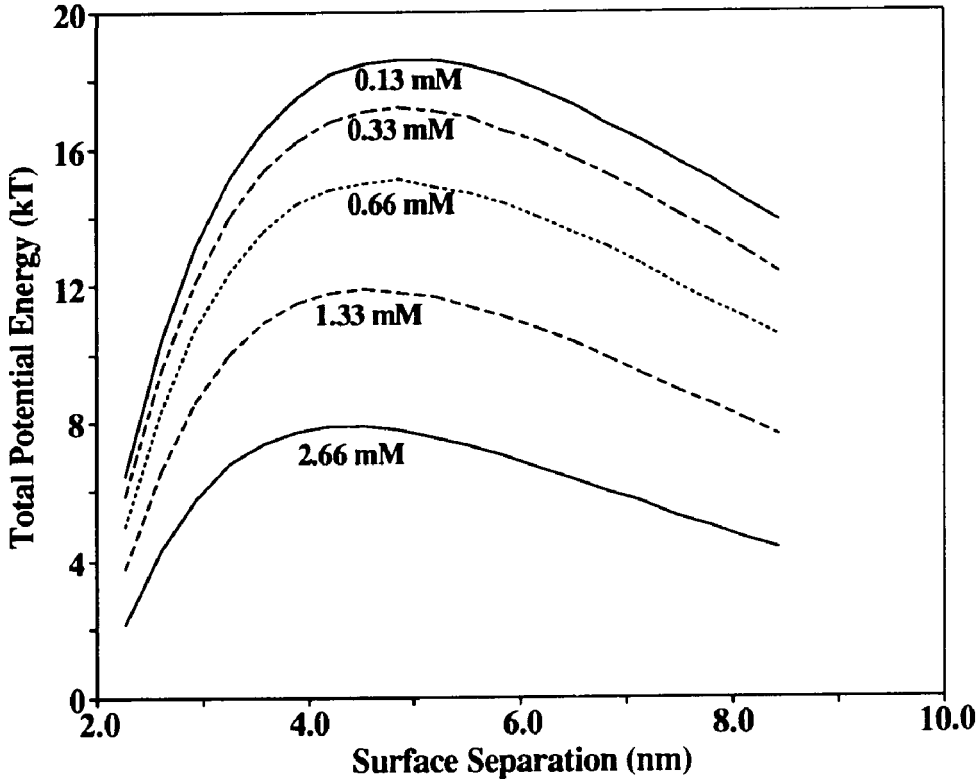

Figure 4-13: Total potential energy versus particle-droplet surface separation calculated for different initiator concentrations using r_p = 50 nm, r_d = 15 nm and $N_p = N_d = 5 \times 10^{17}$ dm^3.

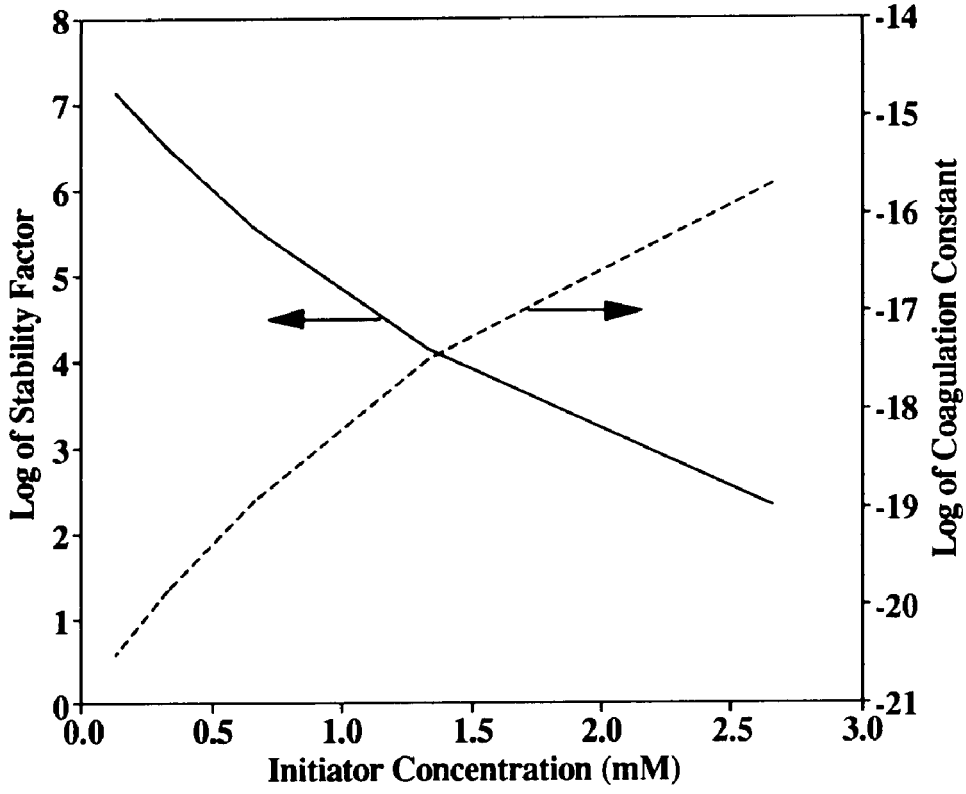

Figure 4-14: Stability factor and the coagulation coefficient versus intiator concentration calculated using r_p = 50 nm, r_d = 15 nm and N_p = N_d = 5 x 10^{17} dm^3.

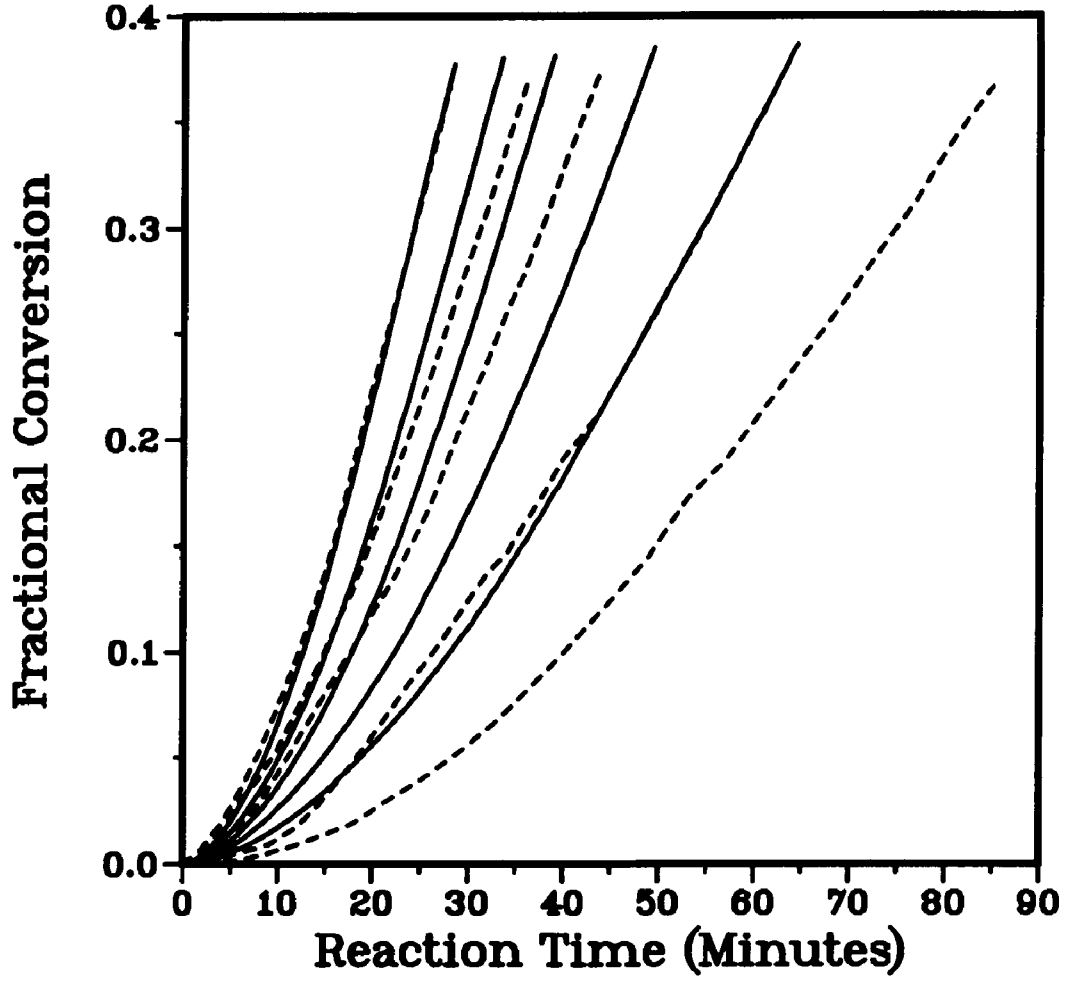

Figure 4-15: Comparison of simulated versus experimental conversion histories for the miniemulsion polymerization of styrene using various initiator concentrations (2.66 mM, 1.33 mM, 0.66 mM, 0.33 mM and 0.13 mM, from left to right respectively); simulation using the DLVO theory and the Muller Equation to calculate the coagulation coefficient; dashed lines: Choi's experimental data, solid lines: simulations.

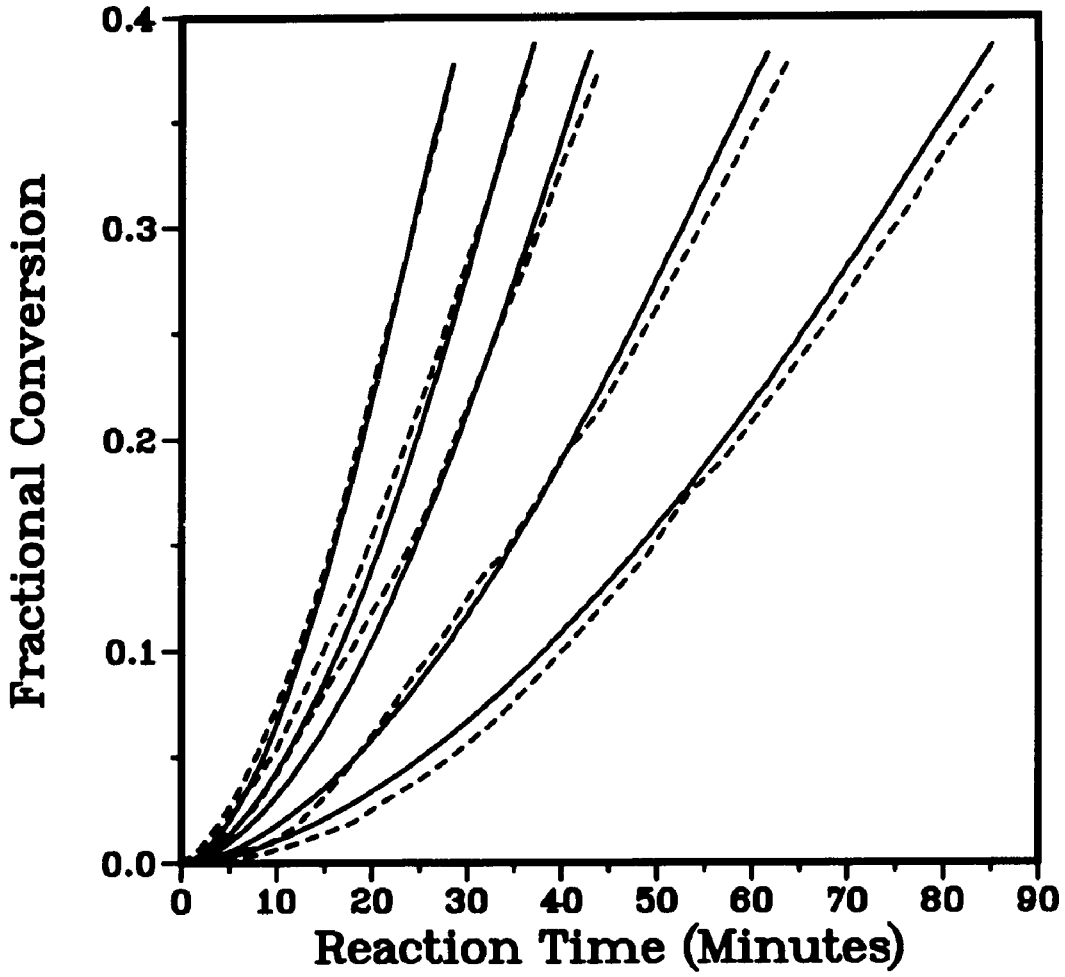

Figure 4-16: Comparison of simulated versus experimental conversion histories for the miniemulsion polymerization of styrene using various initiator concentrations (decreasing from left to right); simulation using the DLVO theory and the Muller Equation to calculate the coagulation coefficient and adjusting k_a^p with initiator concentration: 1.25 x 10^6 dm^3 mol^{-1} s^{-1} for 2.66 mM [I], 1.12 x 10^6 dm^3 mol^{-1} s^{-1} for 1.33 mM [I], 1.10 x 10^6 dm^3 mol^{-1} s^{-1} for 0.66 mM [I], 0.81 x 10^6 dm^3 mol^{-1} s^{-1} for 0.33 mM [I], 0.73 x 10^6 dm^3 mol^{-1} s^{-1} for 0.13 mM [I]; dashed lines: Choi's experimental data, solid lines: simulations.

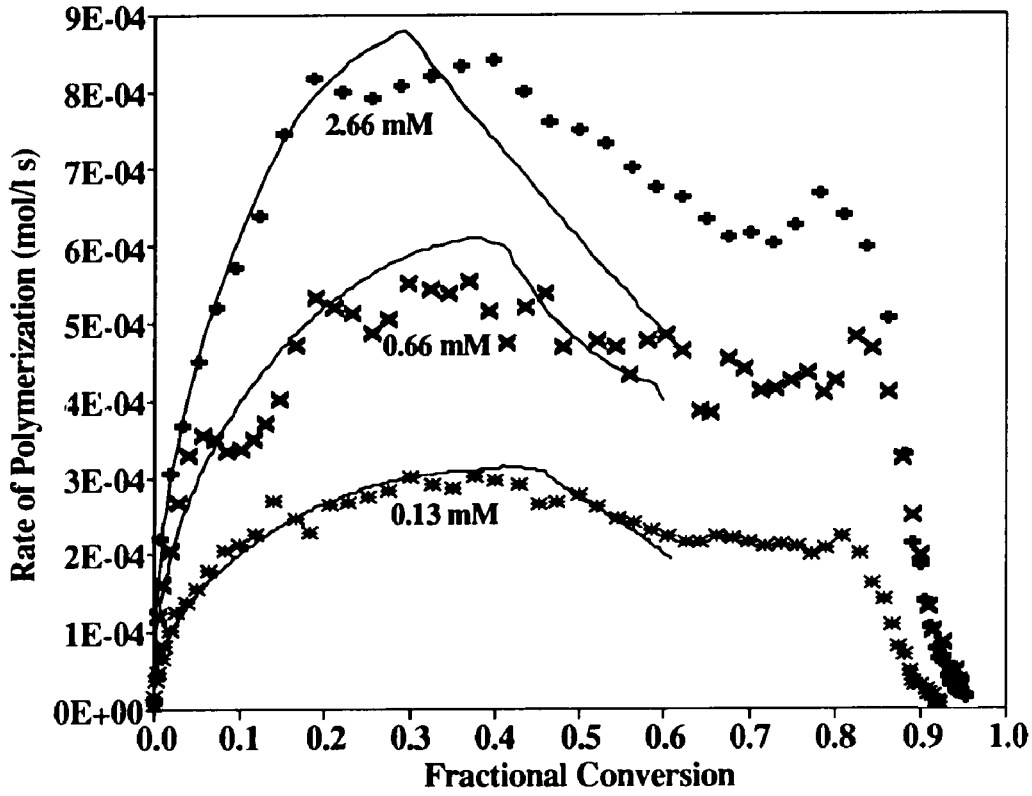

Figure 4-17: Rate of polymerization versus fractional conversion by using the DLVO theory and the Muller Equation to calculate the coagulation coefficient, and adjusting k_a^p with initiator concentration: 1.25 x 10^6 dm^3 mol^{-1} s^{-1} for 2.66 mM [I], 1.10 x 10^6 dm^3 mol^{-1} s^{-1} for 0.66 mM [I], 0.73 x 10^6 dm^3 mol^{-1} s^{-1} for 0.13 mM [I]; dashed lines: Choi's experimental data, solid lines: simulations.

However, their computation of the maximum total potential energy is a major task and is not practically incorporated into this model. Nevertheless, based on their results and the range of ionic strength used in this study, we may use a constant ionic strength for all calculations (e.g., that of 0.13 mM initiator concentration). When a constant ionic strength is assumed, the model is able to predict the experimental data better (Figure 4-18).

The results from Figures 4-10 and 4-16 indicate that using the simple equation (4.50) and the DLVO theory to calculate the coagulation coefficient for droplets and particles provide similar results in prediction of the conversion-time data. However, for a wide droplet size distribution system, equation (4.50) may not be usefull and the extented DLVO theory should be applied.

4.3.4 Other Comparisons With Experimental Data

This model can be used to predict the critical size of the monomer droplets at which they become unstable towards polymer particles. The results are shown in Figure 4-19, which indicate that when the coagulation coefficient depends on the ionic strength, the unstable droplet size is predicted to vary greatly with the initiator concentration. When coagulation is assumed to be independent of initiator concentration, the model predicts the unstable droplet size to be around 15 nm in radius which is similar to the predictions assuming that the coagulation coefficient is a function of conversion (using equation (4.50)). These results indicate that monomer droplet disappearance is a function of the size and number of droplets and particles. In other words, the assumption that the monomer droplet disappearance is a function of a specific conversion for a given set of experimental conditions may not be valid for another sets of experimental conditions. This is likely the main reason for the improvement over Choi's model[6], in which the monomer droplets were assumed

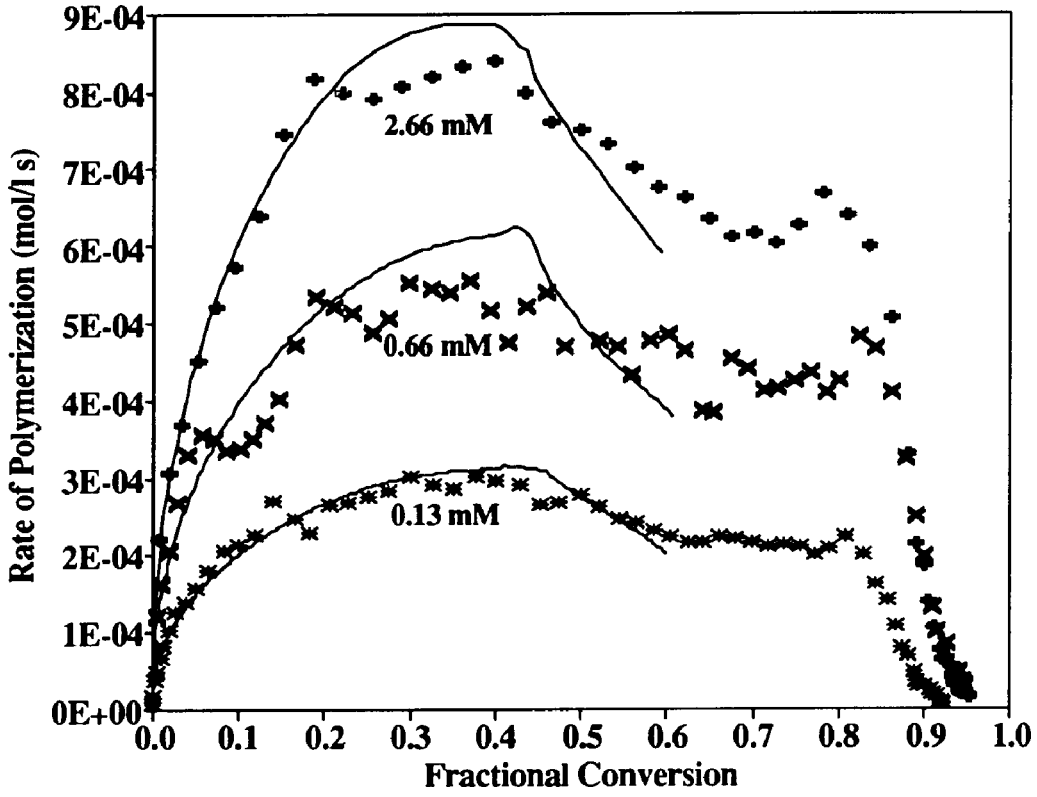

Figure 4-18: Rate of polymerization versus fractional conversion by using the DLVO theory, the Muller Equation and assuming constant ionic strength to calculate the coagulation coefficient, and adjusting k_a^p with initiator concentration: 1.25 x 10^6 dm^3 mol^{-1} s^{-1} for 2.66 mM [I], 1.10 x 10^6 dm^3 mol^{-1} s^{-1} for 0.66 mM [I], 0.73 x 10^6 dm^3 mol^{-1} s^{-1} for 0.13 mM [I]; dashed lines: Choi's experimental data, solid lines: simulations.

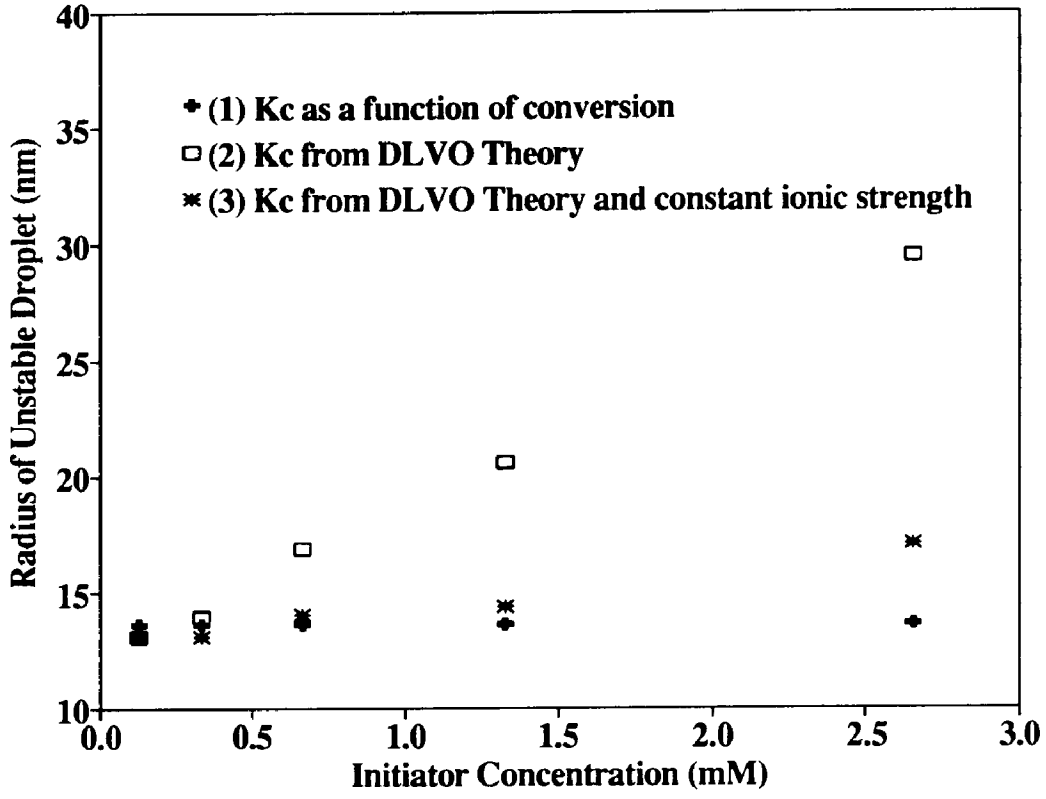

Figure 4-19: Radius of unstable droplets versus initiator concentration for the three cases where the coagulation coefficient was calculated as: (1) a function of conversion (Equation (4.50)); (2) using DLVO theory; and (3) using DLVO theory and a constant ionic strength.

Table 4-3: Experimental and Simulated Data of Final Particle Radius and Number.

[I], mM	r^{*e}, nm	r^{*c}, nm	r^{*t}, nm	$N_p{}^{*e}$,$10^{18}dm^{-3}$	$N_p{}^{*t}$,$10^{18}dm^{-3}$
2.66	46	64	48	0.68	0.60
1.33	52	70	51	0.47	0.49
0.66	56	76	53	0.38	0.45
0.33	63	85	57	0.26	0.35
0.13	66	95	62	0.23	0.27

*e: Experimental data[6]

*c: Prediction from Choi's work[6]

*t: Prediction from this work

to disappear at 30% of conversion, as can be seen from Table 4-3. The final particle radius and number experimental results are from Choi's work on styrene miniemulsion polymerization using cetyl alcohol as cosurfactant and the range of initiator concentration from 0.13 to 2.66 mM. The predictions of this work for the final particle radius and number was extracted from the simulated results of Figure 4-16. Table 4-3 indicates that the predictions of the final particle radius and number from this work are much closer to the experimental values as compared to those predicted by Choi's work[6].

The most difficult result to predict is the number of particles over a wide range of initiator concentration. The experimental data show a particle concentration versus initiator concentration power dependency of 0.37 as shown in Figure 4-20. The model using the DLVO theory and the Muller Equation predict a power dependency of 0.17 (Figure 4-21) and the model assuming the coagulation coefficient as a function of conversion predicts a power dependency

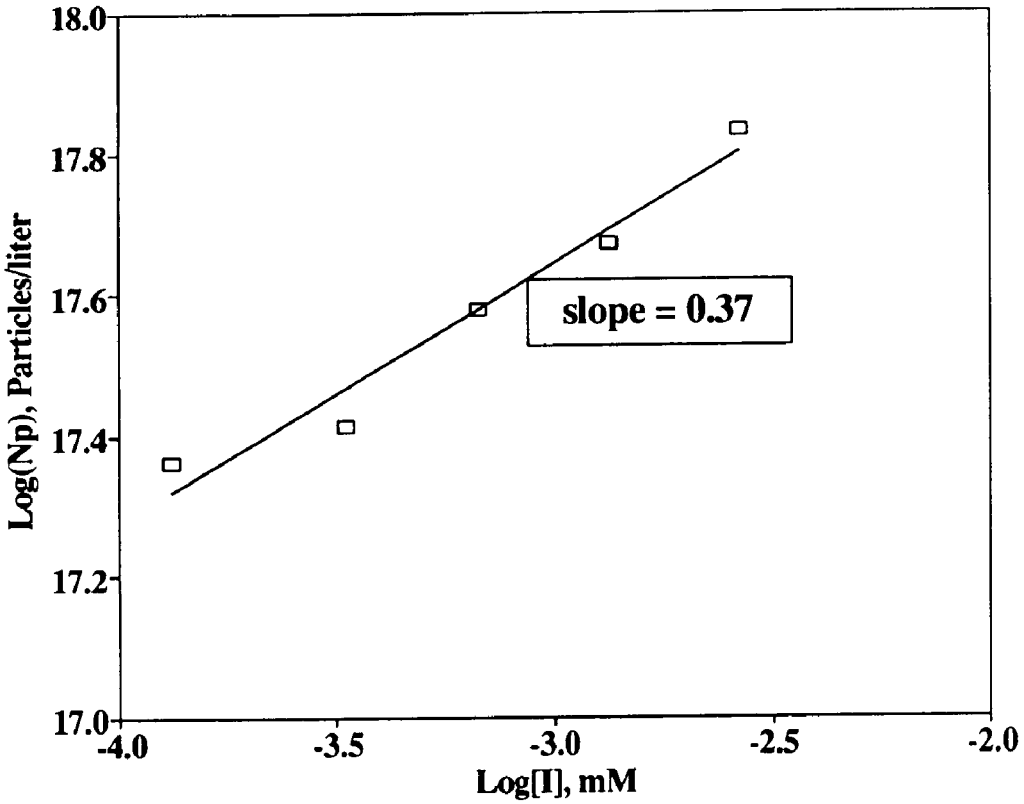

Figure 4-20: Final particle concentration versus initiator concentration from Choi's experimental data of styrene miniemulsion polymerization using 10 mM SLS/30 mM CA.

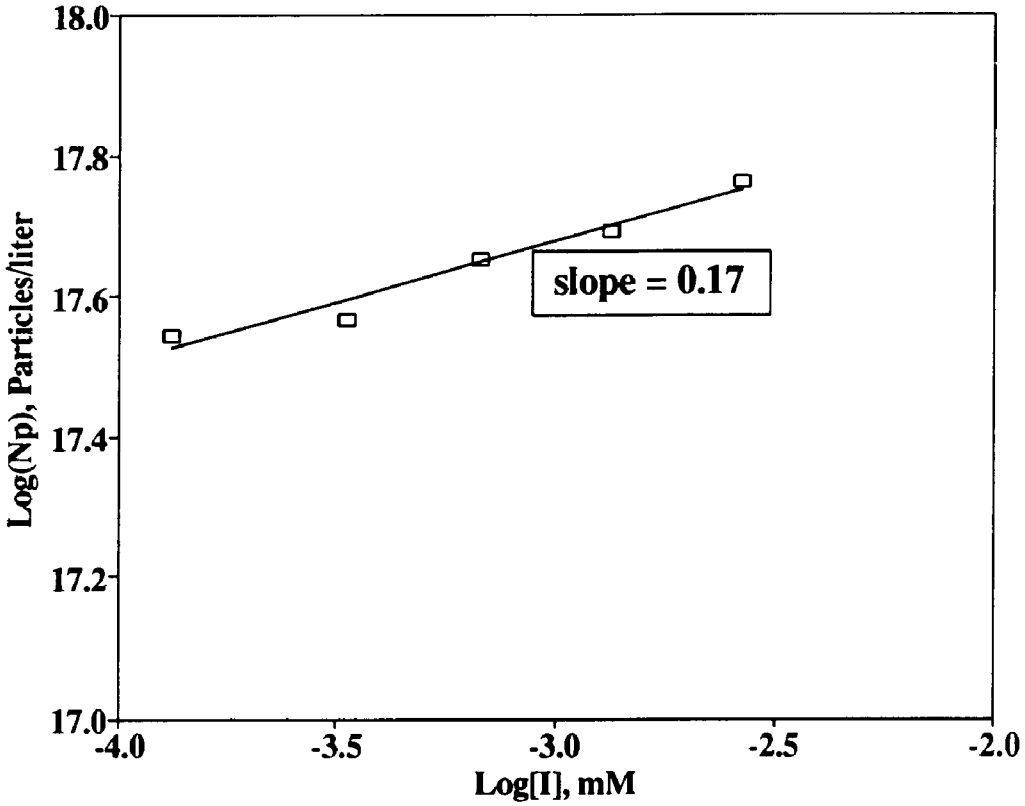

Figure 4-21: Final particle concentration versus initiator concentration from simulation of styrene miniemulsion polymerization using 10 mM SLS/30 mM CA and using the DLVO theory and the Muller Equation.

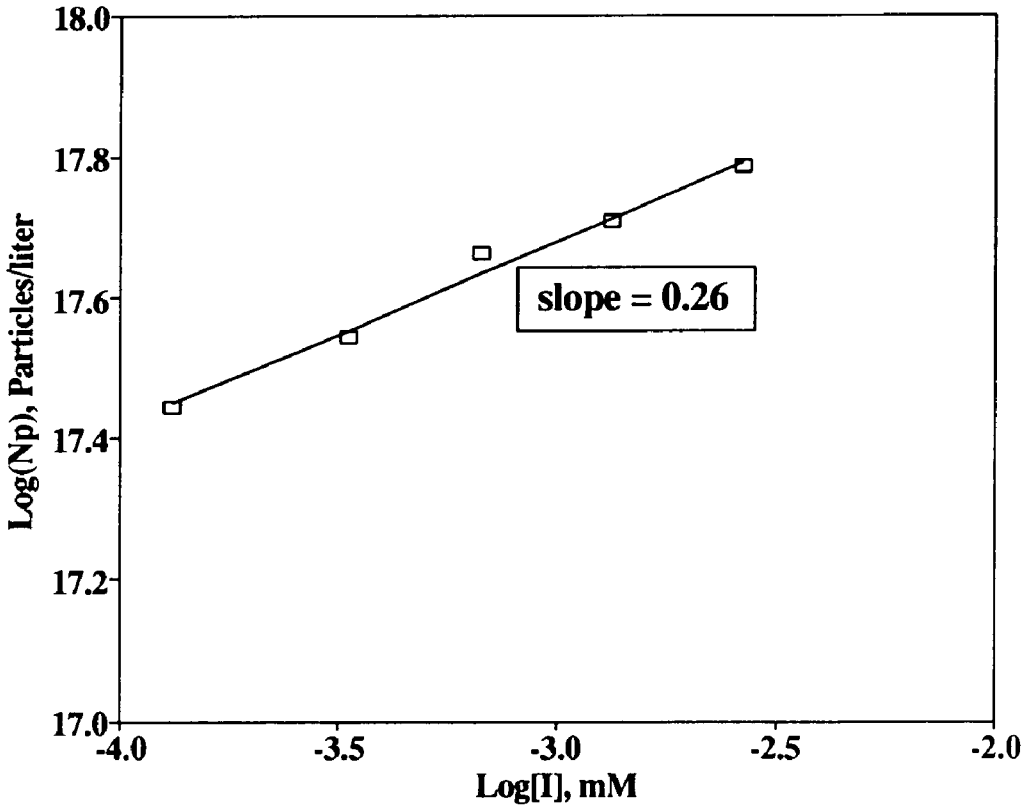

Figure 4-22: Final particle concentration versus initiator concentration from simulation of styrene miniemulsion polymerization using 10 mM SLS/30 mM CA and assuming the coagulation coefficient as a function of conversion ($k_c = 10^{-15}exp[40(x - 0.60)]$).

of 0.26 (Figure 4-22). However, when the individual simulated results of the particle size and number are compared to the experimental ones, the model shows much improvement over the similation results by Choi[6] as can be seen on Table 4-3. The main sources of these improvements are attributed to the incorporation of the equilibrium swelling thermodynamics and coagulation between droplets and particles.

4.3.5 Application of the Model

The model was also applied to miniemulsion polymerizations at different sets of experimental conditions, particularly the results of runs M10 and M12 presented in Chapter 2. Run M10 is the miniemulsion polymerization of styrene using 5 mM SLS/15 mM CA and 2.66 mM potassium persulfate and run M12 is the miniemulsion polymerization of styrene using 5 mM SLS/20 mM HD and 2.66 mM potassium persulfate. The differences between these experimental data and Choi's experimental data are the concentrations of surfactant and co-surfactant and the type of co-surfactant, thus the initial droplet size from these data would be different from that of Choi's data. Therefore, the investigated variables in the model are the initial monomer droplet diameter and the value of the entry rate coefficient for radicals into the monomer droplets. An entry rate coefficient for radicals into the polymer particles of 1.25×10^6 dm^3 mol^{-1} s^{-1} was used, and other constants (see Table 4-1) are the same as those applied to predict Choi's experimental data.

The results of the model predictions for the styrene miniemulsion polymerization of run M10 are shown in Figure 4-23. These indicate that the model predicts the experimental data very well when the initial monomer droplet diameter of 132 nm and the entry rate coefficient for radicals into the droplets of 0.087×10^6 dm^3 mol^{-1} s^{-1} were used. This value of the entry rate

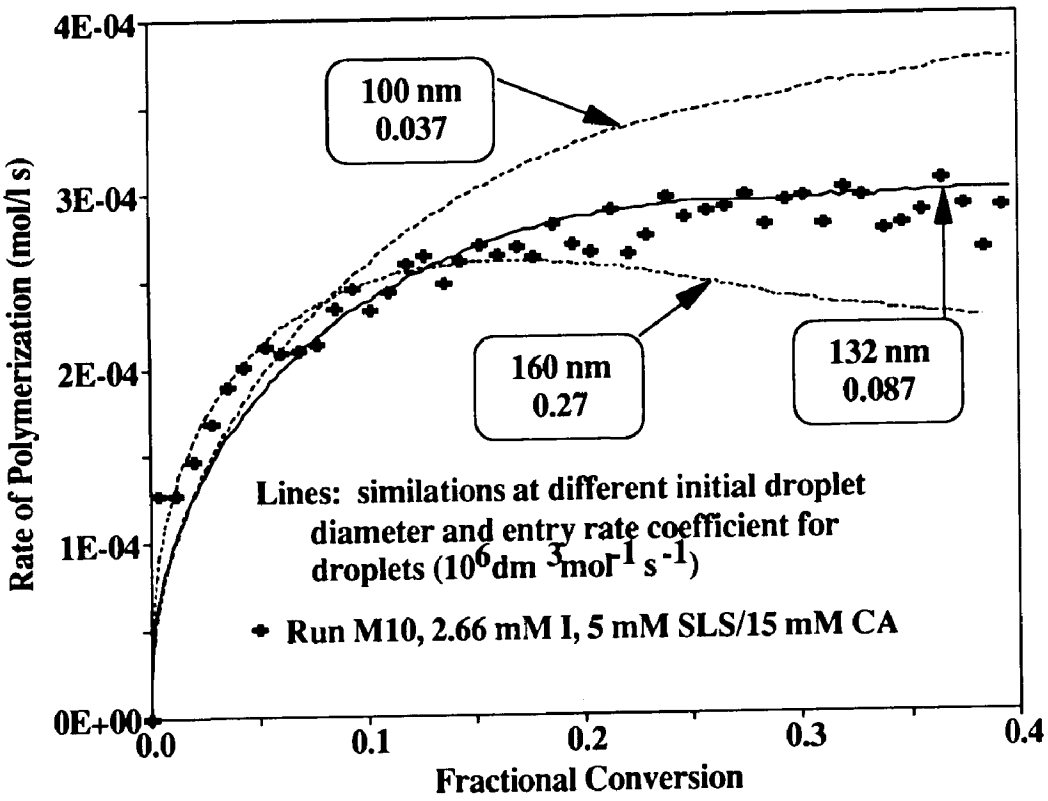

Figure 4-23: Comparison of simulated and experimental rate of polymerization versus fractional conversion for the styrene miniemulsion polymerization using 5 mM SLS/15 mM CA and 2.66 mM potassium persulfate; lines: simulations at different initial monomer droplet diameter and the entry rate coefficient for radicals into the droplets (# x $10^6 dm^3 mol^{-1} s^{-1}$), symbol: experimental data from run M10.

coefficient for radicals into the droplets was also used previously to predict Choi's experimental data. Different initial monomer droplet diameters (100 nm and 160 nm) were also used to test the model predictions, thus the value of the entry rate coefficient for radicals into the droplets had to be adjusted to obtain the best fit to the experimental data. The results from Figure 4-23 show that when the initial monomer droplet diameters of 100 nm and 160 nm are used, the model is unable to predict the experimental data well.

The above predictions indicate that the initial average droplet size for run M10 is about 132 nm. The final particle sizes for runs M10 and M12 were found to be similar, therefore an initial average droplet size of 130 nm was used for the simulation of the experimental results of run M12. The model did not produce a good fit of the data for run M12 in which hexadecane was used as cosurfactant; the results are shown in Figure 4-24. At a lower value of the entry rate coefficient for radicals into the monomer droplets (0.087×10^6 dm^3 mol^{-1} s^{-1}) the model fit the experimental polymerization rate at higher conversions ($x > 0.15$) but failed to predict the experimental data at lower conversions ($x < 0.15$). When a higher value of the entry rate coefficient for radicals into the monomer droplets (0.37×10^6 dm^3 mol^{-1} s^{-1}) was used, the model did not follow the experimental data at higher conversions ($x > 0.03$) but was better at lower conversions ($x < 0.03$). These results suggest that the entry rate coefficient for radicals into the monomer droplets may be higher for the hexadecane case as compared to that of the cetyl alcohol case.

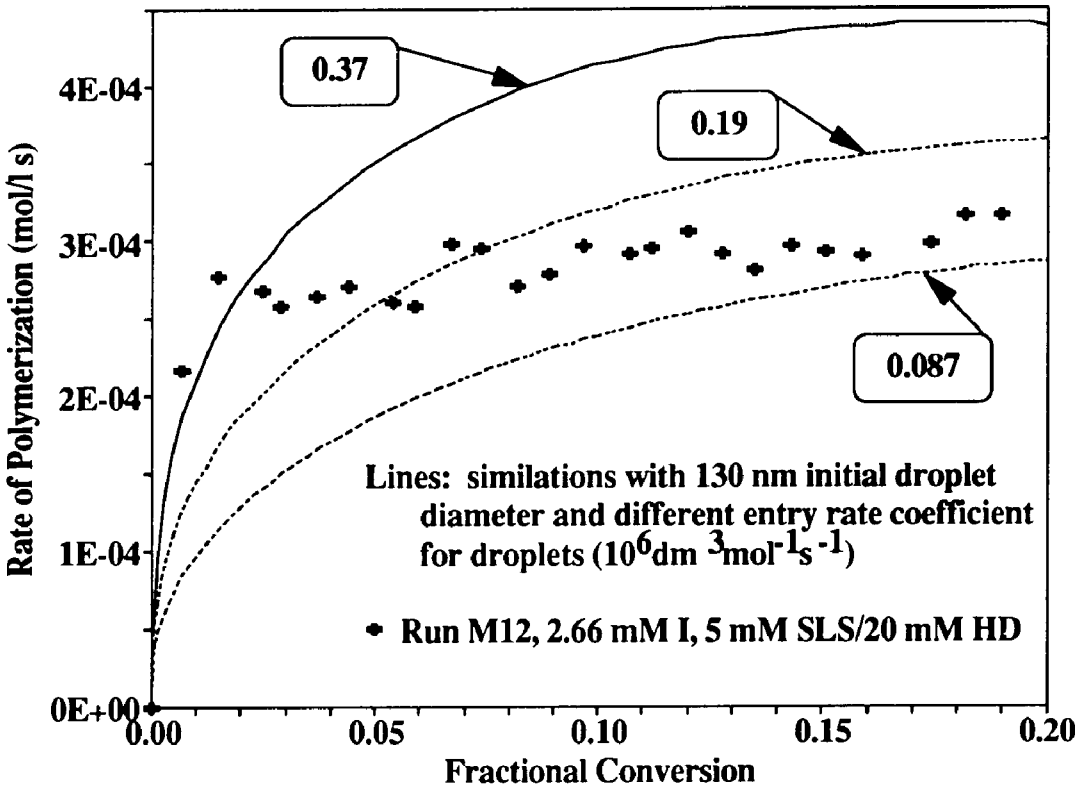

Figure 4-24: Comparison of simulated and experimental rate of polymerization versus fractional conversion for the styrene miniemulsion polymerization using 5 mM SLS/20 mM HD and 2.66 mM potassium persulfate; lines: simulations with 130 nm initial monomer droplet diameter and with a different ratio of the entry rate coefficient for radicals into the droplets (# x 10^6dm^{3}mol^{-1}s^{-1}), symbol: experimental data from run M12.

4.3.6 Incorporation of Radical Exit from Monomer Droplets

In an attempt to explain the experimental data of the styrene miniemulsion polymerization using hexadecane as cosurfactant (run M12), it was assumed that when a radical enters a monomer droplet for the first time it can exit the monomer droplet if it does not propagate first. Thus, a particle is nucleated from a monomer droplet when a radical enters a droplet and starts to propagate. By neglecting the effect of coagulation between droplets and particles at low conversion, the rate of monomer droplet disappearance can be written as:

$$\frac{dN_{d,0}}{dt} = -k_a^d C_R^w N_{d,0} + k^d N_{d,1} \tag{4.51}$$

where $N_{d,0}$ is the number of monomer droplets containing no radicals, $N_{d,1}$ the number of monomer droplets containing one radical, k^d the exit rate coefficient for a radical from the monomer droplets, and thus the balance for the number of droplets containing one radical can be expressed as:

$$\frac{dN_{d,1}}{dt} = k_a^d C_R^w N_{d,0} - k^d N_{d,1} \tag{4.52}$$

These are based on the extreme case that all entering radicals can desord, thus the exit rate for the droplets would be higher than the case when only monomeric radicals can desord. The rate of change of the number of particles containing one radical is written as:

$$\frac{dN_1}{dt} = k_a^p C_R^w (N_0 - N_1) + k(2N_2 - N_1) + k_a^d C_R^w N_{d,0} - k^d N_{d,1} \tag{4.53}$$

The above equations were used to simulate the results of run M12. The entry rate coefficient for radicals into the monomer droplets was assumed to be the same as that of the particles (1.25×10^6 dm^3 mol^{-1} s^{-1}). The average initial droplet size of 130 nm and the exit rate coefficient for radicals from the droplets containing one radical of 2.8×10^{-3} s^{-1} were used. Figure 4-25 indicates that the

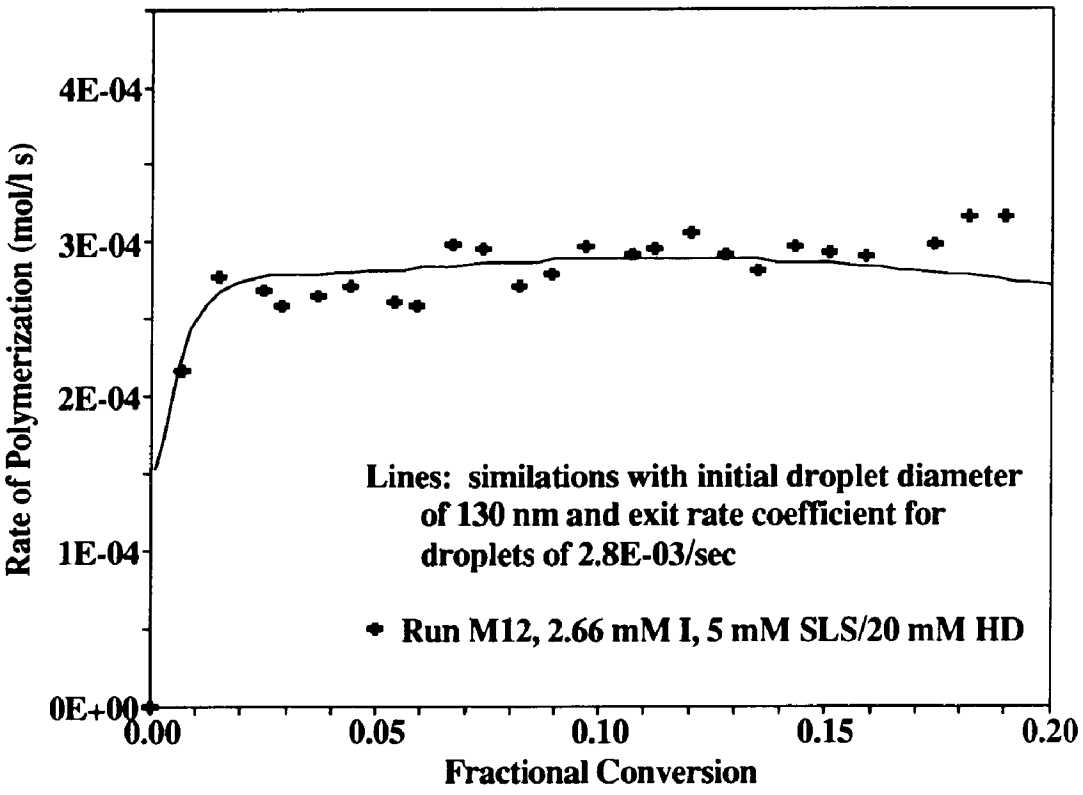

Figure 4-25: Comparison of simulated and experimental rate of polymerization versus fractional conversion for the styrene miniemulsion polymerization using 5 mM SLS/20 mM HD and 2.66 mM potassium persulfate; lines: simulations with 130 nm initial monomer droplet diameter and exit rate coefficient for droplets containing one monomeric radical of 2.8 x 10^{-3} s^{-1}, symbol: experimental data from run M12.

model predicts the experimental data of run M12 well. These results indicate that initially there is a fast increase in the polymerization rate due to a large number of particles nucleated from the entry of the radicals into the monomer droplets, and the polymerization rate does not increase much due to the exit of the radicals from the monomer droplets containing one radical. However, this may not explain the nucleation of particles in the styrene miniemulsion polymerizations using cetyl alcohol as cosurfactant, because the results of run M10 indicate an initially slower increase in the polymerization rate as compared to that of run M12 (hexadecane as cosurfactant).

Radical exit from the monomer droplets was also applied to the case of miniemulsion polymerization using cetyl alcohol as cosurfactant (run M10) and the results are shown in Figure 4-26. The entry rate coefficient for radicals into the particles of 1.25×10^6 $dm^{-3}mol^{-1}s^{-1}$ and the average initial droplet size of 132 nm were used in the similation. The entry rate coefficient for radicals into the droplets and the exit rate coefficient for radicals from the monomer droplets containing one radical were adjusted to fit the shape of the polymerization rate-conversion data of run M10. The best fit to the experimental data was obtained when the entry rate coefficient for radicals into the droplets of 0.17×10^6 $dm^3mol^{-1}s^{-1}$ and the exit rate coefficient for radicals from the droplets containing one radical of $0.4 \times 10^{-3}s^{-1}$ were used. These results indicate that the entry rate coefficient for radicals into the monomer droplets is about an order of magnitude smaller than that of the particles (1.25×10^6 $dm^{-3}mol^{-1}s^{-1}$), and the exit of radicals from the droplets is also about an order of magnitude smaller for the cetyl alcohol case as compared to that of the hexadecane case.

The above studies suggest that the assumption that a particle is nucleated when a radical enters a monomer droplet for the first time is not valid for the hexadecane case, but this assumption may be valid for the cetyl alcohol case if

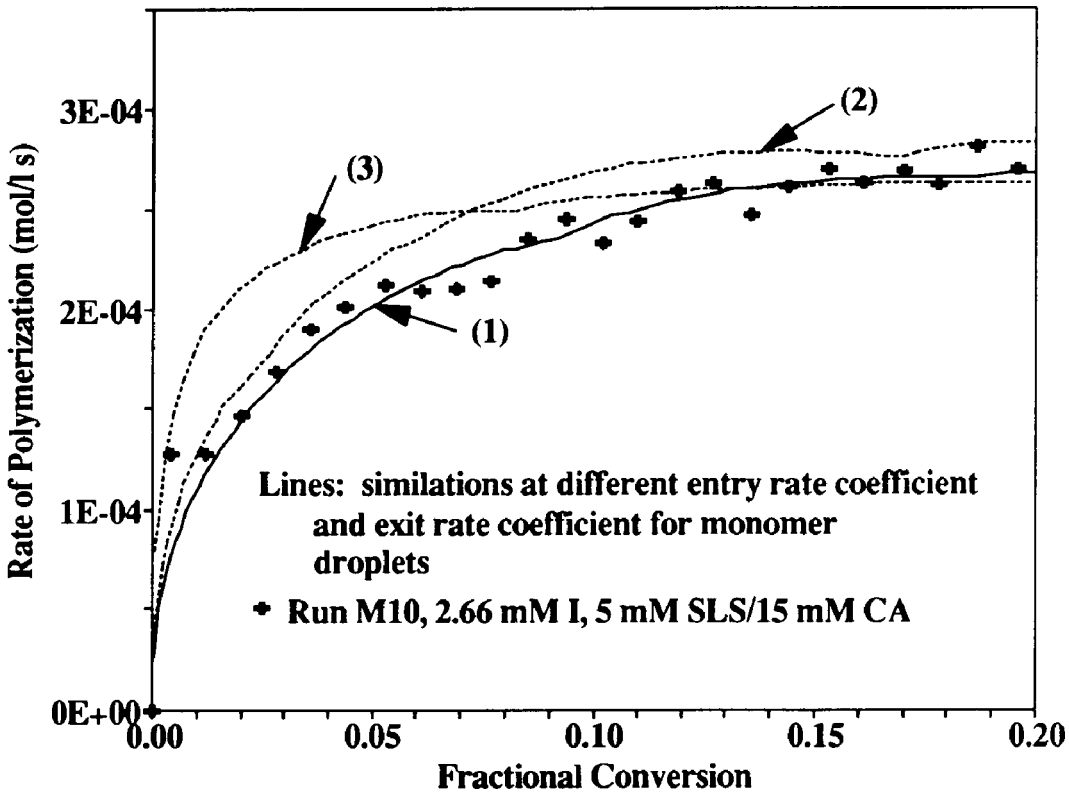

Figure 4-26: Comparison of simulated and experimental rate of polymerization versus fractional conversion for the styrene miniemulsion polymerization using 5 mM SLS/15 mM CA and 2.66 mM potassium persulfate; lines: simulations with different entry rate coefficients for radicals into the monomer droplets and exit rate coefficients for radicals from the droplets, respectively as: (1) k_a^d = 0.17 x $10^6 dm^3 mol^{-1} s^{-1}$ and k^d = 0.4 x 10^{-3} s^{-1}; (2) k_a^d = 0.25 x $10^6 dm^3 mol^{-1} s^{-1}$ and k^d = 0.5 x 10^{-3} s^{-1}; and (3) k_a^d = 0.62 x $10^6 dm^3 mol^{-1} s^{-1}$ and k^d = 2.0 x 10^{-3} s^{-1}, symbol: experimental data from run M12.

cetyl alcohol affects both the entry of radicals into the droplets and the exit of radicals from the droplets containing a radical.

4.3.7 Summary and Conclusions

A mathematical model which takes into account the nucleation of monomer droplets, the equilibrium swelling thermodynamics, the desorption of radicals from the polymer particles, and the coagulation of droplets and particles based on the DLVO theory and the Muller Equation was applied to predict the experimental data. This theoretical study has enhanced the understanding of many mechanisms in miniemulsion polymerization. The entry rate coefficient for radicals into the monomer droplets is about an order of magnitude smaller than that of the particles when cetyl alcohol was used as cosurfactant, and this smaller value contributes to the slow nucleation rate in miniemulsion polymerization using cetyl alcohol as a cosurfactant. The stability of the monomer droplets was found to play a very important role in particle nucleation, more particles being formed with more stable droplets. This stability may not correlate well with the fractional conversion, and a better correlation of the droplet stability should be found with the size, number and surface charge density of the droplets and particles. Thus, for the case of a wide size distribution of monomer droplets, the stability of monomer droplets should be important at lower conversions. The co-surfactant was found to be very important in the nucleation of particles in miniemulsion polymerization. The simulated results show that the entry rate of radicals into the monomer droplets was faster for the hexadecane system as compared to that of the cetyl alcohol system. The co-surfactant was also found to be important in miniemulsion polymerization kinetics, because it causes a decrease in the concentration of monomer in the particles while monomer droplets continue to exist, which in

turn decreases the rate of polymerization.

4.4 Reference

1. J. Ugelstad, M. S. El-Aasser and J. W. Vanderhoff, *Polym. Lett.*, **11**, 503 (1973).

2. B. J. Chamberlain, D. H. Napper and R. G. Gilbert, *J. Chem. Soc., Faraday Trans. I*, **78**, 591 (1982).

3. B. S. Hawkett, R. G. Gilbert and D. H. Napper, *J. Chem. Soc. Faraday trans. I*, **71**, 2288 (1975).

4. J. Delgado, *Miniemulsion Copolymerization of Vinyl Acetate and n-Butyl Acrylate*, Ph. D. Dissertation, Lehigh University, 1986.

5. Y. T. Choi, M. S. El-Aasser, E. D. Sudol and J. W. Vanderhoff, *J . Polym. Sci., Polym. Chem. Ed.*, **23**, 2973 (1985).

6. Y. T. Choi, *Formation and Stabilization of Miniemulsions and Latexes*, Ph. D. Dissertation, Lehigh University, 1986.

7. V. S. Rodriguez, *Interparticle Monomer Transport in Miniemulsion Copolymerization*, Ph. D. Dissertation, Lehigh University, 1988.

8. J. M. Asua, V. S. Rodriguez, C. A. Silebi and M. S. El-Aasser, *Makromol. Chem., Macromol. Symp.*, **35/36**, 59 (1990).

9. W. V. Smith and R. W. Ewart, *J. Chem. Phys.*, **16**, 592 (1948).

10. J. M. Asua, E. D. Sudol and M. S. El-Aasser, *J. Polym. Sci., Polym. Chem. Ed.*, **27**, 3903 (1989).

11. J. Ugelstad, P. C. Mork, H. R. Mfutakamba, E. Soleimany, I. Nordhuus, K. Nustad, R. Schmid, A. Berge, T. Ellingsen and O. Aune, in *"Sci. and Tech. of Polymer Colloids"*, G. W. Poehlein, R. H. Ottewill, J. W. Goodwin, Ed., NATO ASI Ser. Vol. I, 1983, p. 51.

12. J. Delgado, M. S. El-Aasser C. A. Silebi, J. W. Vanderhoff and J. Guillot, *J. Polym. Sci. Polym. Phys.*, **26**, 1495 (1988).

13. J. Th. G. Overbeek, in *Colloid Science*, H. R. Kruyt, Ed., Elsevier, Amsterdam, 1952.

14. H. Muller, *Kolloid.-Beih.*, **26**, 257 (1928).

15. M. Morton, S. Kaizerman and M. W. Altier, *J. Colloid Sci.*, **9**, 300 (1954).

16. C. M. Tseng, M. S. El-Aasser and J. W. Vanderhoff, in *"Computer Applications in Applied Polymer Science"*, T. Provder, Ed., ACS Symp Ser. No. 197. 1982, P. 197.

17. J. Guillot, *Acta Polym.*, **32**, 592 (1981).

18. V. S. Rodriguez, J. Delgado, C. A. Silebi and M. S. El-Aasser, *I&EC Research*, **28**, 65 (1989).

19. P. J. Flory, *"Principles of Polymer Chemistry"*, Cornell University Press, New York, 1953.

20. J. C. Gardon, *J. Polym. Sci., Part A-1*, **6**, 623 (1968).

21. R. M. Fitch and C. H. Tsai, in *"Polymer Colloids"*, R. M. Fitch, Ed., Plenum, New York, 1971, p.73.

22. R. M. Fitch and L. B. Shih, *Progr. Colloid Polym. Sci.*, **56**, 1 (1975).

23. J. Ugelstad and F. K. Hansen, *Rubber Chem. Technol.*, **49**, 536 (1976).

24. P. J. Feeney, D. H. Napper and R. G. Gilbert, *Macromolecules*, **17**, 2520 (1984).

25. B. R. Morrison, I. A. Maxwell, R. G. Gilbert and D. H. Napper, *"II Inter. Symp. on Copolymerization and Copolymers in Dispersed Media"*, Lyon, 1989.

26. I. A. Penboss, R. G. Gilbert and D. H. Napper, *J. Chem. Soc. Faraday Trans. I*, **82**, 2247 (1986).

27. J. C. de la Cal and J. M. Asua, presented at *"64th Colloid and Surface Science Symposium"*, Lehigh University, Bethlehem, PA, June 18-20, 1990.

28. M. Nomura, M. Harada, K. Nakagawara, W. Eguchi and S. Nagata, *I. Chem. Eng. Jpn.*, **4**, 160 (1971).

29. M. Nomura, in *"Emulsion Polymerization"*, Irja Piirma, Ed., Acadamic Press, New York, 1982, p. 191.

30. E. D. von Meerwall, E. J. Amis and J. D. Ferry, *Macromolecules*, **18**, 260 (1985).

31. O. Fuchs, *Z. Phys.*, **89**, 736 (1934).

32. R. H. Ottewill, in *"Emulsion Polymerization"*, I. Piirma, Ed., Academic, New York, 1982, p. 1.

33. J. R. Richards, J. P. Congalidis and R. G. Gilbert, *J. Appl. Polym. Sci.*, **37**, 2727 (1989).

34. H. Reerink and J. Th. G. Overbeek, *Discuss. Faraday Soc.* **18**, 74 (1954).

35. H. C. Hamaker, *Physica*, **4**, 1058 (1937).

36. R. Hogg, T. W. Healy and D. W. Fuerstenau, *Trans. Faraday Soc.*, **62**, 1638 (1966).

37. A. S. Dunn and L. C. H. Chong, *Br. Polym. J.*, **2**, 49 (1970).

38. R. J. Goetz, *Formation and Stabilization of Oil-in-water Miniemulsions*, Ph. D. Dissertation, Lehigh University, 1990.

39. J. S. Guo, *Polymerization of Styrene Oil-in-Water Microemulsions*, Ph.D. Dissertation, Lehigh University, 1990.

40. S. M. Ahmed et al., in *"Polymer Colloids II"*, R. M. Fitch, Ed., Plenum, New York, 1980, p. 265.

41. P. J. Feeney, D. H. Napper and R. G. Gilbert, *Macromolecules*, **20**, 2922 (1987).

42. R. H. Perry, *Chemical Engineers' Handbook*, 6th ed., McGraw-Hill, New York, 1984.

43. *CRC Handbook of Chemistry and Physics*, 63rd ed., CRC Press, Boca Raton, Florida, 1982-1983.

44. H. J. van den Hul and J. W. Vanderhoff, in *"Polymer Colloids I"*, R. M. Fitch, Ed., Plenum, New York, 1971, p. 1.

45. N. Friis and A. E. Hamielec, *J. Polym. Sci., Polym. Chem Ed.*, **12**, 251 (1974).

46. E. L. Cussler, *"Diffusion--Mass Transfer in Fluid Systems"*, Cambridge University, Cambridge, 1984.

47. S. M. Ahmed, *Preparation and Characterization of Latexes*, Ph. D. Dissertation, Lehigh University, 1979.

48. R. J. Goetz, A. Khan and M. S. ElAasser, *J. Colloid Interface Sci.*, **137**, 395 (1990).

49. *"Solubilities of Inorganic and Organic Compounds"*, New York, D. Van Nostrand Co., 1952.

50. F. K. Hansen and J. Ugelstad, *J. Polym. Sci. Polym. Chem. Ed.*, **16**, 1952 (1978).

51. G. Lichti, R. G. Gilbert and D. H. Napper, *J. Polym. Sci. Polym. Chem. Ed.*, **21**, 269 (1983).

52. E. Barouch and E. Matijevic, *J. Chem. Soc., Faraday Trans. I*, **81**, 1797 (1985).

53. E. Barouch, E. Matijevic and T. H. Wright, *J. Chem. Soc., Faraday Trans. I*, **81**, 1819 (1985).

Chapter 5
Conclusions and Recommendations

5.1 Conclusions

From the studies of the effect of preparative variables on the kinetics of miniemulsion polymerization, the following conclusions can be made:

1) When the concentration of SLS is above its cmc, the overall rate of the conventional polymerization is faster than that of the miniemulsion system. However, it is the opposite when the concentration of SLS is below its cmc.

2) When the emulsion without a co-surfactant was allowed to age, thereby increasing the monomer droplet size, the polymerization was found to decrease with aging time (or with increasing droplet size). However, the miniemulsions prepared with cetyl alcohol or hexadecane were found unchanged within four hours of aging at room temperature.

3) Different temperatures used in preparing cetyl alcohol miniemulsions with the same recipe can also result in different kinetics; the miniemulsion prepared with styrene added to the gel solution at 65°C had a faster reaction rate than the one prepared with styrene added to the gel solution at 25°C.

4) Under the reported conditions, the Microfluidizer provides a greater and more uniform shear than the sonifier and the Omni mixer, thus resulting in smaller and more uniform final particle size distributions.

5) The finest droplet size miniemulsions are obtained by: i) using a co-surfactant; ii) homogenizing at elevated temperature when cetyl alcohol is used as co-surfactant; iii) homogenizing using a uniform high shear device (Microfluidizer); and iv) limiting the aging time prior to polymerization when no co-surfactant is used.

From the studies of the effect of cetyl alcohol on the entry and exit of

radicals, the following conclusions can be made:

6) In determining the entry and exit rate coefficients, the method applying the slope and intercept data and the parameter estimation method were found to be in relative agreement.

7) The presence of cetyl alcohol with the polymer particles increases the rate of polymerization.

8) The presence of cetyl alcohol was found not to affect entry but instead to affect exit by acting as a chain transfer agent competing with monomer and decreasing the exit of monomeric radicals.

9) The chain transfer constant to cetyl alcohol was found to be more than an order of magnitude greater than that of styrene.

10) The effect of cetyl alcohol on the exit of radical from the polymer swollen particles in seeded (92 nm in diameter) emulsion polymerization was found to increase in importance with decreasing initiator concentration.

From the studies of the mathematical model on the kinetics of styrene miniemulsion polymerization, the following conclusions can be made:

11) The entry rate coefficient into the monomer droplets prepared with cetyl alcohol was found to be about an order of magnitude smaller than that of the particles.

12) The entry rate coefficient into the monomer droplets prepared with hexadecane was found to be similar with that of the particles.

13) The monomer droplets were suggested to disappear around 50 percent of conversion.

14) The concentration of monomer in the particles in miniemulsion polymerization is below the normal equilibrium concentration even during the nucleation period. The concentration of monomer in the aqueous phase in a miniemulsion system is about half that of its solubility at the same

temperature.

15) The radius at which the monomer droplets become unstable toward polymer particles was predicted to be about 15 nm in this study.

5.2 Recommendations

Based on the observations and findings of the present investigation, the following research areas are recommended:

1) A method of high swelling, at least 100 to 1 monomer to polymer ratio, of the seed using cetyl alcohol should be developed in order to have a better chance to obtain the entry rate coefficient of radicals into the monomer droplets. The method of Chapter 3 or direct emulsification of polymer solution should be used as a starting point.

2) A monomer that has a higher chain transfer constant than that of cetyl alcohol should be investigated to confirmed that cetyl alcohol affects the exit of radicals in a seeded system.

3) The method of using cetyl alcohol as a swelling agent (Chapter 3) should be investigated to produce large monodisperse particles in a few swelling steps.

4) The mathematical model should be expanded by incorporating the particle size distribtution for polymer particles and monomer droplets to investigate the effect of different sizes on the stability of monomer droplets during the polymerization.

5) For the mathematical model, the relationship between the second order entry rate coefficients for droplets and particles as a function of conversion should be investigated to evaluate the validity of the assumption that once a monomer droplet captures a radical, it instantaneously becomes a polymer particle (in terms of radical absorption behavior).

6) The calculation of the coagulation coefficient as a function of the droplet size may be used in the case of semicontinuous feed of miniemulsions to a reactor to account for the instability of the monomer droplets during the polymerization.

Appendix A
Nomenclature

English

a = slope of $-ln(1-x)$ versus time curve (s^{-1})

a_{si}' = area occupied by a surfactant molecule for droplet or particle (dm^{-2})

b_{si} = Langmuir isotherm constant ($dm^3\ mol^{-1}$)

b = intercept of a $-ln(1-x)$ versus time curve

c = rate coefficient for bimolecular termination of radicals in a particle (s^{-1})

d_p = diameter of the particle (dm)

e_I = electronic charge (C)

f = initiation efficiency factor

g_m^o = initial mass of monomer (g)

g_p^o = initial mass of polymer (g)

k = rate coefficient for radical desorption from the particles (s^{-1})

k_B = Boltzmann constant

k_c = coagulation coefficient for droplet and particle ($dm^3\ s^{-1}$)

k_{fm} = monomer chain transfer constant ($dm^3\ mol^{-1}\ s^{-1}$)

k_I = rate constant for initiator decomposition (s^{-1})

k_p = rate constant for propagation ($dm^3\ mol^{-1}\ s^{-1}$)

k_{tw} = rate constant for radical termination in water ($dm^3\ mol^{-1}\ s^{-1}$)

k_a^d = second order entry rate coefficient for droplets ($dm^3\ mol^{-1}\ s^{-1}$)

k_a^p = second order entry rate coefficient for particles ($dm^3\ mol^{-1}\ s^{-1}$)

m_d = partition coefficient of monomeric radicals between particles and aqueous phase

m_{ij} = ratio of the equilvalent number of molecular segments between i and j

n = the number of radicals

$\bar{n}$ = average number of radicals per particle

r_d = radius of the droplet (dm)

r_p = radius of the particle (dm)

s = ratio of the center-to-center distance to the radius

x = fractional conversion

x_e = experimental fractional conversion

x_c^h = calculated fractional conversion

t = reaction time (s)

z_+ = valency of cation

A = Hamaker constant (J)

A_i = total surface area for droplets or particles (dm^2)

$B = k_p / N_A V_s$ (s^{-1})

C_I = initiator concentration (mol dm^{-3})

C_{st} = total concentration of surfactant (mol dm^{-3})

C_{sw} = total concentration of surfactant in water (mol dm^{-3})

C_m^p = concentration of monomer in the polymer particles (mol dm^{-3})

C_m^w = concentration of monomer in water (mol dm^{-3})

C_R^w = concentration of radicals in water (mol dm^{-3})

D_p = diffusion constant for monomeric radicals in the particles ($dm^2\ s^{-1}$)

D_w = diffusion constant for monomeric radicals in the aqueous phase ($dm^2\ s^{-1}$)

G = number of experimental points

I_e = ionic strength (mol dm^{-3})

K = vector of adjustible parameters

K_o = diffusion rate of monomeric radicals out of particles (s^{-1})

L_{dp} = surface separation between droplet and particle (dm)

M_o = molecular weight of monomer (g mol^{-1})

M_i^o = initial number of moles of component i (mol dm^{-3})

N_A = Avogadro's number (molecule mol^{-1})

N_n = number of particles containing n radicals (dm^{-3})

N_d = number of droplets per unit volume of continuous phase (dm^{-3})

N_p = number of particles per unit volume of continuous phase (dm^{-3})

R = gas constant

R_c = rate of radical capture by particles (dm^{-3} s^{-1})

R_{dp} = center-to-center distance between droplet and particle (dm)

R_f = rate of radical flocculation (dm^{-3} s^{-1})

R_i = rate of radical generation (dm^{-3} s^{-1})

R_p = rate of polymerization (mol dm^{-3} s^{-1})

$[R\cdot]$ = concentration of radicals in the particles (mol dm^{-3})

S = vector of the state variables

T = temperature (K)

$V_D(t)$ = volume of a droplet at time t (dm^3)

V_q = volume of phase q (dm^3)

V_s = swollen volume of a latex particles (dm^3)

V_t = total volume of the system (dm^3)

V_w = volume of water (dm^3)

$\overline{V}_i$ = molar volume of component i

W_{dp} = stability ratio

Y = vector of the independent variables

Greek

β = probability a desorbed radical reacts in the aqueous phase

χ_{ij} = Flory-Huggins interaction parameter

δ = Stern layer thickness (dm)

ε = permitivity of the dispersion medium (C V^{-1} dm^{-1})

ε_o = permitivity of vacuum (C V^{-1} dm^{-1})

ε_r = dielectric constant

$\phi_{i,q}$ = volume fraction of component i in phase q

ϕ_w = volume fraction of water in the continuous phase

γ = interfacial tension (J dm^{-2})

κ = inverse electric double layer thickness (dm^{-1})

μ = viscosity of the medium (kg dm^{-1} s^{-1})

ρ = first order radical entry rate coefficient into particles (s^{-1})

ρ_m = density of monomer (g dm^{-3})

ρ_p = density of polymer (g dm^{-3})

ρ_D = first order radical entry rate coefficient into droplets (s^{-1})

σ_{si} = surface charge density from surfactant contribution for droplet or particle (C dm^{-2})

σ_{oi} = total surface charge density for droplet or particle (C dm^{-2})

σ_{Ii} = surface charge density from initiator contribution for particle (C dm^{-2})

θ_{si} = surface coverage for droplet or particle

ω = fraction of the ionic groups on the surface of particle

ψ_{oi} = surface potential of droplet or particle (V)

ζ_i = zeta potential of droplet or particle (V)

Φ_T = total potential energy (J)

Φ_A = attractive potential energy (J)

Φ_R = repulsive potential energy (J)

Appendix B
Concentration of Cetyl Alcohol As Determined by Gas Chromatography

B.1 Conditions of Running the Gas Chromatograph

About 0.5 μl of sample was injected into the gas chromatograph (GC). The injecting sample was prepared by dissolving a known amount of cetyl alcohol, CA, in ethanol (solvent) containing a known amount of benzyl alcohol, BA, (standard). At the beginning of the run, the oven temperature was at 118°C for 2 minutes. Then it was heated at 30°C/min to the final temperature of 160°C. The detailed program is shown in Table B-1

Table B-1: Parameters Used in the GC Program

```
* LIST: METH  a:CABAET  @

RUN PARAMETERS
ZERO   =  5
ATT 2^ =  8
CHT SP =  0.5
AR REJ =  5000
THRSH  = -1
PK WD  =  0.05

TIMETABLE EVENTS
   0.000 INTG # = -7
   0.000 INTG # =  2
   0.000 INTG # =  8

OVEN TEMP = 124    SETPT = 118
 EQUIB TIME   = 1.00        CRYO OFF
 OVEN MAXIMUM = 280
 INITIAL TEMP = 118
 INITIAL TIME = 2.00

TEMP PRGM: RATE   FINAL TEMP   FINAL TIME
           30.0       160         8.00

RUN LENGTH = 11.40 MIN

INJ A TEMP = 200   SETPT = 200
INJ B TEMP = 200   SETPT = 200
DET A TEMP = 100   SETPT = 300  (OFF)
DET B TEMP = 200   SETPT = 200

SIGNAL 1 = B
 INET FULL RANGE DATA ON
 RANGE = 0
 ZERO  = 11.8
 ATTN  = 0
```

When a sample was injected into the GC, a result was obtained and is shown in Figure B-1. Peak (1) is that of benzyl alcohol and peak (2) cetyl alcohol.

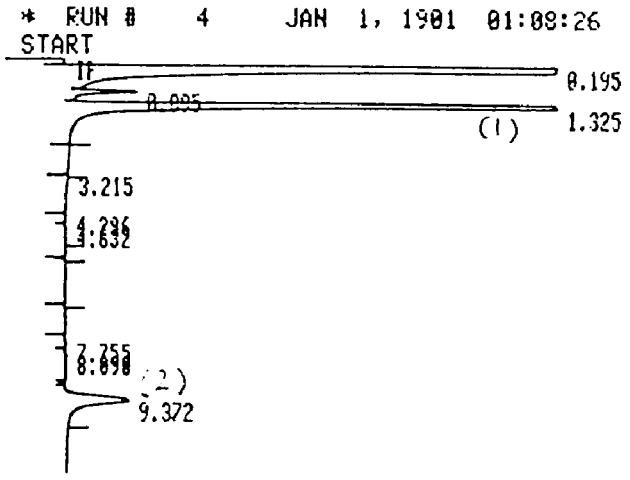

STOP

Closing signal file M:SIGNAL .RAW

RUN# 4 JAN 1, 1901 01:08:26

METHOD NAME: a:CABAET.MET

SIGNAL FILE: M:SIGNAL.RAW

CALIBRATION

AREA%

RT	AREA	TYPE	WIDTH	AREA%
.195	895494720	SBB	.064	93.52243
.895	1110616	BB	.083	.11599
1.325	56742944	BB	.090	5.92604
7.755	9014	PB	.171	.00094
8.090	6834	BB	.159	.00071
9.372	4154917	PB	.281	.43393

TOTAL AREA=9.5752E+08
MUL FACTOR=1.0000E+00

Figure B-1: Actual GC data of one sample from the calibration curve, indicating peaks for benzyl alcohol (1) and cetyl alcohol (2), and the associated computer integration.

The GC calibration curve was developed by injecting samples of known CA/BA weight ratio into the GC to obtain an area ratio of CA/BA. The results are plotted on Figure B-2. This plot was used to obtain the cetyl alcohol/bezyl alcohol weight ratio when a sample mixture was injected into the GC.

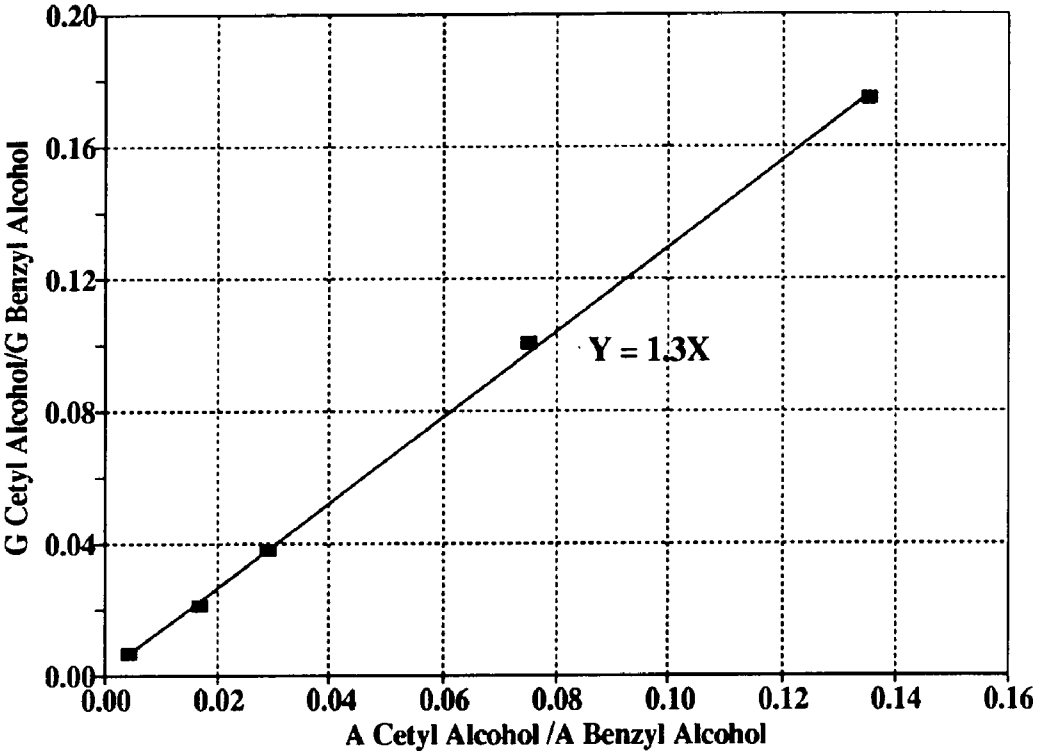

Figure B-2: Plot of GC calibration curve data for cetyl alcohol sample using benzyl alcohol as standard and ethanol as solvent.

Vita

Phan Linh Tang was born on July 25, 1961 in Camau, Viet Nam, the fourth son of Quyen Toung Tang and Hoa Thu Quach. Phan came to America in 1980. After a year and a half of attending Ludington High School in Michigan, he received a high school diploma in June, 1981; more importantly, he "adopted" a second family, the Beatty family, to whom he owes all his bright future.

After four years of attending Michigan Technological University where there was nothing else but school work and bars (luckily he chose the former), Phan recieved a B.S. degree in Chemical Engineering. After spending two years in the Development Laboratory at the Dow Chemical Company in Ludington, Michigan, he decided that more education would be valuable to his career in chemical research and thus came to Lehigh University to pursue higher education. In June of 1989, he received a M.S. degree in Chemical Engineering. After talking to Dr. El-Aasser about the advantages of getting a Ph.D. degree (Phan ignored the disadvantages), he continued to pursue a higher education. Upon completion of a Ph.D. degree, he will join Du Pont in Louisville, Kentucky.

In 1990, Phan received the Hoechst-Celanese Polymer Science and Engineering Award for outstanding research in the field of polymer science, and in 1991, he received the Kenneth A. Earhart Award for scholarly achievement and contributions to the activities of the EPI. Phan has published a paper from his M.S. Research and a paper from his Ph.D. work, and has presented part of his work at the ACS meeting in Atlanta, Georgia, April 19-25, 1991. Phan is a member of the American Chemical Society.

Phan is married to Lan Diem Tran whose love and cooking kept him alive during the 'best time of his life' (according to Dr. Sudol) at Lehigh.